The functional relationship between Inhibitor-3, SDS22, and PP1 in the process of bipolar spindle attachment

Inaugural-Dissertation

zur

Erlangung des Doktorgrades

Dr. rer. nat.

der Fakultät für

Biologie

an der

Universität Duisburg-Essen

vorgelegt von

Annika Eiteneuer

aus Olpe

März 2014

Die der vorliegenden Arbeit zugrunde liegenden Experimente in der Abteilung Molekularbiologie I der Fakultät für Biologie der Universität Duisburg-Essen durchgeführt.

1. Gutachter: Prof. Dr. Hemmo Meyer
2. Gutachter: prof. Dr. Andrea Musacchio

Vorsitzender des Prüfungsausschusses:
Prof. Dr. Bernhard Horsthemke

Tag der mündlichen Prüfung: 13.08.2014

Table of Contents

List of Figures

List of Tables

Summary

The identification of bipolar kinetochore-microtubule attachments is essential for proper progression through mitosis. This is achieved by dynamic Aurora B-mediated phosphorylation of its targets at the kinetochore. Centromere-localized Aurora B phosphorylates kinetochore proteins in a tension-dependent manner, thereby destabilizing wrong kinetochore-microtubule attachments, which are without tension. PP1-mediated dephosphorylation of Aurora B substrates at kinetochores, which are under tension and thereby pulled out of the reach of Aurora B, leads to stabilization of kinetochore-microtubule attachments. Targeting of PP1 to the kinetochore by KNL1 and SDS22 (as well as CENP-E and KIF18A) is thought to regulate PP1 activity at the kinetochore in mammalian cells. However, the exact mechanism of PP1 regulation by SDS22 remained unclear so far, as contradictory data exist concerning the kinetochore-localization of SDS22 and its relevance for the activity of Aurora B on metaphase chromatin. Furthermore, in yeast, also Iinhibitor-3 (I3), which builds a trimeric complex with PP1-SDS22, is known to be relevant for PP1-mediated counteraction of the Aurora kinase.

In this thesis, we resolved the contradictory data, published on SDS22 and we provided additional information, which clarifies its role in PP1 regulation. Furthermore, we elucidated the function of I3 in mammalian cells. Our data demonstrate that SDS22 does not localize to kinetochores quantitatively and also does not function as a targeting subunit of PP1. Moreover, we find that SDS22 is required for PP1-mediated counteraction of Aurora B activity. However, increased levels of SDS22 at kinetochores inhibit PP1 activity. From these data we conclude that SDS22-bound PP1 is inactive, although SDS22 is required for PP1 activity. Therefore, we suggest that SDS22 may act as a general chaperone, stabilizing inactive PP1 for re-activation. Furthermore, we show for the first time that I3 is required for proper chromosome congression and PP1-mediated counteraction of Aurora B in mammalian cells. Our data indicate that I3 ensures localization of active PP1 to KNL1 by restricting SDS22 localization to KNL1-bound PP1. Increased SDS22 localization to kinetochore-bound PP1 due to I3 knockdown causes not only

metaphase defects, but also leads to anaphase defects and persistence of active Aurora B on anaphase chromatin. Additionally, our data provide initial hints that the mechanism of PP1-SDS22 sequestration by I3 could be regulated via phosphorylation of I3 during mitosis. Finally, investigating the function of I3 and SDS22 provides a basis for exploring the functional link between I3-PP1-SDS22 and p97-p47/p37, which were found to interact physically.

Zusammenfassung

Die Bildung und Identifikation von bipolaren Kinetochor-Mikrotubuli-Verbindungen ist essentiell für den erfolgreichen Verlauf der Mitose. Beides wird erreicht durch die Aurora B abhängige Phosphorylierung von Kinetochor-Proteinen. Am Zentromer lokalisiertes Aurora B phosphoryliert seine Kinetochor-lokalisierten Substrate wenn Kinetochor-Mikrozubuli-Verbindungen nicht unter Spannung stehen. Dadurch wird erreicht, dass falsche Kinetochor-Mikrotubuli-Verbindingungen, die nicht unter Spannung stehen, destabilisiert werden. Kinetochore, die durch bipolare Verbindung mit Mikrotubuli unter Spannung stehen, können von dem, am Zentromer lokalisierten, Aurora B nicht mehr erreicht werden, wodurch PP1-abhängige Dephosphorylierung der Kinetochor-Substrate favorisiert wird. Aufgrund von Experimenten in Säugerzellen wird angenommen, dass die Aktivität von PP1 am Kinetochor über dessen Lokalisierung durch SDS22 (als auch KNL1, CENP-E, und KIF18A) reguliert wird. Der genaue Mechanismus ist bisher jedoch ungeklärt, da widersprüchliche Daten bezüglich der Lokalisierung von SDS22 und des Einflusses von SDS22 auf die Aktivität von Aurora B publiziert wurden. Zusätzlich haben Experimente in Hefe gezeigt, dass auch Inhibitor-3 (I3), welches einen trimeren Komplex mit PP1 und SDS22 bildet, für das antagonistische Wechselspiel von PP1 und Aurora B benötigt wird.

In dieser Arbeit wurden die Widersprüche bezüglich der Lokalisierung und Funktion von SDS22 aufgeklärt, sowie weitere Erkenntnisse gewonnen, die neue Schlussfolgerungen über die Rolle von SDS22 auf PP1 erlauben. Des Weiteren wurde die Funktion von I3 in Säugerzellen aufgeklärt. Diese Ergebnisse zeigen, dass SDS22 nicht quantitativ an den Kinetochoren lokalisiert und es auch nicht die Lokalisierung von PP1 zu den Kinetochoren reguliert. Jedoch ist SDS22 für ein funktionierendes Wechselspiel von PP1 und Aurora B am Kinetochor essentiell, auch wenn sich eine erhöhte Lokalisierung von SDS22 an den Kinetochor inhibierend auf die Aktivität von PP1 auswirkt. Dies führt zu der Schlussfolgerung, dass SDS22-gebundenes PP1 inaktiv ist, trotzdem aber SDS22 für PP1 Aktivität benötigt wird, woraus sich die Hypothese ergibt, dass SDS22 die Funktion eines Chaperons zur

Stabilisierung inaktiven PP1s übernimmt, welches zur Reaktivierung von inaktivem PP1 benötigt werden könnte. Desweiteren wird erstmalig gezeigt, dass auch I3 für die erfolgreiche Bildung einer Metaphase Platte und für ein funktionierendes Wechselspiel von PP1 und Aurora B in Säugerzellen erforderlich ist. Die Daten belegen zusätzlich, dass I3 die Bindung von aktivem PP1 an KNL1 durch die Restriktion der Lokalisierung von SDS22 an KNL1-gebundenes PP1 sichert. Eine Störung der Lokalisierung von SDS22 verursacht nicht nur Defekte in Metaphase, sondern auch in Anaphase, da Segregationsdefekte und persistierendes aktives Aurora B auf Anaphase Chromatin gefunden wurde. Die Ergebnisse liefern darüber hinaus erste Hinweise auf eine Regulierung I3 abhängiger Sequestrierung von PP1-SDS22 durch Phosphorylierung von I3 in Mitose.

Schließlich vereinfacht die Entschlüsselung der Funktionsweise von SDS22 und I3 die weitere Suche nach der funktionellen Verbindung zwischen den, physikalisch interagierenden Komplexen I3-PP1-SDS22 und p97-p47/p37.

1 Introduction

1.1 Mitosis

Mitosis is a complex process, which has to be tightly regulated to assure error-free cell division. The accompanying tremendous cellular reorganization is controlled by multiple regulatory mechanisms, like phosphorylation-dependent switches and ubiquitin-dependent degradation (Musacchio, 2011).

Mitotic entry

The satisfaction of the G2-M checkpoint marks the beginning of mitosis. Only cells, whose genome has been accurately replicated and which are free of DNA damage, can pass the checkpoint. With mitotic entry, the decision is made to undergo mitosis and there is no way back, but finishing mitosis or undergoing mitotic catastrophe (Lobrich and Jeggo, 2007). Mitotic entry is driven by the kinase CDK1. Together with its activating subunit Cyclin B, it builds the maturation-promoting factor (MPF). Satisfaction of the G2-M checkpoint allows the phosphatase CDC25 to dephosphorylate CDK1 and thereby activate the MPF. Phosphorylation of many mitotic substrates, among them further mitotic kinases like Plk1, Aurora A and B, and PKA, generates the signal for the structural reorganization of the cell (Ma and Poon, 2011). The cell rounds up, the chromatin condenses to the mitotic chromosomes, the mitotic spindle assembles, and Golgi and ER reorganize (Guttinger et al., 2009). With nuclear envelope break down (NEBD) many mitotic proteins gain access to their site of action. One example of this is the assembly of the outer kinetochore, which is assembled on the inner kinetochore shortly after NEBD (Jia et al., 2013). Next, the microtubules of the spindle start to attach to the kinetochores, thus the chromosomes can be arranged in a horse-shoe form around the spindle.

Chromosome congression

The following migration of the two centrosomes of the mitotic spindle to the opposite poles of the cell allows an arrangement of the chromosomes in a vertical plate between both spindle poles – the metaphase plate. Here, the challenging task is to

achieve a bipolar attachment of every chromatid pair to the opposite spindle poles so that all sister chromatids will be equally distributed into the two daughter cell when separation starts in anaphase. Every erroneous microtubule-kinetochore attachment has to be detected and corrected, as already a single undetected misaligned chromosome will cause aneupoidy and can lead to cancer (Kops et al., 2005; Tanaka, 2013). Two mechanisms exist to assure faithful segregation. First, bi-oriented chromosomes are detected by sensing the tension (Lampson and Cheeseman, 2011), which arises when microtubules pull from opposite spindle poles. And second, the spindle assembly checkpoint (SAC) prevents premature anaphase, as long as it is activated (Musacchio, 2011). Members of the SAC build the mitotic checkpoint complex (MCC), which binds CDC20, a subunit of the anaphase promoting complex, also called cyclosome, (APC/C), thereby precluding association of CDC20 with the APC/C and activation of the APC/C (Acquaviva and Pines, 2006; Jia et al., 2013). Together both mechanisms assure bipolar attachment of all chromosomes before the cell starts mitotic exit. How the spindle assembly checkpoint and the sensing of bi-orientation are organized, and how they act in concert will be explained in detail below.

Mitotic exit

When bipolar spindle attachment of all chromosomes is achieved, mitotic exit is initiated (Sullivan and Morgan, 2007). Activation of the APC/C is crucial for mitotic exit. Upon satisfaction of the SAC, the MCC releases CDC20, thereby allowing its binding to the APC/C. This complements the recognition site for two key substrates, Cyclin B and Securin. The APC/C^{CDC20} ubiquitinates them and thereby targets them for proteasomal degradation (Jia et al., 2013). Cyclin B degradation inactivates the CDK1 and thereby drives mitotic exit. Besides inactivation of the kinase, also dephosphorylation of the CDK1 substrates by the phosphatases PP2A, PP1 and CDC14 is of importance (Bollen et al., 2009; Wurzenberger and Gerlich, 2011). The second important substrate, Securin, is an inhibitor of the protease Separase. Upon degradation of Securin, Separase cleaves Cohesin, which before tightly connected both sister chromatids. Now, segregation of the sister chromatids to the opposite spindle poles is possible. This is also facilitated by the help of the central spindle, consisting of antiparallel microtubules, which assemble between both chromatin

masses at anaphase onset. In telophase, when the chromatin decondenses and the nuclear envelope forms again, the central spindle in the midzone condenses to a bundle of microtubules, the midbody (Guttinger et al., 2009). After reorganization of the Golgi and ER, cytokinesis takes place at the midbody and separates the last connection between both daughter cells (Fededa and Gerlich, 2012).

1.2 Chromosome congression

1.2.1 The kinetochore

The centromere is located in a distinct region on every chromosome, which is epigenetically marked by exchange of histone 3 for its variant, CENP-A (Black and Bassett, 2008). Here, two kinetochores are assembled to link the two sister chromatids to the +ends of microtubules coming from the opposing spindle poles. The kinetochore can be structurally divided into the inner and the outer kinetochore. The inner kinetochore consists of the CENP proteins. They build the constitutive centromere associated network (CCAN) connecting the kinetochore with the chromatin. Microtubule attachment is facilitated by the outer kinetochore, which is only assembled in mitosis (Takeuchi and Fukagawa, 2012). Linking microtubules to kinetochores is complex, as it must be dynamic enough to allow correction of erroneous attachments and it must be stable enough to bear the forces of sister chromatid separation. The KMN network takes over this task. It consists of KNL1 (kinetochore null protein 1), the Mis12 (missegregation 12) complex and the Ndc80 (nuclear division cycle 80) complex. Among these complexes, the Ndc80 complex directly binds microtubules, even though also KNL1 was shown to have microtubule-binding capacity and is able to synergistically enhance the binding capacity of the KMN network to microtubules (Cheeseman et al., 2006). The Mis12 complex connects the KMN network with the CCAN (Petrovic et al., 2010).

When kinetochores bind microtubules different scenarios of erroneous binding are possible. Next to the correct amphitelic (or bipolar) attachment, also a monotelic, syntelic, or merotelic attachments are possible (Figure 1.1). As microtubules bind kinetochores according to the principle of trial and error, also wrong attachments are relatively frequent (Nicklas, 1997).

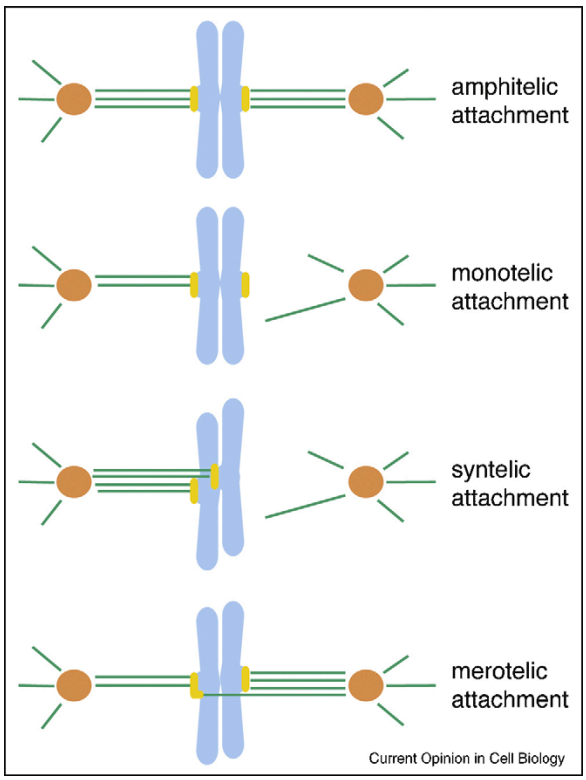

Figure 1.1 Classification of kinetochore-microtubule attachments. Amphitelic, or bipolar attached chromosomes have sister kinetochores which are correctly attached to microtubules of both mitotic spindle poles. In the case of monotelic and syntelic attachments, one or both kinetochores of a chromosome are connected to one spindle pole. Merotelic attachment describes the case, when both kinetochores are connected to the opposing spindle poles, but one kinetochore is additionally connected to microtubules of the other spindle pole (Kelly and Funabiki, 2009).

A mechanism to detect and correct erroneous attachments is therefore essential to achieve bi-orientation. Aurora B takes over this task. How Aurora B is able to sense bi-orientation of sister chromatids will be discussed in detail below. Briefly, Aurora B is able to destabilize erroneous kinetochore-microtubule attachments by phosphorylating several kinetochore-localized substrates dynamically in a tension-dependent manner. Monotelic, merotelic, and syntelic kinetochore-microtubule attachments are tensionless so that centromere-localized Aurora B will phosphorylated its substrates at the kinetochore, thereby provoking dissociation of erroneous attached microtubules (Funabiki and Wynne, 2013; Lampson and Cheeseman, 2011). Only when kinetochore-microtubule attachments are amphitelic,

force is generated from the opposing spindle poles pulling the kinetochores out of the reach of centromere-localized Aurora B, thereby shifting the dynamic balance of phosphorylation and dephosphorylation towards dephosphorylation of kinetochore proteins, leading to the stabilization of kinetochore-microtubule attachments (Lesage et al., 2011; Tanaka, 2013). Additionally, Aurora B phosphorylates and thereby regulates CENP-E, the Ska complex and MCAK. The plus end-directed kinetochore motor, CENP-E, transports polar-localized chromosomes towards the metaphase plate, thereby helping to form a metaphase plate (Kim et al., 2010). The Ska complex stabilizes the microtubule ends by preventing depolymerization when attached bipolar to kinetochores (Chan et al., 2012) and the kinesin-related protein MCAK binds the outer kinetochore to further stabilize the microtubule attachment (Lan et al., 2004).

1.2.2 The spindle assembly checkpoint

The spindle assembly checkpoint (SAC) translates the alignment state of the kinetochore to a cellular signal, which indicates whether progression to anaphase is allowed (Foley and Kapoor, 2013). It keeps the APC/C^{Cdc20} inactive, as long as congression defects are present and activates it, as soon as all chromosomes are aligned. The key players of the SAC are Bub1 (budding uninhibited by benomyl 1), Bub3, BubR1 (Bub1-related 1), Mad1 (mitotic arrest deficient 1), MAD2, as well as Aurora B and Mps1 (monopolar spindle protein 1) (Jia et al., 2013). A subset of these proteins, Mad2, BubR1 and Bub3 build together with Cdc20 the mitotic checkpoint complex (MCC) which prevents binding of Cdc20 to the APC/C as long as the checkpoint is activated (Musacchio, 2011; Musacchio and Salmon, 2007). To facilitate a fast release of Cdc20 from the MCC upon checkpoint satisfaction, Cdc20 binding to the MCC has to be dynamic (Jia et al., 2013). Hence, the MCC does not bind Cdc20 stably, but targets it for degradation. New Cdc20 is synthesized and again bound by the MCC (Jia et al., 2013). This creates a dynamic system, thereby allowing a prompt response upon SAC silencing. While the MCC acts as an effector, the other checkpoint proteins, MAD1 and the kinases Bub1, and Mps1 are signal amplifiers (Tanaka, 2013). They multiply the signal, originating from a single

misaligned chromosome, so that it keeps the spindle assembly checkpoint active (Tanaka, 2013).

Both, the MCC and the amplifiers localize to the outer kinetochores in prometaphase. Mps1 is thought to bind Ndc80 in an Aurora B-dependent manner (Saurin et al., 2011), furthermore it was shown to phosphorylate KNL1 in its MELT motif, which allows binding of Bub1 to that site (London et al., 2012). Besides that, also localization of a Mad1-Mad2 complex to Ndc80 is Mps1 and Aurora B dependent (Jia et al., 2013; Martin-Lluesma et al., 2002; Santaguida et al., 2011). Bub3 and BubR1 localize to the kinetochore by binding Knl1-localized Bub1 (Kiyomitsu et al., 2007). And additionally, further interdependencies were found, as Bub1 binding depends on Bub3 recruitment (Krenn et al., 2012) and Aurora B also contributes to kinetochore localization of Mps1, Bub1 and BubR1 (Santaguida et al., 2011). Upon microtubule binding, the checkpoint proteins are transported via dynein motors along the microtubules towards the spindle poles (Howell et al., 2001), although microtubule-binding to kinetochores was also shown to directly displace checkpoint proteins from kinetochores without the help of dynein motors (Espeut et al., 2012; Jia et al., 2013). Whether the kinetochore-microtubule attachment is of amphitelic, syntelic or merotelic nature is not sensed by the SAC (Kelly and Funabiki, 2009). It is rather believed that the destabilizing effect of Aurora B phosphorylation quickly generates unattached kinetochores so that the SAC proteins stay bound to kinetochores (Kelly and Funabiki, 2009). Only after shut down of Aurora B signaling due to the emergence of tension upon bipolar microtubule attachments, the SAC proteins dissociate from the kinetochore and only after all chromosomes are bipolar attached, the SAC is satisfied (Funabiki and Wynne, 2013). However, besides the function of Aurora B in error correction, Aurora B also might play a direct role in the SAC, as there is evidence that Aurora B is required for the maintenance of the SAC in the presence of microtubule-depolymerizing drugs (Kallio et al., 2002; Petersen and Hagan, 2003; Santaguida et al., 2011).

1.3 Aurora B

1.3.1 The Chromosomal Passenger Complex

Three Aurora homologues are known in vertebrates, Aurora A, B, and C, while in budding yeast only one Aurora homolog was found, which is named Ipl1 (Chan and Botstein, 1993; Ruchaud et al., 2007). The three mammalian homologues differ in function, localization and tissue specificity. Whereas Aurora C is mostly expressed in the testis, Aurora A and B are expressed in all tissues (Ruchaud et al., 2007). However, Aurora A and B localize differently in the cell and build distinct complexes. While Aurora A was found to bind Bora and to localize to centrosomes in mitosis, being involved in spindle maturation, Aurora B acts as part of the chromosomal passenger complex (CPC) and changes its localization dynamically during mitosis (Ruchaud et al., 2007). In prophase it is found at the chromatin and concentrates in prometaphase at the centromeric region. With anaphase onset, Aurora B relocalizes from centromeres to the spindle midzone, and then to the midbody in telophase.

Besides the kinase Aurora B, the CPC consists of three scaffold proteins: inner centromere protein (INCENP), Survivin, and Borealin (also known as Dasra-B). Aurora B binds INCENP at the IN box, which is located near the C-terminus (Adams et al., 2000). At its N-terminal region INCENP binds Borealin and Survivin. Survivin belongs to the inhibitor of apoptosis (IAP) family and has a baculovirus IAP repeat (BIR) domain, which is responsible for dimerization of Survivin (Verdecia et al., 2000). However, in the CPC Survivin is bound as monomer. It connects the N-terminus of INCENP with Aurora B and also binds Borealin (Carmena et al., 2012). Additionally, Borealin may stabilize the interaction between INCENP and Survivin by binding the N-terminus of INCENP (Vader et al., 2006).

At mitotic entry, INCENP, as well as Survivin are phosphorylated by Aurora B (Bishop and Schumacher, 2002; Wheatley et al., 2004). The phosphorylation of INCENP by Aurora B at two sites on the C-terminus was shown to increase Aurora B activity in a positive feedback loop (Bishop and Schumacher, 2002). This positive feedback may include stimulation of Aurora B activity by autophosphorylation at T232 (Yasui et al., 2004). Additionally, phosphorylation of Survivin by CDK1 further activates Aurora B (Tsukahara et al., 2010). INCENP is also phosphorylated by CDK1, which effects the localization of the CPC, as dephosphorylation of this site at anaphase onset triggers

localization from centromeres to the central spindle (Pereira and Schiebel, 2003). Both, Survivin and INCENP were furthermore shown to be also relevant for targeting the CPC to centromeres (Ainsztein et al., 1998). Besides posttranslational modification of the CPC members, the localization is regulated by the creation of binding sites. In prophase, Haspin phosphorylates Histone 3 at T3 (H3T3) and thereby triggers binding of the CPC to chromatin (Kelly et al., 2010; Wang et al., 2010). At the same time, PP1 with its targeting subunit Repo-Man dephosphorylates this site (Qian et al., 2013). A balance between phosphorylation and dephosphorylation is generated, which can be shifted towards phosphorylation by Aurora B itself, since Aurora B is able to phosphorylate Repo-Man, thereby inhibiting PP1-Repo-Man mediated dephosphorylation of H3pT3. So, Aurora B supports its own chromosomal targeting (Qian et al., 2013). Bound to H3pT3, Aurora B in turn phosphorylates histone 3 at S10 (H3S10) (Crosio et al., 2002). The function of this phosphorylation is still to be elucidated, but it may play a role in organizing the chromosome structure, as additional acetylation of L14, adjacent to the phospho-site, causes dissociation of the heterochromatin protein 1 (HP1) from chromatin (Fischle et al., 2005). Nevertheless, H3S10 phosphorylation is a well established marker for mitosis, which persists until telophase (Lipp et al., 2007; Ruchaud et al., 2007; Takemoto et al., 2007).

In prometaphase and metaphase Aurora B concentrates from the chromosomal arms to the inner centromeres, where it acts in chromosome congression and maintains the spindle assembly checkpoint (Lampson and Cheeseman, 2011). The accumulation in the centromeric region might be achieved by Bub1-mediated phosphorylation of Histone 2A T120 (Kawashima et al., 2010). This creates a binding site for Shugoshin, which in turn binds Borealin that has been phosphorylated by CDK1 (Kawashima et al., 2007; Tsukahara et al., 2010). Work from Yamagishi and colleagues suggests that the combination of Histone 2A and Histone 3 phosphorylation determines Aurora B localization to the inner centromere (Yamagishi et al., 2010). An additional mechanism keeps Aurora B localization at the centromere dynamic, as Survivin and Aurora B were shown to turn over rapidly at centromeres in a ubiquitin-dependent manner (Beardmore et al., 2004; Murata-Hori and Wang, 2002; Vong et al., 2005). Finally, Mps1 promotes Aurora B clustering at centromeres, potentially by Mps1-mediated phosphorylation of Borealin at T230 (Jelluma et al.,

2008; van der Waal et al., 2012). This local clustering increases Aurora B activity by facilitating autophosphorylation at Thr232 (Carmena et al., 2009). Now fully active, Aurora B can fulfill its function in correcting erroneous kinetochore-microtubule attachments by phosphorylating its kinetochore substrates, thereby destabilizing wrong attachments (Lampson and Cheeseman, 2011). Its targets are the members of the KMN network (especially Ndc80 at various sites of its N-terminus), MCAK, CENP-E, and the Ska complex (Chan et al., 2012; Cheeseman et al., 2006; DeLuca et al., 2006; Kim et al., 2010; Ohi et al., 2004; Welburn et al., 2010).

With onset of anaphase, Aurora B again changes its localization to the midzone, where it is involved in the formation and stabilization of the central spindle (Ruchaud et al., 2007). For translocation from centromeres to the midzone, Aurora B is ubiquitinated by the E3 ligase Cullin 3 with help of the Kelch proteins KLHL9, KLHL13, and KLHL21 (Sumara and Peter, 2007; Sumara et al., 2007). In a next step, p97 with its cofactors Ufd1 and Npl4 extracts Aurora B from chromatin (Dobrynin et al., 2011) and the site for Aurora B targeting to chromatin, H3pT3, is removed by Repo-Man-mediated dephosphorylation. Additionally, localization to the midzone requires binding of Aurora B and INCENP to Mklp2 (mitotic kinesin-like protein 2), a kinesin 6 protein, which is regulated by removal of the CDK1-mediated phosphorylation (Gruneberg et al., 2004; Hummer and Mayer, 2009). At the midzone, Aurora B builds a gradient. Experiments, in which Aurora B substrate phosphorylation was measured with the help of a fluorescence resonance energy transfer (FRET) sensor, showed that substrate phosphorylation decreased with increasing distance from the central spindle (Fuller et al., 2008). Thereby Aurora B substrates at the chromosomal arms exhibit higher phosphorylation then substrates at the centromeric regions. This gradual phosphorylation allows a specific axial shortening of the chromosomal arms, which ensures that the nucleus will include all chromatin when it is formed (Mora-Bermudez et al., 2007).

In telophase, when the midzone contracts to the midbody, Aurora B is part of the equatorial contractile ring and involved in cytokinesis. Here, it plays a role in the regulation of cytoskeletal dynamics and in regulating RhoA activity, which is of importance for maturation of the contractile ring (Carmena et al., 2012; Petronczki et al., 2007; Yuce et al., 2005).

1.3.2 Aurora B sensing tension

Already in 1969 Nicklas and Koch found that artificially pulling on unipolar attached kinetochores with a glass microneedle stabilized microtubule attachments, which were otherwise unstable (Lampson and Cheeseman, 2011; Nicklas, 1997; Nicklas and Koch, 1969). This experiment gave the first hint that bipolar kinetochore-microtubule attachments are recognized and stabilized. Furthermore, it suggests that the detection is based on the occurrence of tension. With such a mechanism not only unattached and monopolar, but also merotelic and syntelic attached kinetochores become detectable. But how does the cell sense the occurrence of tension? Inhibition of Aurora B stabilizes kinetochore-microtubule attachments independent of the type of attachment and wash out of the inhibitor again destabilizes erroneous attachments allowing error-correction (Ditchfield et al., 2003; Hauf et al., 2003; Lampson et al., 2004). This finding suggests that Aurora B translates the occurrence of mechanical force into a cellular signal, which stabilizes the attachment. Furthermore, DeLuca and colleagues found the N-terminal tail of Ndc80, which is responsible for microtubule binding, to be phosphorylated by Aurora B in vitro and a nonphosphorylatable mutant of Ndc80 to cause an increase in merotelic attachments (DeLuca et al., 2006). Additionally, an Ndc80 mutant, simulating constitutive phosphorylation, caused metaphase arrest in yeast, although bipolar attachments were achieved (Kemmler et al., 2009). Besides Ndc80, Aurora B also phosphorylates Knl1 and Mis12, when unattached to microtubules, leading to a highly phosphorylated KMN network. Phosphorylation of these sites does not serve for signal transduction, but decreases the affinity of the KMN network for microtubules, as Welburn and colleagues found full phosphorylation of the KMN network to strongly compromise microtubule binding (Welburn et al., 2010).

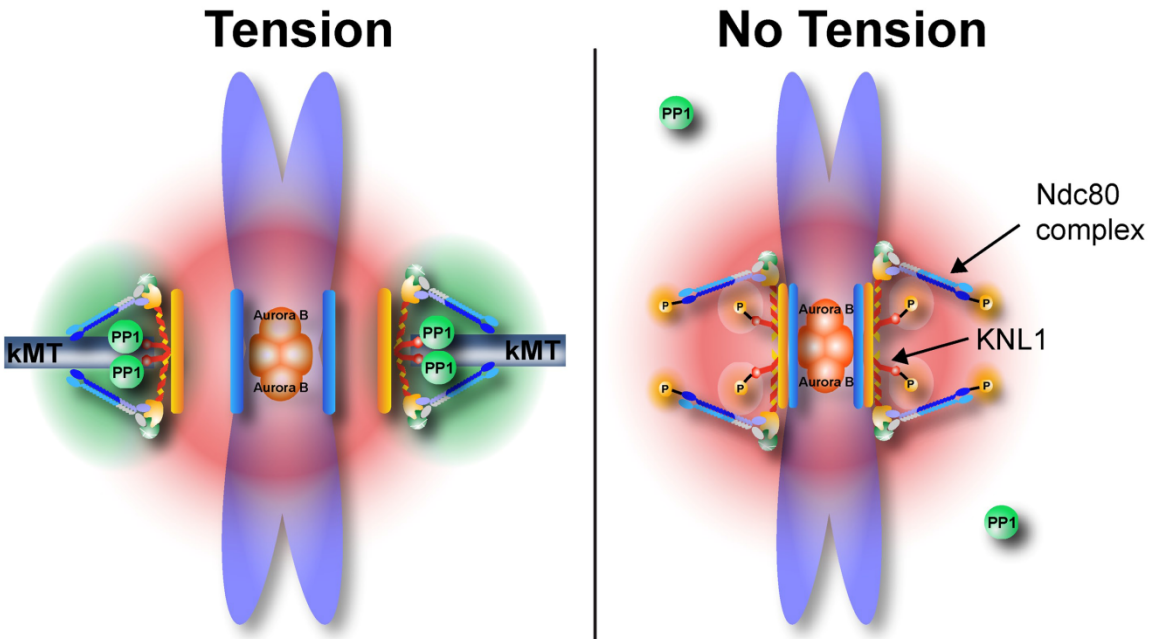

Figure 1.2 Model of Aurora B sensing tension. Kinetochores, unattached to microtubules are tensionless which enables centromeric Aurora B to phosphorylate kinetochore substrates. Kinetochores correctly attached to microtubules, are under tension, whereby the Aurora B substrates at the kinetochore are pulled out of its reach and the counteracting phosphatase (PP1) can dephosphorylate such targets. (Liu et al., 2010).

However, the KMN network phosphorylation sites are not collectively dephosphorylated, but gradual levels of phosphorylation are generated, whereby gradual levels of affinity of kinetochores for microtubules are generated (Welburn et al., 2010). This effect was also explored by Liu and colleagues by targeting a FRET-based sensor for Aurora B substrate phosphorylation to different sites at the kinetochore, representing different distances from the inner centromere, where Aurora B is localized (Liu et al., 2009). They found the level of phosphorylation to depend on the distance, the FRET-based sensor had from the inner centromere. Additionally, the degree of change in phosphorylation upon bipolar attachment depended on the localization of the FRET-based sensor at the kinetochore. A sensor, located at the inner kinetochore, adjacent to Aurora B at the inner centromere, was highly phosphorylated independent of the occurrence of tension, whereas phosphorylation of a sensor located at the outer kinetochore was highly tension-sensitive. And also, artificial repositioning of Aurora B closer to kinetochores, thereby

increasing outer kinetochore phosphorylation, prevented stabilization of bi-orientated attachments (Liu et al., 2009). All these results lead to the widely accepted hypothesis that, upon bipolar kinetochore-microtubule attachment, the kinetochore-localized substrates of Aurora B are pulled out of the area, which Aurora B can reach from its inner centromeric localization, thereby allowing dephosphorylation of these targets (Figure 1.2) (Liu et al., 2009). However, it is still unclear how Aurora B reaches its substrates at all, as the kinetochore substrates are separated by 100 nm from the inner centromere. Currently, there are two models, which try to explain this effect. Santaguida and Musacchio proposed a leash model, explaining the gradual phosphorylation by Aurora B with the physical character of the CPC (Santaguida and Musacchio, 2009). They suggest that Aurora B could have an increased radius of action, because its CPC member INCENP contains a flexible coiled-coil region, which would allow the CPC, located at the outer edge of the inner centromere, to reach even distant targets at kinetochores. However, when Liu and colleagues tested the effect of an INCENP mutant, which was missing the flexible leash, error correction was still functional (Vader et al., 2007). A second model was proposed, which explains the gradual phosphorylation with a diffusion gradient of Aurora B from the inner centromere to the outer kinetochore (Lampson and Cheeseman, 2011), like it is observed in anaphase when the CPC localizes at the midzone, but phosphorylates targets on chromatin (Fuller et al., 2008). Clustering at the centromere fully activates Aurora B, which then would be released to diffuse away from centromeres. The model is supported by the fact that high turnover of centromeric Aurora B and Survivin was found (Beardmore et al., 2004; Murata-Hori and Wang, 2002). However, it is not clear whether an Aurora B gradient could act on such a short distance, as the size of a single kinetochore (Musacchio, 2011).

1.4 Phosphatases in mitosis

Only for a decade, researchers have investigated the relevance of phosphatases as dynamic counteractors of kinases in mitosis. Previously one thought of rather static and constitutively active dephosphorylation machineries (Trinkle-Mulcahy and Lamond, 2006). Only after discovering that substrate dephosphorylation does not necessarily occur concurrently with deactivation of the respective phosphorylating

kinase, the interest in the regulation of mitotic phosphatases increased (Sullivan and Morgan, 2007).

Five phosphatases were shown to act in mitosis: PP1, PP2A, PP4, CDC25, and Cdc14 (Bollen et al., 2009). Whereas CDC25, CDC14, and PP4 apparently act in distinct events during mitosis, PP1 and PP2A have more general roles (Bollen et al., 2009). Both are structurally closely related and carry two catalytic metal ions in the active site (Bollen et al., 2010; Guo et al., 2014). Recently, it was shown that the protein α4 stabilizes inactive PP2A, which is perturbed at the active site (Jiang et al., 2013) and that the PP2A phosphatase activator, PTPA, binds PP2A to enhance with the help of ATP binding the proper coordination of catalytic metal ions, thereby activating PP2A (Guo et al., 2014). A similar chaperone mechanism was proposed for Inhibitor-2 (I2) on PP1 (Alessi et al., 1993). Both phosphatases gain specificity by binding different subunits and dephosphorylate the majority of all serine and threonine residues during mitosis (Bollen et al., 2009). They often act in one pathway having synergistically, as well as antagonistically functions. Nevertheless, they have mostly non-overlapping substrates (Bollen et al., 2009).

Upon satisfaction of the G2-M checkpoint, CDC25 initiates mitotic entry by dephosphorylating CDK1, thereby activating the kinase (Karlsson-Rosenthal 2006). Also PP1 and PP2A are involved in mitotic entry, acting antagonistically on the G2-M checkpoint. PP2A with its subunit B’ (also called B56) participates in G2-M checkpoint maintenance by inhibitory binding to CDC25, if B’ is phosphorylated by CHK1, whereas PP1 activates CDC25 upon checkpoint satisfaction, thereby driving mitotic entry (Margolis et al., 2006a; Margolis et al., 2006b; Margolis et al., 2003). Additionally, PP1 and PP2A regulate Plk1, as well as Aurora A and B activation at mitotic entry (Bayliss et al., 2003; Sun et al., 2008; Yamashiro et al., 2008). Also during spindle assembly, both phosphatases act antagonistically in the same pathway. PP2A together with its subunit B’’ is a positive regulator of spindle assembly (Schlaitz et al., 2007). It inhibits MCAK in its microtubule depolymerization activity and promotes TPX2-binding to centrosomes, thereby protecting Aurora A from inactivating dephosphorylation by PP1 (Bayliss et al., 2003; Satinover et al., 2004; Schlaitz et al., 2007). Furthermore, the PP1 subunit I2 regulates PP1 activity with respect to Aurora A by inhibitory binding to PP1 (Li et al., 2007; Satinover et al., 2004).

During chromosome congression PP1 and PP2A seem to act synergistically (Foley et al., 2011; Lesage et al., 2011; Xu et al., 2013). Dephosphorylation of Aurora B substrates at kinetochores to stabilize bipolar kinetochore-microtubule attachments was earlier thought to be solely PP1-mediated, but recent data also show involvement of PP2A. PP1 localizes to kinetochores in prometaphase, where it is involved in SAC silencing, not only by dephosphorylating kinetochore-localized Aurora B substrates (Ditchfield et al., 2003; Musacchio and Salmon, 2007), but also by activating the dynein motor, which transports the SAC proteins from kinetochores to the spindle (Whyte et al., 2008). PP2A-B' binds to kinetochore-localized SAC member BubR1, when the KARD domain of BubR1 is phosphorylated by Plk1 and CDK1 (Kruse et al., 2013; Suijkerbuijk et al., 2012) and depletion of PP2A-B' causes severe misalignment, which can be partially rescued by Aurora B silencing or inhibition, suggesting that also PP2A counteracts Aurora B (Foley et al., 2011; Xu et al., 2013).

For exit from mitosis inactivation of CDK1 is essential (Sullivan and Morgan, 2007). In yeast, Cdc14 was shown to drive exit from mitosis by inhibiting CDK1 (Stegmeier and Amon, 2004; Yeong et al., 2000). However, such role of CDC14 was not found in mammals. As here the APC/C^{CDC20}-dependent degradation of the CDK1 subunit Cyclin B is much more efficient than in yeast, additional inactivation by a phosphatase does not seem to be required (Berdougo et al., 2008; Surana et al., 1993). Nevertheless, numerous CDK1 substrates have to be dephosphorylated in anaphase. The collected data so far indicate that PP1 or PP2A are taking over the task of bulk CDK1 substrate dephosphorylation, but it is still unclear which phosphatase is responsible for that (Bollen et al., 2009; Queralt and Uhlmann, 2008). PP2A with its subunit B (also called B55) takes part in the regulation of exit from mitosis, as found in a live-cell imaging RNAi screen searching for phosphatases with mitotic exit functions (Schmitz et al., 2010). However, also PP1 was found to act on different sites during exit from mitosis. It is required for kinetochore disassembly, as well as chromosome segregation (Emanuele et al., 2008). The PP1 subunits Repo-Man and PNUTS furthermore target PP1 to chromatin in anaphase and telophase, respectively, where it acts in chromatin decondensation (Landsverk et al., 2005; Trinkle-Mulcahy and Lamond, 2006; Vagnarelli et al., 2006). And finally, PP1 is involved in nuclear envelope formation (Ito et al., 2007; Steen et al., 2000).

1.4.1 Protein phosphatase 1

PP1 is one of the most abundant phosphatases (Wurzenberger and Gerlich, 2011). From yeast to mammals, it is highly conserved and shows > 80 % sequence homology (Gibbons et al., 2007). Besides its function in mitosis, it also regulates the glycogen metabolism, transcription, cell polarity, vesicle trafficking, as well as DNA damage response (Ceulemans and Bollen, 2004). Eukaryotes express three closely related isoforms of PP1 (PP1α, PP1β, and PP1γ), which show similar enzymatic properties and also most PP1 binding proteins bind all three isoforms (Heroes et al., 2013).

PP1 has broad substrate specificity *in vitro* (Bollen et al., 2010; Ceulemans et al., 2002). However, in a cellular context PP1 acts highly specific, because it is bound by PP1-interacting proteins (PIPs) (Heroes et al., 2013). PIPs are available in excess and compete for PP1-binding. This makes PP1 substrate binding flexible, depending on the actual composition of its interactome. So far, close to 200 PIPs were identified, which accurately regulate PP1 localization and activity (Heroes et al., 2013). They act as substrate specifiers, provide additional docking sites for substrates, or prevent recruitment of other substrates (Figure 1.3) (Heroes et al., 2013; Lesage et al., 2011). Furthermore, PP1 may bind more than one PIP at once and some PIPs may bind each other, which highly increases the number of possible holoenzymes. Often, such complexes are trimers, comprising of a second PIP, which acts as an inhibitor, binding the dimer only temporarily to regulate its function (Heroes et al., 2013).

The high combinatorial potential is structurally achieved by a variety of short PP1 docking motifs of 4-8 aa, which bind to small hydrophobic grooves that are present on the PP1 surface (Terrak et al., 2004). Still, PP1-binding is highly specific, as PIPs combine docking motifs, which bind to overlapping, as well as distinct areas on the PP1 surface (Terrak et al., 2004). Of all docking motifs, the RVxF motif is best studied. Proteins containing an RVxF motif bind PP1 at a hydrophobic channel remote from the catalytic site (Wakula et al., 2003). With its high PP1-binding affinity, the motif acts as an anchor, which facilitates binding of additional weaker docking motifs (Wakula et al., 2003). KNL1, for instance, binds PP1 via an RVxF motif. Additionally, it contains a weaker SILK motif, which is not required for binding, but may stabilize it (Liu et al., 2010).

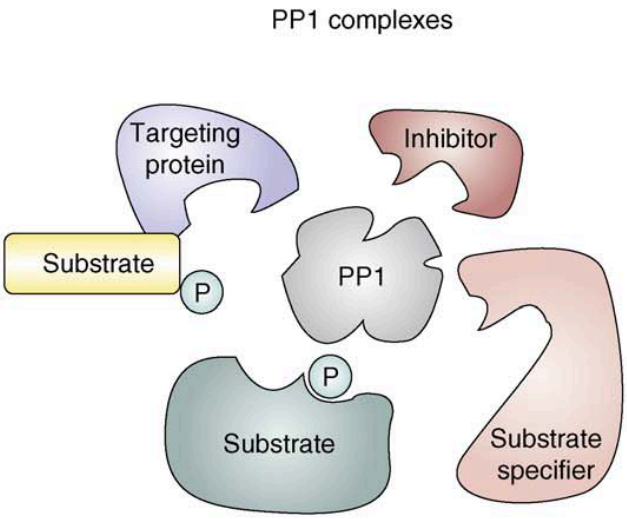

Figure 1.3 PP1-interacting protein functions in PP1 complexes. PP1-interacting proteins (PIPs) function as PP1 inhibitors, substrate specifiers, substrates, or targeting proteins. As PIPs bind to different grooves on the PP1 surface, combined PIP binding is possible (Bollen et al., 2009).

Moreover, PP1 docking motifs are degenerative so that there are also PIPs with weaker RVxF motifs, lacking the anchoring function (Heroes et al., 2013). The actual sequence of the RVxF motif varies from PIP to PIP, thus the residue occurrence among the RVxF-motif containing PIPs corresponds to $[K_{55}R_{34}][K_{28}R_{26}][V_{94}I_{6}]\{FIMYDP\}[F_{83}W_{17}]$ with small numbers indicating the percentage of the residues' occurrence and excluding the residues in curly brackets (Meiselbach et al., 2006). This degeneracy of docking motifs leads to different binding affinities even of proteins, binding to the same groove, which further increases the complexity of PIP binding (Heroes et al., 2013). Additionally, the binding affinity might additionally be altered transiently by posttranslational modifications, like phosphorylation in or near the docking motif (Bollen et al., 2010; Heroes et al., 2013). Such modification was found in the RVxF motif of CENP-E and KNL1. Here, the x is represented by a threonine and serine, respectively, which is phosphorylated by Aurora B to inhibit PP1 binding (Liu et al., 2010; Rosenberg et al., 2011).

PP1 in chromosome congression

A large number of studies aimed to investigate the role of Aurora B in chromosome segregation. In contrast, the role of PP1 in that context only recently became a matter of interest. A fast cellular response upon bipolar kinetochore-microtubule attachment can only be achieved by dynamic dephosphorylation of Aurora B substrates at the kinetochore. This discloses an additional layer of regulation, which also allows the establishment of switch-like responses (Vanoosthuyse and Hardwick, 2009).

First evidence for the importance of dephosphorylation in chromosome congression came from experiments showing that expression of phospho-mimicking mutants of the KMN network members or checkpoint proteins lead to a constitutively activated SAC (Huang and Lee, 2008; Kemmler et al., 2009; Kim et al., 2010). Furthermore, expression of an inactive PP1 in yeast made the SAC hypersensitive, whereas overexpression of PP1 prevented SAC activation (Pinsky et al., 2009). These experiments indicate that PP1 activity is required for SAC silencing. To participate in SAC silencing, PP1 localizes to kinetochores (Trinkle-Mulcahy et al., 2003). Here, its major binding partner is the KMN network protein KNL1, which binds PP1 via its RVxF motif. Mutation of the docking motif prevents PP1 targeting to kinetochores, thereby impeding SAC silencing by PP1 (Rosenberg et al., 2011). Artificial targeting of PP1 to kinetochores by expression of CENP-B-PP1 or KNL1mutant-PP1 rescued the phenotype, whereas expression of KNL1-PP1, which increases the amount of PP1 at kinetochores twofold, is lethal in yeast (Rosenberg et al., 2011). Additionally, it was found that the absence of PP1 from kinetochores causes an increase in Aurora B substrate phosphorylation (Meadows et al., 2011; Rosenberg et al., 2011). Therefore, PP1 localization is necessary for SAC silencing by counteracting Aurora B activity. This could be confirmed in mammals, where Liu and colleagues additionally found that Aurora B prevents PP1 localization to KNL1 by phosphorylating its RVxF motif (Liu et al., 2010). This feedback loop, which makes PP1 localization to kinetochores Aurora B-dependent and thereby tension-dependent, allows a switch-like response leading to fast and definite checkpoint signaling. However, it is unclear yet, which phosphatase is responsible for dephosphorylating KNL1 and thereby allowing PP1 binding (Lesage et al., 2011). Further investigations are also required to elucidate which phospho-sites at the kinetochore are directly targeted by PP1. Only

MCAK was shown to be directly dephosphorylated by PP1 (Moore and Wordeman, 2004). An open question is also whether PP1 is only required for proper chromosome congression and thereby influences the SAC, or whether it also acts directly in silencing the SAC. Data from Vanoosthuyse and colleagues indicate that at least in yeast PP1 acts additionally in SAC silencing independently from its function in chromosome congression (Vanoosthuyse and Hardwick, 2009).

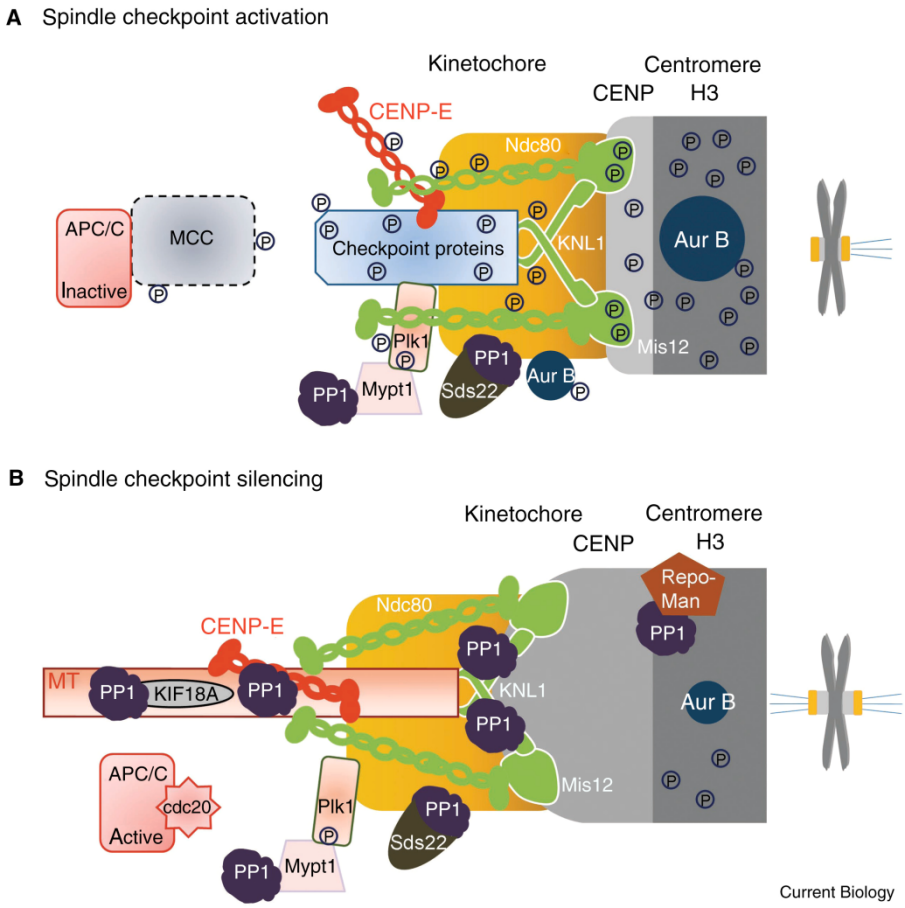

Figure 1.4 Model of PP1 localization and counteraction of Aurora B at the kinetochore. A Tensionless kinetochores are highly phosphorylated by Aurora B. Only SDS22- and Mypt1-mediated PP1 binding to the kinetochore is possible. This destabilizes wrong kinetochore-microtubule attachments. **B** Upon the generation of tension due to amphitelic kinetochore-microtubule attachment, Aurora B gets spatially separated from its kinetochore targets, the consequential dephosphorylation of PP1-binding sites at the kinetochore on CENP-E and KNL1 allows additional binding of PP1 and a switch-like dephosphorylation of Aurora B substrates occurs (Lesage et al., 2011).

Besides KNL1, further PIPs are involved in PP1-targeting in the process of metaphase to anaphase transition. First to mention here is SDS22, which is subject of this thesis and its function will be explained in detail below. Briefly, PP1 and SDS22 binding to kinetochores are thought to depend on each other and SDS22 seems to be required for proper Aurora B counteraction by PP1 (Posch et al., 2010; Wurzenberger et al., 2012). However, the exact function of SDS22 is unclear, as depletion of SDS22 increases Aurora B autophosphorylation but decreases Aurora B substrate phosphorylation (Posch et al., 2010), although contradictory data on this were published recently, which show that Aurora B autophosphorylation is not influenced by SDS22 (Wurzenberger et al., 2012). Though, CENP-E, a motor protein, which tows polar chromosomes towards the cell center, when phosphorylated by Aurora B, targets PP1 to kinetochores. PP1 only binds the unphosphorylated form of CENP-E. However, in contrast to KNL1 phosphorylation, CENP-E phosphorylation was shown to be reversed by PP1 itself, thereby allowing PP1 to regulate its own targeting (Kim et al., 2010; Liu et al., 2010). Another PIP involved in PP1 targeting to kinetochores is the kinesin-8 motor KIF18A (Klp5/6 in yeast), which was shown to be relevant for Aurora B counteraction and SAC silencing in yeast (Meadows et al., 2011). The PP1-Repo-Man holoenzyme regulates Aurora B targeting by dephosphorylating H3T3, which is not only important in anaphase to prevent re-initiation of the SAC, but also during metaphase to constrain Aurora B targeting to the centromeric region of chromatin (Qian et al., 2013; Vagnarelli et al., 2011; Vazquez-Novelle et al., 2010). Additionally, Myosin phosphatase 1 (Mypt1), another PIP involved in SAC silencing, binds PP1 via an N-terminal element (MyPhoNE) to target it to Plk1, whereby Plk1-mediated phosphorylation of SAC components and Aurora B recruitment to unattached kinetochores is inhibited (Hendrickx et al., 2009; Salimian et al., 2011; Yamashiro et al., 2008). And finally, experiments performed by Rieder and colleagues showed that SAC silencing also generates diffusible checkpoint inhibitors, suggesting the possible existence of further cytoplasmic PP1 holoenzymes acting in SAC silencing (Lesage et al., 2011; Rieder et al., 1997). Taken together, there are multiple ways of PP1 targeting to kinetochores, but the relevance and interdependency of PP1-binding to the different PIPs is not clear yet.

1.4.2 The PP1 interacting proteins SDS22 and Inhibitor-3

In yeast, it is well established that PP1 (Glc7 in yeast) counteracts Aurora B (Ipl1 in yeast), as the lethality of a yeast strains carrying the temperature sensitive Ipl1 mutants *ipl1-321, ipl1-1*, or *ipl1-2* is suppressed by the Glc7 mutants *glc7-10, glc7-1*, or *glc7-127* (Chan and Botstein, 1993; Francisco et al., 1994; Peggie et al., 2002; Pinsky et al., 2006). However, Glc7 does not directly regulate Ipl1, since Ipl1 kinase activity is not altered in immunoprecipitates from mitotic *glc7-10* cell extracts in comparison to mitotic Glc7 wild type cell extracts (Pinsky et al., 2006). Additionally, Pinsky and colleagues showed that Glc7 does not counteract Ipl1 by dephosphorylating Ipl1 at the site of autophosphorylation (T260), as *glc7-10* suppresses defects in *ipl1-T260A* cells (Pinsky et al., 2006). Consequently, Glc7 rather counteracts Ipl1 by dephosphorylating its substrates in yeast.

In screens searching for further genes that suppress *ipl1* lethality, mutant genes of the Glc7-interacting proteins Sds22 and Ypi1 (SDS22 and Inhibitor-3 in mammals) were found (Bharucha et al., 2008; Pedelini et al., 2007; Peggie et al., 2002). MacKelvie and colleagues first identified Sds22 as a potential Glc7 regulator in 1995. He found that overexpression of Sds22 suppressed temperature sensitive lethality of *glc7-12* cells, which is caused by an arrest in mitosis (MacKelvie et al., 1995). Additionally, Gosh and Cannon recently showed that cells carrying a heterozygous deletion of Sds22 could suppress defects caused by Glc7 overexpression (Ghosh and Cannon, 2013). Consistent with this, the Sds22 mutants *sds22-5* and *sds22-6* suppress *ipl1-1* and *ipl1-2* phenotypes, indicating Sds22 to be positive regulator of Glc7 in mitosis (Ghosh and Cannon, 2013; Peggie et al., 2002; Robinson et al., 2012). However, in a screen searching for high copy number suppressors of *ipl1-321*, high levels of Sds22 were found to suppress *ipl1-321* defects as well (Pinsky et al., 2006), which suggests Sds22 to be rather a negative regulator of Glc7.

In yeast strains carrying s*ds22-5* or *sds22-6* mutant genes, which are mutated in the leucine-rich repeats (LRRs) whereby Glc7 binding is impeded, Peggie and colleagues furthermore observed chromosome instability, hinting to a chromosome segregation defects, without evidence for a mitotic arrest (Peggie et al., 2002). However, when Pedelini and colleagues revisited the phenotypes in s*ds22-5*, and *sds22-6* strains, they found lethality caused by an anaphase arrest (Pedelini et al., 2007). Both chromosome instability and anaphase arrest indicate that Sds22 mutants

have an inhibitory effect on Ipl1 counteraction by Glc7, which would mean that Sds22 is a positive regulator of Glc7 activity.

Ypi1 was discovered in 2003 as being a Glc7-binding protein (Garcia-Gimeno et al., 2003) and Ypi1 mutant strains were found to suppress the temperature sensitive *ipl1* lethality (Bharucha et al., 2008; Robinson et al., 2012). Furthermore, Ypi1 deletion is lethal due to SAC arrest (Bharucha et al., 2008; Garcia-Gimeno et al., 2003; Pedelini et al., 2007). These findings point to a positive regulation of Glc7 by Ypi1, although Ypi1 overexpression, equal to Sds22 overexpression, rescues *ipl1-321* temperature sensitivity (Pedelini et al., 2007), which hints to an inhibitory role of Ypi1. However, for fulfilling its function, the ability of Ypi1 to bind Glc7 via its RVxF motif is required, as the Glc7-binding deficient mutant *ypi1 V51A/W53A* is not able to rescue the lethality of an Ypi1 deletion (Bharucha et al., 2008). Furthermore, Bharucha and colleagues showed that Ypi1 is important to maintain the nuclear localization of Glc7 and Sds22 during closed mitosis in yeast (Bharucha et al., 2008).

Where the examination of yeast data on the function of Sds22 and Ypi1 cannot unambiguously identify the role of both proteins on Glc7 avtivity, *in vitro* experiments come to a clear result. Sds22, as well as Ypi1 inhibit Glc7 *in vitro*, showing an additive inhibitory capacity when added together to Glc7 (Pedelini et al., 2007). In contrast, human SDS22 and Inhibitor-3 (I3), both inhibit PP1, but don't act synergistically (Lesage et al., 2007). The fact that SDS22 and I3 are able to interact directly in yeast, but lost this capability in mammals, explains this discrepancy (Lesage et al., 2007). Nevertheless, Lesage and colleagues found in a yeast two-hybrid assay the best interaction between human orthologues when all three members of the complex were expressed, suggesting PP1 to build a sandwich complex with SDS22 and I3 (Figure 1.5 A) (Lesage et al., 2007). The trimeric complex was reconstituted *in vitro* and complex formation between SDS22, PP1, and I3 was also confirmed to be specific, as SDS22 was not found in a complex with PP1 and a truncated form of the PIP NIPP1, which has the molecular weight as I3 and also contains an RVxF motif (Lesage et al., 2007). Lesage and colleagues also detected the complex, when immunoprecipitating GFP-tagged I3 or FLAG-tagged SDS22 from COS1 cells (Lesage et al., 2007). However, complex formation was abolished, when the RVxF motif of I3, E192A in SDS22, or W302A in SDS22 was mutated. Next to the degenerative RVxF motif, which consists of the residues

KVEW40-43 in I3, Zhang and colleagues identified a second PP1-binding site in I3, containing the residues 65-77, as found by experiments testing for PP1 activity in the presence of wild type I3, I3 with partial deletions, or I3 with site-directed mutations (Zhang et al., 2008). Furthermore, Zhang and colleagues propose binding of the second PP1 interaction site of I3 directly at or near the active site of PP1, whereby I3 could possibly inhibit the phosphatase (Zhang et al., 2008). Such inhibitory mechanism was also previously proposed for binding of I1, DARP-32, I2, and Mypt1 (Barford et al., 1998; Hurley et al., 2007; Terrak et al., 2004). Additionally, Dephoure and colleagues identified four residues of the second PP1 interaction site to be phosphorylated in mitosis in a screen using a mass spectrometry approach to detect mitotic phospho-sites (Figure 1.5 B) (Dephoure et al., 2008). Thereby the inhibition of PP1 by I3 could possibly be regulated.

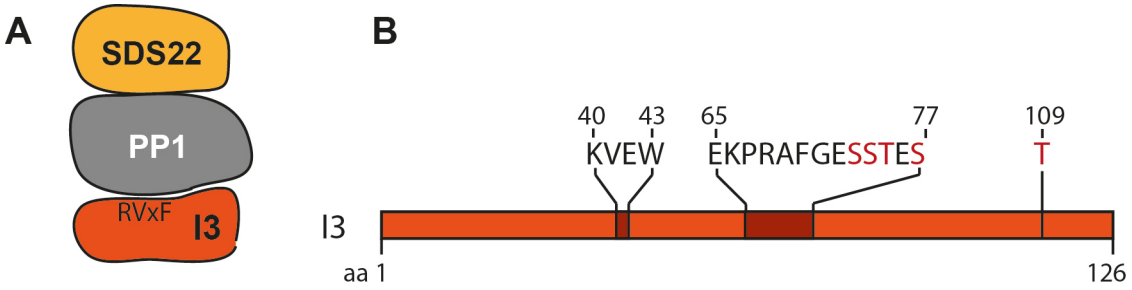

Figure 1.5 Scheme of I3 interaction with PP1. A I3 interacts via its RVxF motif with PP1 and builds a ternary complex with SDS22. **B** Sites for interaction with PP1. Amino acids 40-43 of human I3 correspond to the RVxF motif and amino acids 65-77 correspond to the second PP1 interaction site. Amino acids which were identified to be phosphorylated in mitosis (Dephoure et al., 2008), are marked in red (adapted from Zhang et al., 2008).

I3 and SDS22 both inhibit PP1 reversibly in a substrate dependent way, as they inhibit PP1 phosphatase activity towards Casein and Phosphorylase, but not towards MBP and H2A (Lesage et al., 2007). This could indicate SDS22 and I3 being substrate specifiers. However, additional to the reversible inhibition of PP1, SDS22 was found to convert PP1 slowly and irreversibly into an inactive form, which is sensitive to trypsin digestion, which is an indication for a conformational change of PP1 (Lesage et al., 2007). A similar trypsin-sensitive inactivation of PP1 was found

for I2, where the conformational change may include the loss of a metal ion from the catalytic site (Hurley et al., 2007).

I3, as well as PP1 is found in the nucleus, as well as in nucleoli in mammalian interphase cells, (Huang et al., 2005; Lesage et al., 2007; Trinkle-Mulcahy et al., 2003). Like I3, also SDS22 is found in the nucleus, although it accumulates less in the nucleus, as almost the same concentration of SDS22, is found in the cytoplasm (Lesage et al., 2007). However, it is not clear if that difference has relevance for the function of the trimeric complex in mammalian mitosis, as the nuclear membrane breaks down at mitotic entry.

The role of I3 during mammalian mitosis is still unclear, whereas the function of SDS22 has been evaluated by Swedlow's group and Gerlich's group. Both find that depletion of SDS22 causes a delay in progression through mitosis, which is accompanied by chromosome congression defects, as well as anaphase defects and Gerlich's group additionally observed paused segregation of individual chromatids (Posch et al., 2010; Wurzenberger et al., 2012). Both groups also agree on SDS22 counteracting Aurora B, but disagree on how SDS22 counteracts Aurora B. In the background of SDS22 depletion Wurzenberger and colleagues find an increase in Aurora B substrate phosphorylation (Dsn1 pT100) in metaphase and anaphase cells, but no effect on Aurora B activity, monitored as the level of autophosphorylation at T232, suggesting SDS22-mediated PP1 counteracts Aurora B solely by dephosphorylating its substrates (Wurzenberger et al., 2012). In contrast, Posch and colleagues detect an increase in Aurora B activity in metaphase cells upon silencing of SDS22, but a decrease in Aurora B substrate phosphorylation (MCAK pS92, Hec1 pS55, and CENP-A pS7) (Posch et al., 2010). As a consequence, Posch and colleagues propose SDS22 to mediate Aurora B dephosphorylation by PP1. They furthermore suggest that a different PP1 holoenzyme or a different phosphatase may dephosphorylate Aurora B substrates (Posch et al., 2010). Posch and colleagues additionally show that SDS22 localizes (interdependently with all PP1 isoforms) to kinetochores from prometaphase until telophase (Ceulemans et al., 2002; Posch et al., 2010). However, three other groups failed to detect SDS22 at kinetochores (Liu et al., 2010) (Gerlich and Bollen, personal communication).

1.5 The AAA ATPase p97

p97 (also called VCP, and Cdc48 in yeast) belongs to the AAA (ATPases associated with diverse cellular activities) protein family and was first identified in yeast, where *cdc48-1* was found to cause defects in cell cycle progression (Moir et al., 1982). From its first identification as a cell cycle regulator, until now many other functions of p97 have been found. Today p97 is known as a crucial regulator being involved in protein degradation, membrane fusion, DNA replication, gene expression, DNA damage response, apoptosis and autophagy (Jentsch and Rumpf, 2007) (Dantuma and Hoppe, 2012; Dargemont and Ossareh-Nazari, 2012) (Meyer et al., 2012; Ye, 2006).

p97 contains two ATPase domains D1 and D2, which comprise of a Walker A and a Walker B motif for ATP binding and hydrolysis (Ogura and Wilkinson 2001). Six p97 proteins assemble in a hexameric, barrel-like structure with a central pore (DeLaBarre and Brunger, 2005; Ogura and Wilkinson, 2001; Pye et al., 2006; Wang et al., 2004). p97 hexamers convert the energy of ATP hydrolysis into mechanical force, for instance, to extract substrates from binding partners or cellular surfaces (Meyer et al., 2012). During ATP hydrolysis, the D2 domain undergoes major structural changes, suggesting the D2 domain to be required for ATPase-dependent functions of p97 (DeLaBarre and Brunger, 2005; Erzberger and Berger, 2006; Pye et al., 2006; Wang et al., 2004). Besides the ATPase domains, p97 contains an N-domain and a C-terminal tail, where a large number of cofactors bind to regulate p97 activity and localization. As p97 regulates ubiquitin-dependent and SUMO-dependent processes, several cofactors have ubiquitin-binding affinity (Bergink et al., 2013; Buchberger, 2013; Dai and Li, 2001; Meyer et al., 2002; Wang et al., 2004). Cofactor binding is mediated by a variety of p97-binding motifs, as there are the UBX (ubiquitin regulatory X) domain, the UBX-like element, the SHP box (also called BS1 , binding site 1), the VBM (VCP-binding motif), the PUB (PNGase/UBA or UBX domain), and the VIM (VCP-interacting motif) (Decottignies et al., 2004; Madsen et al., 2009; Schuberth et al., 2004). Some of the cofactors bind p97 concurrently, whereas others bind mutual exclusively (Bruderer et al., 2004; Schuberth and Buchberger, 2008). Based on that finding a hierarchical model was proposed (Hanzelmann et al., 2011; Jentsch and Rumpf, 2007; Wang et al., 2004; Yeung et al., 2008), differentiating between major substrate-recruiting cofactors determining the

cellular pathway by mutually exclusive binding, additional substrate-recruiting cofactors improving substrate binding or providing additional spatial regulation, and substrate-processing cofactors, like ubiquitin-ligases, ubiquitin-chain editing factors, and deubiquitinating enzymes, bringing in additional enzymatic activities (Alexandru et al., 2008; Ballar et al., 2006; Ernst et al., 2009; Kuhlbrodt et al., 2011). This tool kit regulates the many different functions of p97. Besides the extraction of substrates from chromatin, ER, mitochondrial membranes or binding partners, p97 also segregates substrates during endosomal sorting, may assist the proteasome by unfolding substrates and is thought to disassemble aggregates (Beskow et al., 2009; Heo et al., 2010; Kobayashi et al., 2007; Meusser et al., 2005; Meyer et al., 2012; Ramadan et al., 2007; Stolz et al., 2011; Wilcox and Laney, 2009; Xu et al., 2011).

Best understood is the function of p97 in ER-associated degradation (ERAD). Misfolded proteins are recognized, labeled with ubiquitin chains, and transported to the proteasome for degradation. Thereby, p97 clears the ER from these proteins. Cofactor-binding of p97 tightly associates it with the ER membrane. Here, the attached E3 ligases gp78 and Ufd2 ubiquitinate misfolded proteins and p97 extracts them from the ER membrane (Richly et al., 2005; Vembar and Brodsky, 2008; Wolf and Stolz, 2012; Ye et al., 2001; Ye et al., 2004). However, not only proteasomal degradation is regulated by p97, but also lysosomal degradation via endosomal sorting and autophagy is p97-mediated (Chou et al., 2011; Ju and Weihl, 2010; Kirchner et al., 2013; Tresse et al., 2010). Together with its cofactors Npl4 and Ufd1, p97 furthermore acts in the DNA damage response, where it is required for CDT1 degradation in S-Phase at the replication checkpoint, as well as for CDC25 degradation at the G2-M checkpoint (Franz et al., 2011; Meerang et al., 2011; Mouysset et al., 2008; Raman et al., 2011; Riemer et al., 2014).

During mitosis in mammalian cells, p97 counteracts Aurora A and Aurora B with the help of p37/p47 and Ufd1-Npl4, respectively. The p97-p37/p47 complex antagonizes Aurora A localization to centrosomes, thereby inhibiting centrosome maturation in mammalian cells and *C. elegans* embryos (Kress et al., 2013). In parallel, the p97-Ufd1-Npl4 complex extracts ubiquitinated Aurora B from chromatin to limit Aurora B localization to the centromeric region (Dobrynin et al., 2011). Depletion of Ufd1-Npl4 from mammalian cells increases of Aurora B protein level and activity on

prometaphase and metaphase chromatin, and causes chromosomal misalignment, as well as delay in progression through mitosis (Dobrynin et al., 2011).

1.5.1 The p47 subfamily and its role in mitosis

All members of the p47 subfamily of p97-binding proteins contain a UBX domain and a SHP box (also called BS1, binding site 1) for p97 binding, and a SEP (Shp1, eye-closed, p47) domain which triggers trimerization (Beuron et al., 2006; Yuan et al., 2004). Additionally, the mammalian p47 and most of its eukaryotic orthologues, like Shp1 in *S. cereviseae*, UBXN-2 in *C. elegans*, and Ubx3 in *S. pombe*, contain a UBA domain for ubiquitin binding (Meyer et al., 2002; Schuberth and Buchberger, 2008; Yuan et al., 2004). Interestingly, besides p47, mammals additionally express three orthologues lacking the UBA domain, namely p37, UBXD4, and the more distantly related Socius (also called UBXD5) (Rezvani et al., 2009; Schuberth and Buchberger, 2008; Uchiyama et al., 2006). The function of Socius is unclear and only little is known about UBXD4, whereas the function of p47 and p37 is already better understood (Rezvani et al., 2009; Schuberth and Buchberger, 2008).

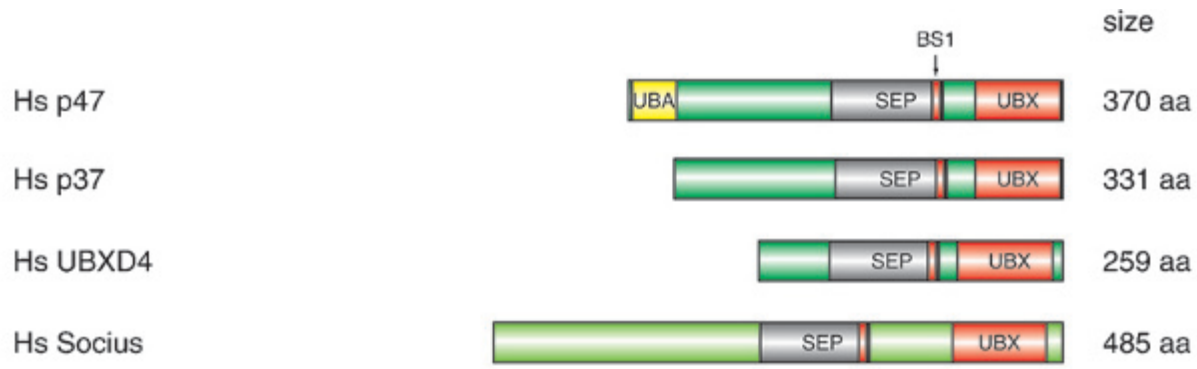

Figure 1.6 The p47 subfamily of p97 cofactors. Subfamilies were termed according to their sequence homologies outside the UBX domain (red) as identified by systematic PSI-BLAST searches. All p47 subfamily proteins comprise of a SEP domain (grey) with an adjacent C-terminal binding site 1 (BS1, red) for p97 binding. p47 is the only human orthologue with the ability to bind ubiquitin, due to its UBA domain (yellow) (Schuberth and Buchberger, 2008).

First identified was the yeast homologue of p47, Shp1 (Suppressor of High-copy PP1), in a genetic screen searching for suppressors of the otherwise lethal phenotype caused by overexpression of Glc7 (Zhang 1995). Zhang and colleagues suggested Shp1 to be a positive regulator of Glc7, as the Shp1 mutant rescued Glc7 overexpression (Zhang et al., 1995). 15 years later, Cheng and Chen further investigated the function of Shp1, because they found it in a screen searching for p97 (Cdc48) cofactors in yeast, which show the same mitotic defects as the temperature sensitive mutant *cdc48-3*. Inducible deletion of Shp1 caused a metaphase arrest due to activation of the SAC, chromosomal alignment defects, and spindle defects, whereas cells expressing the temperature sensitive mutants *ufd1-2* or *npl4-1* had no clear cell cycle defects (Cheng and Chen, 2010). Similar defects were found in cells expressing the p97-binding deficient mutants *shp1-a1* and *shp1-b1*, pointing out that the function of Shp1 in mitosis is p97 dependent (Bohm and Buchberger, 2013). Additionally, Böhm and Buchberger recently showed, that Shp1 does not only genetically but also physically interact with Glc7 (Bohm and Buchberger, 2013). Furthermore they found Shp1 to counteract Ipl1, as deletion of Shp1 partially rescued the lethality of temperature sensitive *ipl1-321* cells (Bohm and Buchberger, 2013). The role of Cdc48-Shp1 in Glc7-mediated Ipl1 counteraction was further confirmed, by Robinson and colleagues found two Shp1 mutants (*shp1-FS99*, *shp1-FS105*) in a screen searching for *ipl1-2* suppressors (Robinson et al., 2012).

Recently mammalian p47/p37 and the *C. elegans* orthologue UBXN-2 have been implicated in mitosis. Kress et al found that p47, p37, and UBXN-2 localize to centrosomes at the beginning of mitosis and that depletion of UBXN-2 in *C. elegans* embryos or p37 together with p47 in mammalian cells cause spindle orientation defects, as well as delayed centrosome separation (Kress et al., 2013). Though, cells depleted for p47 alone had no spindle defects. They furthermore found that depletion of p37 and p47, or UBXN-2 increased Aurora A protein level and activity at prophase centrosomes, while total cellular Aurora A protein level stayed unchanged, indicating a function of p37/p47 in segregation rather than in degradation of Aurora A (Kress et al., 2013).

Additionally, a mass spectrometry screen searching for p97 interacting proteins, which was performed in our laboratory, indicated that mammalian p97 interacts with PP1 and its subunits SDS22 and I3 (PhD thesis D. Ritz). This interaction was

confirmed by co-immunoprecipitation experiments. Bremer found endogenous PP1 and SDS22 to co-immunoprecipitate with p97-Strep, and importantly also with HA-p47 but not with UBXD1-HA, HA-Npl4, or Ufd1-HA (S. Bremer unpublished data). SDS22, PP1, and I3, as well coprecipitated with GFP-p37 (J. Seiler, unpublished data). This physical interaction between p97-p47/p37 and SDS22-PP1-I3 could for instance reveal a functional link between SDS22-PP1-I3 and Aurora A, or might hint to an involvement of p97-p47 in the Aurora B and PP1 interplay. Enzymatically, p97-p47/p37 could act on the, potentially ubiquitinated, SDS22-PP1-I3 complex, as well as PP1-SDS22-I3 could act on p97-p47/p37 by dephosphorylating complex members. Both scenarios are possible, especially as Glc7 was found to be ubiquitinated in two independent screens (Peng et al., 2003; Starita et al., 2012), and as p47 and p37 were found to phosphorylated in mitosis (Dephoure et al., 2008; Uchiyama et al., 2003).

1.6 The aim of the thesis

Chromosome segregation is a fundamental process during mitosis. Tension-dependent phosphorylation of kinetochore proteins by the kinase Aurora B assures bipolar attachment of all chromosomes to the mitotic spindle before onset of anaphase (Lampson and Cheeseman, 2011). It is established that PP1 is the counteracting phosphatase, which is thought to mediate dephosphorylation of Aurora B and its substrates at the kinetochore, when tension arises between sister kinetochores (Lesage et al., 2011). A dynamically regulated switch-like dephosphorylation of bipolar attached kinetochores is achieved by the complex interplay between Aurora B and PP1. SDS22 was found to be relevant for PP1 function at the kinetochore. However, the function of SDS22 at the kinetochore is highly controversial, as two research groups published contradictory data on SDS22 localization as well as on the function of SDS22-regulated PP1. Furthermore, in yeast, I3 is required for proper regulation of the Aurora homologue Ipl1 by PP1 (Bharucha et al., 2008; Robinson et al., 2012). Although I3 is known to build a ternary complex with PP1-SDS22 in mammals (Lesage et al., 2007), its function in mammalian cells is still unclear.

Therefore, this study aimed to unravel the controversy on the role of SDS22 at the kinetochore, as well as to reveal the role of I3 as member of the ternary complex I3-PP1-SDS22 in mammalian cells, To carefully clarify the roles of SDS22 and I3, we made use of stable cell lines expressing SDS22, I3, or PP1 near endogenous levels to avoid disturbance of the system by overexpression. Furthermore, we applied siRNA-mediated depletion, as well as transient overexpression to consciously perturb the system. These tools are to be applied to examine the localization of SDS22 and I3, as well as the mitotic defects caused by depletion or overexpression of the proteins. In a next step, we aimed to investigate the regulation of PP1 localization and activity by SDS22 and I3, to evaluate the impact of SDS22 and I3 on the PP1-mediated counteraction of Aurora B activity.

The data obtained from this work shall then provide a basis for further studies revealing the functional relationship between I3-PP1-SDS22 and p97-p47/p37.

2 Material and Methods

2.1 Cloning

Polymerase chain reactions (PCRs) were performed with Pfu Ultra II DNA-polymerase (Aligent Technologies) or Phusion High-Fidelity DNA Polymerase (Thermo Scientific) according to the manufacturer's protocols. Restriction digestions, oligonucleotide dephosphorylation reactions and DNA ligations were done with enzymes from New England Biolabs according to the manufacturer's protocol. The QIAquick Gel Extraction Kit (Qiagen) was used for DNA extraction from agarose gels and the NucleoSpin® Gel and PCR Clean-up kit (Macherey-Nagel) was used for purification of DNA amplified with PCR.

Transformation of *E. coli* DH5-α with plasmid DNA was performed according to standard protocol. Amplified plasmid DNA was purified with the NucleoSpin® Plasmid kit and the NucleoBond® Xtra Maxi kit from Macherey-Nagel.

2.1.1 Generation of plasmid constructs

I3 constructs

peGFP.C1 I3 (clone 450) was generated by Micheal Welti. N-terminal GFP was exchanged for mcherry via digestion with AgeI and EcoRI to get *pmcherry.C1 I3* (clone 634). *pcDNA5 FRT/TO GFP-I3* (clone 606) was obtained by transferring GFP-I3 via HindIII and BamHI from *peGFP.C1 I3* into an empty *pcDNA5 FRT/TO* vector. *pcDNA5 FRT/TO GFP-I3 V41A/W43A* (clone 607) was generated from *pcDNA5 FRT/TO GFP-I3* by site directed mutagenesis with the primers 458 and 459. Three silent point mutations were introduced into *pmcherry.C1 I3* to generate an I3 construct, which is resistant to the siRNA I3 S2. The construct *pmcherry.C1 I3 res* (clone 645) was made by site-directed mutagenesis with the primers 896 and 897. I3 phospho-mutants *pcDNA5 FRT/TO GFP-I3 T105A* (clone 721) and *pcDNA5 FRT/TO GFP-I3 T105E* (clone 722) were generated via site-directed mutagenesis with the

primer pairs 960/961 and 962/963, respectively. I3 phospho-mutants *pcDNA5 FRT/TO GFP-I3 TTTET72AAAEA* (clone 723) and *pcDNA5 FRT/TO GFP-I3 TTTET72EEEEE* (clone 724) were generated via site-directed mutagenesis with the primer pairs 964/965 and 966/967, respectively.

Table 2.1 Oligonucleotides used for cloning.

accession number	Oligonucleotide sequence
458	GCCAGAGAAAAAGGCAGAAGCGACAAGTGACACTG
459	CAGTGTCACTTGTCGCTTCTGCCTTTTTCTCTGGC
896	GCTCATCCAAATGCTGTTGTATCTACGAGAAACCTCGGG
897	CCCGAGGTTTCTCGTAGATACAACAGCATTTGGATGAGC
898	CAACTACAGATGCTAGCGCTGGGATCTAACCGC
899	GCGGTTAGATCCCAGCGCTAGCATCTGTAGTTG
900	GAGCTGCAAGAGTTCGCGATGAACGACAATCTCC
901	GGAGATTGTCGTTCATCGCGAACTCTTGCAGCTC
960	GACCGACCCCCACCGCCCCTCCCCAGCC
961	GGCTGGGGAGGGGCGGTGGGGGTCGGTC
962	GACCGACCCCCACCGAGCCTCCCCAGCCTCC
963	GGAGGCTGGGGAGGCTCGGTGGGGGTCGGTC
964	GGGCCTTTGGCGAGGCCGCCGCGGAAGCTGATGAGGAGGAAGAAGAG
965	CTCTTCTTCCTCCTCATCAGCTTCCGCGGCGGCCTCGCCAAAGGCCC
966	GGGCCTTTGGCGAGGAGGAGGAGGAAGAAGATGAGGAGGAAGAAGAGGG
967	CCCTCTTCTTCCTCCTCATCTTCTTCCTCCTCCTCCTCGCCAAAGGCCC

SDS22 constructs

peGFP.C1 SDS22 (clone 605) was a kind gift from Mathieu Bollen (Lesage et al., 2007). N-terminal GFP was exchanged for mcherry via digestion with BsrGI and NheI to get *pmcherry.C1 SDS22 (clone 635)*. Furthermore, two PP1-binding deficient SDS22 mutants were generated. Glutamic acid at position 192 was mutated to

alanine by a site-directed mutagenesis with the primers 898 and 899 (*pmcherry.C1 SDS22 E192A*, clone 646) and tryptophan at position 302 was mutated to alanine in the same way with the primers 900 and 901 (*pmcherry.C1 SDS22 W302A*, clone 647).

NIPP1 constructs

peGFP.N1 NIPP1 (clone 637) was a kind gift from Mathieu Bollen (Jagiello et al., 2000). The C-terminal GFP in *peGFP.N1 NIPP1* was exchanged for RFP via digestion with ApaI and NotI to obtain *pRFP.N1 NIPP1 (clone 644)*.

Anti-GFP nanobody construct

The bacterial expression vector containing the sequence for His-tagged anti-GFP nanobody (clone 765) was a kind gift from Mathieu Bollen.

2.2 Generation and maintenance of cell lines

All cells were grown in DMEM (Sigma) supplemented with 10 % FCS (Gibco) and 1 % Penicillin/Streptamycin (PAA) in an incubator with 5 % CO_2 and at 37 °C. The HeLa cell line stably expressing SDS22-GFP from a BAC was a kind gift from Antony Hyman (Poser et al., 2008). Its medium contained additionally 400 µg/ml G418 (PAA). Medium for HeLa cells stably expressing GFP-PP1γ was supplemented with 200 µg/ml G418. This cell line was a kind gift from Laura Trinkle-Mulcahy (Trinkle-Mulcahy et al., 2003). HeLa cells stably expressing H2B-RFP together with IBB-GFP or H2B-mCherry alone were kind gift from Daniel Gerlich. The HeLa cell line expressing H2B-mCherry was used to generate a stable cell line additionally expressing I3 by transfecting the cells with *peGFP.C1 I3*. HeLa H2B-RFP IBB-GFP and HeLa H2B-mCherry GFP-I3 were maintained in medium containing 500 µg/ml G418 and 0.5 µg/ml Puromycin (PAA).HeLa cells expressing GFP were a kind gift from Andrea Musacchio and were maintained as published (Krenn et al., 2012).

2.3 Transfections

For transfection with DNA plasmids the JetPEI transfection reagent (Polyplus) was used according to the manufacturer's protocol, but with only one fourth of the

recommended amount of DNA. The medium was changed 6 h after transfection and the cells were grown for 48 h before analysis.

The manufacturer's protocol for reverse transfection with Lipfectamine RNAiMAX (life technologies^{TM}) was used for RNAi experiments. After 6 h the medium was changed. The oligonucleotides were used in a final concentration of 10 nM. As a control oligonucleotides silencing Luciferase were used. Cells were depleted for 48 h before analysis.

For experiments involving RNAi silencing and DNA transfection, first a reverse RNAi transfection was done and after 24h DNA was transfected. The cells were grown for additional 48 h before analysis.

KNL1 silencing experiments were performed with 60 nM siRNA (as a mixture of the oligonucleotides KNL1 S1, KNL1 S2, and KNL1 S3) for 24 h. For double knockdown experiments of I3 and KNL1, I3 siRNA was reverse transfected and after 24h, additionally KNL1 siRNA was transfected. The cells were grown for additional 24h before analysis.

Table 2.2 Sequences of oligonucleotides used in RNAi experiments.

Target gene	Name	Sequence	Source
Luciferase	Luc	CGUACGCGGAAUACUUCGATT	Microsynth
I3	I3 S1	GUAGAAUGGACAAGUGACA	designed by S. Bremer
	I3 S2	CUGCUGTAUUUAUGAGAAA	designed by S. Bremer
NIPP1	NIPP1 S1	GGAACCTCACAAGCCTCAGCAAATT	stealth RNA from Invitrogen
SDS22	SDS22 S2	AGAGTTCTGGATGAACGACAA	Wurzenberger et al., 2012
p37	p37 S2	CTCCAGAAGAGGAGGATAATT	Uchiyama et al., 2006
p47	p47 S1	AGCCAGCUCUUCCAUCUUATT	Dobrynin et al., 2011
KNL1	KNL1 S1	CACCCAGUGUCAUACAGCCAAUAUU	Krenn et al., 2013
	KNL1 S2	UCUACUGUGGUGGAGUUCUUGAUAA	Krenn et al., 2013
	KNL1 S3	CCCUCUGGAGGAAUGGUCUAAUAAU	Krenn et al., 2013

2.4 Immunofluorescence staining

For immunofluorescence experiments with HeLa cells, cells were seeded on 18 mm cover slips in 12 well culture dishes. For fixation, the cells were washed once with PBS and then incubated in 4 % paraformaldehyde (PFA) in PBS for 15 min followed by washing the cells again once with PBS for 5 min. To permeabilize the cells, they were incubated in 0.1 % Triton X-100 in PBS for 10 minutes. After washing the cells once with PBS, they were blocked in 3 % BSA in PBS for at 30-60 min. Primary antibody dilutions were prepared in 3 % BSA in PBS. The cover slips with cells were placed upside-down onto a drop of 60 µl antibody solution on Parafilm in a humid chamber. After incubation for 1 h the cells were washed three times with PBS for 5 min. Then, the cells were again incubated in the humid chamber in secondary antibody solution (in 3 % BSA in PBS) for 1 h in the dark. Afterwards, the cells were washed three times in PBS for 5 min. Finally, the cells were mounted on glass slides using Mowiol, which contained 0.5 µg/ml DAPI.

For immunofluorescence experiments with HeLa SDS22-GFP cells, cells were seeded in 8-well µ-slides (ibidi) and processed as HeLa cells, but without mounting in Mowiol.

Table 2.3 Antibodies used for immunofluorescence experiments.

Antibody	Species	Dilution	Company
Aurora B	mouse	1:500	BD
Aurora B pT232	rabbit	1:1000	Rockland
CREST	human	1:400	Antibodies Inc.
mouse IgG Alexa 488	goat	1:600	Invitrogen
mouse IgG Alexa 568	goat	1:600	Invitrogen
rabbit IgG Alexa 488	goat	1:600	Invitrogen
rabbit IgG Alexa 568	goat	1:600	Invitrogen
human IgG Alexa 594	goat	1:600	Invitrogen

2.5 Fluorescence imaging

For live cell imaging cells were grown in 8 well µ-slides (ibidi). 30 min before imaging the medium was changed to imaging medium (DMEM without phenol red from Gibco supplemented with 10 % FCS) and cells were supplied with 5 % CO_2 at 37°C during imaging. HeLa GFP-PP1γ cells were grown in 8 well µ-slides and fixed for imaging with 4 % PFA in PBS containing 0.1 % Triton X-100 for 15 min. Then, the cells were washed once with PBS and incubated for at least 30 min in PBS supplemented with 0.2 µg/ml DAPI. HeLa SDS22-GFP cells were treated for imaging like HeLa GFP-PP1γ, but without permeabilizing.

Confocal images were taken at a Nikon Eclipse Ti microscope with a Yokogawa CSU X-1 spinning disc unit and an Andor iXon X3 EMCCD camera. Images were acquired either with a 100x/1.49 NA Apo TIRF oil-immersion objective or a 20x/0.75 NA Plan Apo air objective.

For time lapse microscopy HeLa H2B-RFP IBB-GFP were imaged with the 20x/0.75 air objective every 45 sec at multiple positions for 12.5 h.

2.6 Cell extracts

Cell extracts were made from cells, grown in 6 well plates. All steps were done on ice and with ice-cold buffers. First cells were washed once with PBS. Then the cells were scraped in 50 µl extraction buffer (150 mM KCl, 50 mM Tris pH 7.4, 5mM $MgCl_2$, 5 % glycerol, 1 % Triton X-100, 2 mM β-Mercaptoethanol supplemented with Roche complete EDTA-free protease inhibitors and Roche PhosSTOP phosphatase inhibitor) and incubated for 20 min. The cell extracts were centrifuged at 13,000 rpm for 20 min. Then the supernatant was collected and the protein concentration was measured with a bicinchoninic acid assay (Interchim).

2.7 Immunoprecipitations

For immunoprecipitations 500-1000 µg of cell extracts were filled up to a volume of 250 µl with IP buffer (extraction buffer supplemented with 1 µg/ml BSA). Then the lysates were cleared again by centrifuging at 13,000 rpm for 10 min at 4 °C. In the

meanwhile, nanobody-coupled Sepharose beads specific for GFP were washed three times with 300 µl IP buffer. After centrifugation, input samples (2-5%) were taken and 20 µl beads were added to the samples. The samples were again shaked for 1 h at 4 °C. After centrifugation at 1000 rpm for 1 min at 4 °C a flow through sample was taken (2-5 %) and then the beads were washed three times with 300 µl IP buffer. Finally, the proteins were eluted from the beads by boiling the samples for 5 min in SDS sample buffer.

GFP-nanobodies were expressed in *E.coli* BL21 and purified with Ni-NTA Superflow resin beads (Qiagen). Affinity-purified nanobodies were coupled to NHS-activated Sepharose 4 Fast Flow (GE) (2 mg per ml bead slurry).

2.8 SDS PAGE and Western blotting

Standard protocols were used for SDS PAGE. The SDS running buffer contained 200 mM glycine, 25 mM Tris-Hcl and 0.1 % SDS and gels were run at 20 mA. Western blotting was performed in semi-dry Trans-Blot® SD transfer cells (Bio-Rad). As blotting buffer, SDS running buffer supplemented with 20 % methanol was used. SDS gels were blotted on a nitrocellulose membrane (Hybond-C super, Amersham Biosciences ®) at a current of 120 mA for 45-60 min. Afterwards the membrane was blocked in 10 % nonfat dried milk powder in PBS-T (PBS supplemented with 0.05 % Tween® 20 (AppliChem)) for 1 h at room temperature. After washing with PBS-T, the membranes were incubated in primary antibody diluted in 3 % BSA in PBS-T over night at 4 °C. The membranes were washed three times with PBS-T for 10 minutes and then incubated in secondary antibody diluted in 3 % BSA in PBS-T for 1 h at room temperature. Afterwards the membranes were washed again three times with PBS-T for 10 min and incubated 2 min with SuperSignal® West Pico Chemoluminescent Substrate (Thermo Scientific) or Super Signal® West Femto Maximum Intensity Substrate (Thermo Scientific) for developing the membranes on X-ray films (FUJIFILM).

Antibodies specific for phospho-sites were diluted in TBS-T (TBS supplemented with 0.05 % Tween® 20 (AppliChem)). Anti-Histone 3 pS10 and anti-dsRED antibodies were diluted in 5 % nonfat dried milk powder in TBS-T and PBS-T, respectively.

Table 2.4 Antibodies used for Western blotting experiments.

Antibody	Species	Dilution	Source
actin	goat	1:1000	Santa Cruz
Cyclin E	mouse	1:500	Santa Cruz
dsRED	rabbit	1:1000	Clontech
GAPDH	mouse	1:10000	Sigma-Aldrich
GFP	mouse	1:1000	Roche
Histone 3 pS10	rabbit	1:4000	Upstate
HSC70	mouse	1:10000	Santa Cruz
I3	rabbit	1:500	Eurogentec, raised against aa115-126, DPSQPPPGPMQH; by J. Seiler
NIPP1	rabbit	1:500	Sigma-Aldrich
PP1γ	goat	1:1000	Santa Cruz
PP1 pT320	rabbit	1:1000	Cell Signaling
SDS22	goat	1:500	Santa Cruz
p37	rabbit	1:100	Kress et al., 2013
p47	rabbit	1:5000	Dobrynin et al., 2011
p97	rabbit	1:2000	Meyer et al., 2000
mouse IgG HRP	goat	1:10000	Bio-Rad
rabbit IgG HRP	goat	1:10000	Bio-Rad
goat IgG HRP	mouse	1:10000	Bio-Rad

2.9 Quantification and statistics

Fluorescence intensities were quantified using Cell Profiler. Therefore, the DAPI image was used to build a mask for measuring only the fluorescence signal on

chromatin. Significance was calculated with Sigma Plot Software (Systat) using a Mann-Whitney *U* test. Box plots show medians, lower and upper quartiles (line and box), 10^{th} and 90^{th} percentiles (whiskers), and outliers (●).

3 Results

3.1 Mitotic phenotypes upon perturbation of I3 or SDS22

A series of publications showed that SDS22 is required for proper progression through mitosis (Bharucha et al., 2008; Pinsky et al., 2006; Robinson et al., 2012). In human cells, silencing of SDS22 was shown to cause mitotic defects as chromosomal misalignment, chromosomal bridges and lagging chromosomes in anaphase, pauses in pole ward segregation and delay in mitotic progression (Posch et al., 2010; Wurzenberger et al., 2012). Although SDS22 is also known to build a trimeric complex with PP1 and I3 (Lesage et al., 2007), the role of I3 in mammalian cells remains unclear. Therefore we started our research on the ternary complex with confirming the data on SDS22 and with elucidating if I3 silencing causes mitotic defects. As readouts for mitotic defects we tested for chromosomal alignment defects and for defects in mitotic progression from nuclear envelope breakdown till anaphase onset. Additionally, we tested if overexpression of SDS22 or I3 has an effect on chromosomal alignment.

3.1.1 I3 and SDS22 are required for faithful chromosome segregation

To clarify, whether SDS22 or I3 silencing causes chromosomal congression defects, we treated HeLa cells with siRNAs targeting SDS22 or I3 for 48h. siRNA specific for Luciferase (Luc), which is absent in mammalian cells, and for NIPP1, which is an RVXF-motif containing PIP without known function in mitosis (Minnebo et al., 2013; Nuytten et al., 2008), were used as negative controls. First, the knockdown efficiency was determined by analyzing lysates of siRNA treated cells by Western blotting. SDS22, I3, and NIPP1 protein levels were monitored by applying antibodies, which specifically detect the respective proteins. Furthermore, HSC70 was stained as a loading control. All three proteins were specifically depleted from the samples treated for the respective siRNA, thus the knockdown is efficient and specific and the experimental setup can be used to explore mitotic phenotypes (Figure 3.1 A).

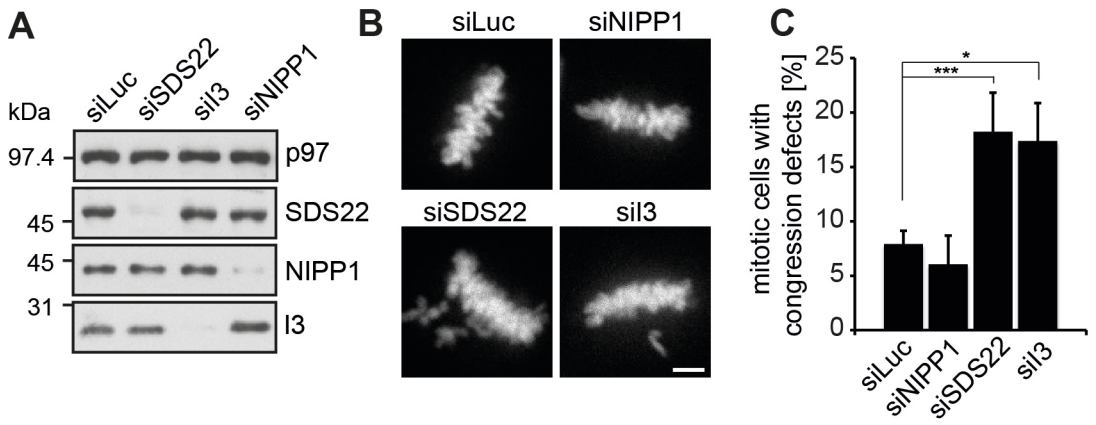

Figure 3.1 siRNA mediated depletion of SDS22 or I3 causes chromosomal alignment defects in mitosis. A HeLa cells were treated with the indicated siRNAs for 48 h, then lysates were prepared and analyzed by Western blotting with respective antibodies. HSC70 served a loading control. **B** Representative confocal micrographs of cells depleted as in **A** after fixation and staining with DAPI. Scale bar, 5 µm. **C** Quantification of **B**. Percentage of mitotic cells with misaligned chromosomes. Data from 3 independent experiments with n ≥ 60 cells per condition. Error bars show the standard deviation. P-values were calculated using a Mann-Whitney-*U* test (***, p ≤ 0.001; *, p ≤ 0.05).

To analyze the chromosomal alignment, cells depleted for Luc, SDS22, I3, or NIPP1 were fixed with paraformaldehyde and stained with DAPI to visualize the chromatin. Afterwards, the samples were analyzed by light microscopy. A metaphase cell was scored as having congression defects, when at least one chromosome was visibly separated from an identifiable metaphase plate. Crucially, apart from SDS22 depletion, also I3 depletion led to an increased number of cells with congression defects, as shown in example images of aligned (siLuc and siNIPP1), and misaligned metaphase cells (siSDS22 and siI3) (Figure 3.1 B). 60 cells in metaphase were counted in three independent experiments to quantify the relative number of cells with congression defects in the different depletion backgrounds. A small number Luc and NIPP1 siRNA-treated cells show alignment defects in metaphase (Figure 3.1 C), as it is typical for HeLa cells, being a cancer cell line with high variation in chromosome number. Silencing of SDS22 and I3 caused misalignment in 18 % and

17 % of all metaphase cells, respectively. Therefore, not only SDS22, but also I3 is necessary for proper chromosome alignment.

3.1.2 Overexpression of SDS22, I3, or NIPP1 cause metaphase plate alignment defects

To further characterize the congression defect, we asked, whether not only silencing but also overexpression of SDS22, or I3 would have an effect on chromosomal alignment. Such information would allow us to reason that also the expression level of SDS22 and I3 is relevant for correct mitosis. HeLa cells were transfected with DNA coding for the protein of interest tagged with a fluorescent marker for 48 h. As a negative control the tag alone was expressed. The expression of SDS22 and I3 mutants, which are deficient in binding to PP1, served as a control for the dependency of potential effects on PP1 binding.

So, next to SDS22 wild type, two PP1-binding deficient mutants, $SDS22^{E192A}$ and $SDS22^{W302A}$, were expressed labeled N-terminally with mCherry. Lysates were prepared from transfected cells to determine the expression levels of the respective overexpressed proteins by Western blotting. By stainingwith dsRED-antibodies, which are binding specifically red fluorophores, the expression levels can be directly compared. SDS22 and both of its mutants were expressed in equal amounts. Only mCherry was expressed less efficiently (Figure 3.2 A). Nonetheless, an accurate microscopic analysis was still guaranteed, since only cells with similar expression levels were used for the quantification.

Thus, transfected cells were prepared for chromosome congression analysis at a confocal microscope by fixation and staining them with DAPI. The alignment in 30 mitotic cells was determined in 3 independent experiments. Remarkably, already transfection with mCherry alone induced misalignment in 26 % of the cells (Figure 3.2 C). Nevertheless, transfection with SDS22 led to a further increase in misalignment to 40 %. Surprisingly, also expression of the SDS22 mutants $SDS22^{E192A}$, and $SDS22^{W302A}$ caused misalignment in 44% and 42 % of all transfected cells, respectively. This suggests that SDS22 overexpression causes chromosomal congression defects, which do not depend on the ability of SDS22 to bind PP1.

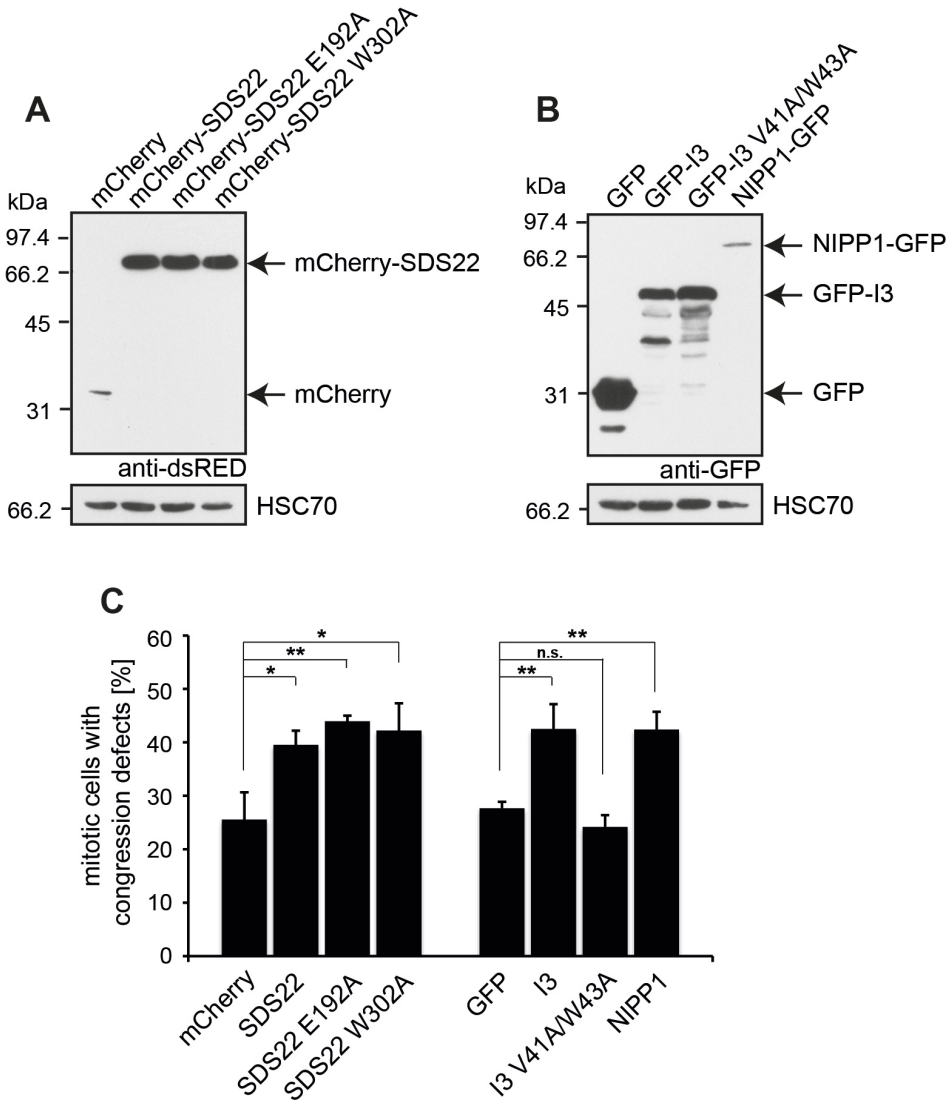

Figure 3.2 Transient overexpression of SDS22, I3, or NIPP1 causes chromosomal alignment defects in mitosis. A HeLa cells were transfected with mCherry, mCherry-tagged SDS22, or with its PP1 binding deficient mutants, $SDS22^{E192A}$ or $SDS22^{W302A}$ for 48 h, and lysates were prepared and analyzed by Western blotting with anti-dsRED antibodies. HSC70 served as a loading control. **B** HeLa cells were transfected with GFP, GFP-tagged I3, its PP1-binding deficient mutant $I3^{V41A/W43A}$, or NIPP1 for 48 h, then lysates were prepared and analyzed as in **A**, but with anti-GFP antibodies. **C** Cells, transfected as in **A** and **B**, were fixed and stained with DAPI. The chromosomal misalignment of cells in metaphase was quantified in 3 independent experiments with n ≥ 30 cells per condition. Error bars indicate the standard deviation. P-values were calculated using a Mann-Whitney-*U* test (***, p ≤ 0.001; **, p ≤ 0.01; *, p ≤ 0.05).

In a second experiment, I3, its PP1-binding deficient mutant $I3^{V41A/W43A}$, or NIPP1 were expressed with a GFP tag. Western blot analysis of the lysates, which were prepared from the transfected cells, revealed that NIPP1-GFP was only expressed in low levels, whereas GFP was highly expressed (Figure 3.2 B). Furthermore, several additional bands occurred in the cases of I3 and $I3^{V41A/W43A}$ expression, probably originating from degradation products. As a next step, transfected cells were fixed and stained with DAPI. Chromosomal congression was analyzed as before in cells with comparable expression levels by confocal microscopy. Transfection with GFP caused congression defects in 28 % of the cells, comparable to the effects in mCherry expressing cells (Figure 3.2 C). I3, as well as NIPP1 overexpression, but not $I3^{V41A/W43A}$ overexpression increased the relative number of metaphase cells with alignment defects up to 42 %, 43 %, and 24 %, respectively, indicating that this is a PP1 dependent effect. However, it is not specific to I3, as also the RVxF motif-containing PIP, NIPP1, caused congression defects

3.1.3 I3 and SDS22 are required for timely progression from nuclear envelope breakdown until anaphase onset

In addition to chromosomal alignment defects, also mitotic progression defects were found in previously published SDS22 silencing experiments (Posch et al., 2010). Therefore, we wanted to confirm the data for SDS22 and test, if also I3 is necessary for proper mitotic progression. To address this question, a HeLa cell line stably expressing Histone 2B (H2B) labeled with RFP and importin ß binding domain (IBB) labeled with GFP was used. Because IBB contains a nuclear localization signal, it is quickly imported into the nucleus. Upon nuclear envelope breakdown (NEBD) in prophase, IBB-GFP spreads throughout the cell, which can be observed as a sudden drop of the GFP-signal intensity. When the nuclear envelope is reassembled in late anaphase (nuclear envelope formation, NEF), IBB-GFP is quickly imported into the newly built nucleus, which can then be observed as a prompt increase in GFP signal. By marking the chromatin with a fluorescently labeled Histone 2B, additionally, anaphase onset (AO) can be observed as the time-point, when the sister chromatids start to separate from each other. This tool allows measuring the time span for mitotic progression from NEBD to AO and the time span for progression through anaphase from AO till NEF by analyzing movies from live cell imaging.

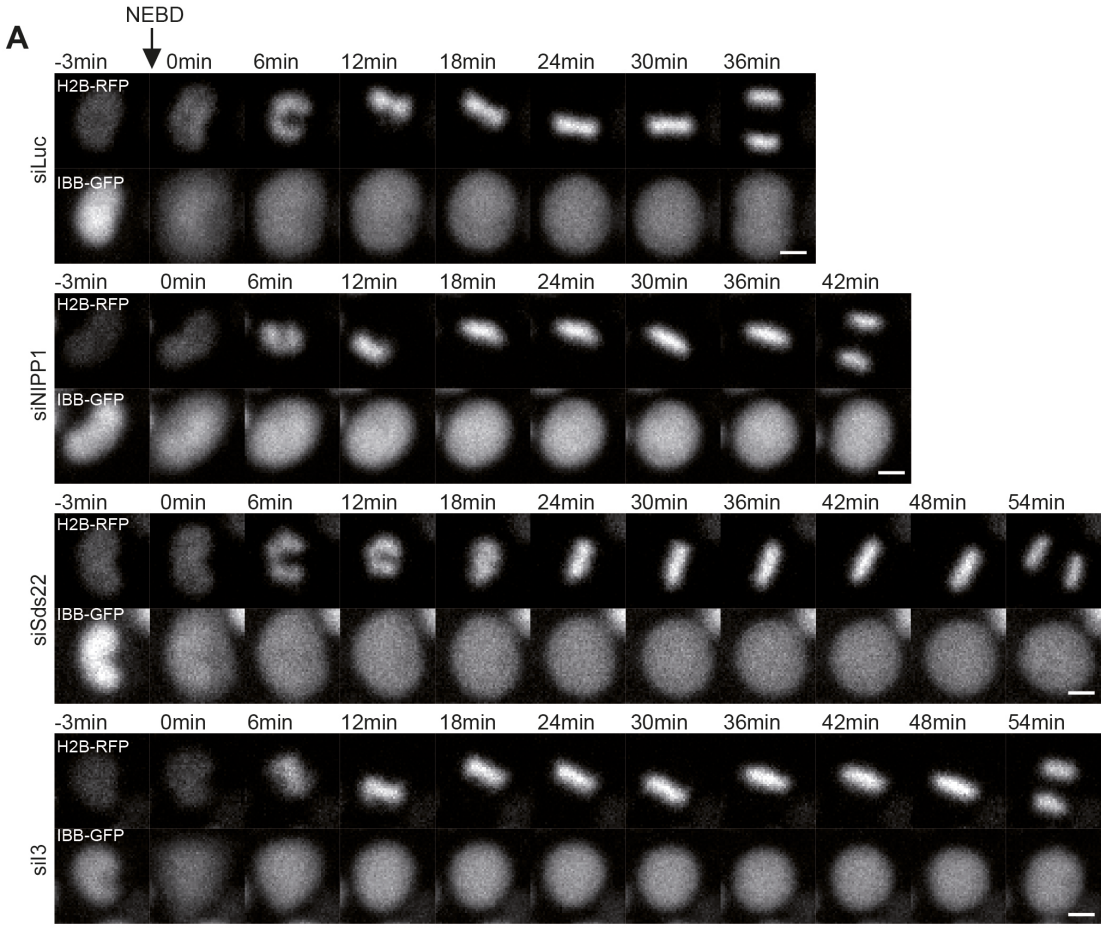
A
NEBD
-3min
0min
6min
12min
18min
24min
30min
36min
42min
48min
54min
H2B-RFP
IBB-GFP
siLuc
siNIPP1
siSds22
sil3

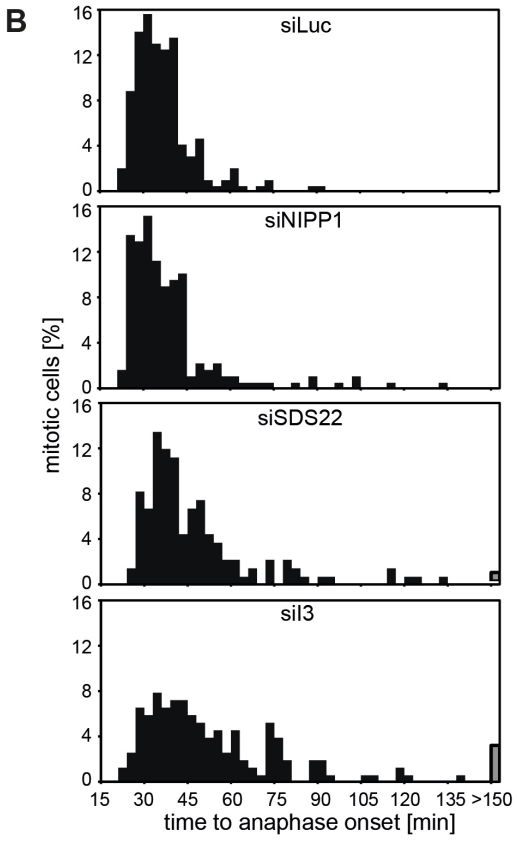
B
siLuc
siNIPP1
siSDS22
sil3
mitotic cells [%]
0
4
8
12
16
15
30
45
60
75
90
105
120
135
>150
time to anaphase onset [min]

Figure 3.3 siRNA mediated depletion of SDS22 or I3 causes a delay in mitotic progression. HeLa cells, stably expressing H2B-RFP and IBB-GFP, were treated with the indicated siRNAs for 48 h, and then imaged in 45 sec intervals for 12.5 h. **A** Representative confocal image sequences from NEBD until AO. Scale bar, 10 µm. **B** Percentage of cells committing to anaphase in the indicated time windows are plotted. n ≥ 133 cells per condition summed up from 3 independent experiments.

HeLa cells stably expressing H2B-RFP and IBB-GFP were treated with I3, SDS22, NIPP1, or Luc siRNA for 48h and then imaged at 37 °C and while supplied with 5 % CO_2 at a confocal microscope. Images were taken every 45 sec for 12.5 h and the obtained movies were analyzed by measuring the time each cell needed for mitotic progression until anaphase onset. As expected, the timing for mitotic progression was prolonged in cells depleted for SDS22 in comparison to Luc or NIPP1 depleted cells. Interestingly, also I3 depleted cells showed delayed anaphase onset (Figure 3.3 A). When plotting the relative number of mitotic cells against the time for mitotic progression in a histogram, a shift to longer duration times for mitotic progression can be observed for SDS22 and I3 depleted cells (Figure 3.3 B). Whereas control cells (siLuc and siNIPP1) needed on average 35.8 min until anaphase onset, SDS22, and I3 depletion delayed anaphase onset to 47.0 min and 58.0 min, respectively. This result confirmes the effect of SDS22 silencing on mitotic progression and indicates that I3 is needed for successful progression through mitosis in mammalian cells.

3.2 Characterization of HeLa cell lines stably expressing GFP-PP1, GFP-I3, or SDS22-GFP

As we found I3 to be required for chromosomal alignment and progression through mitosis, the question arose, if I3 can be found at kinetochores for regulating metaphase plate formation. Also reviewing the localization of SDS22 was of interest, since conflicting data on SDS22 localization to kinetochores are published (Liu et al., 2010; Posch et al., 2010). Finally, we also monitored PP1 localization to test, whether it is influenced by I3 (and SDS22), since PP1 localization to kinetochores was shown to be SDS22 dependent (Posch et al., 2010).

3.2.1 Expression levels in HeLa cell lines stably expressing GFP-PP1, GFP-I3, or SDS22-GFP

Since we found an increased number of metaphase cells with congression defects in the case of SDS22 or I3 overexpression, a localization analysis in cells expressing moderate protein levels is preferable. This can be achieved by generating stable cell lines from single clones, expressing the protein of interest in amounts, close to the respective endogenous protein. Therefore, a HeLa cell line stably expressing GFP-tagged I3 was generated. HeLa cells stably expressing GFP-PP1γ were a kind gift of Laura Trinkle-Mulcahy (Trinkle-Mulcahy et al., 2003) and HeLa cells stably expressing SDS22-GFP were provided by Antony Hyman (Poser et al., 2008).

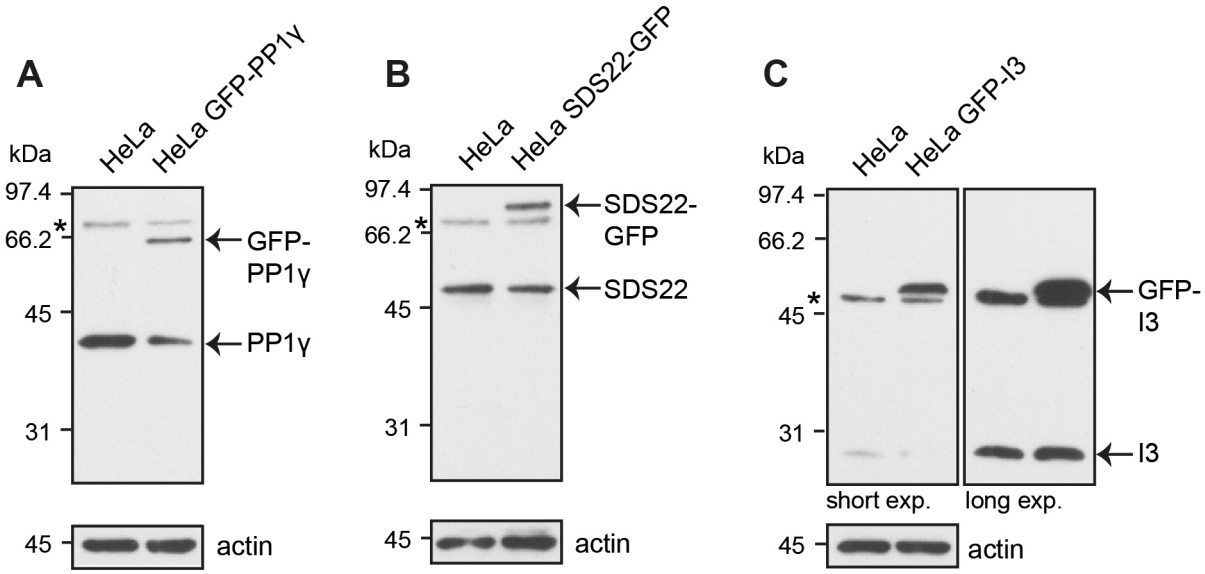

Figure 3.4 Expression levels of the GFP-fusions of PP1γ, SDS22, and I3 in the respective stably expressing HeLa cells. Expression level in HeLa cells stably expressing GFP-PP1γ (**A**), SDS22-GFP (**B**), or GFP-I3 (**C**). Stably expressing HeLa cells and untransfected HeLa cells were compared by Western blot analysis of the corresponding cell extracts. Endogenous and exogenous PP1γ, SDS22, and I3 protein levels were detected with the respective antibodies. Actin served as a loading control. Asterisks mark unspecific bands.

First, we characterized the stable cell lines by comparing the expression levels of exogenous protein to endogenous protein. Additionally, the expression levels in the stable cell lines were compared with expression levels in untreated HeLa cells.

Endogenous and exogenous protein was stained with the respective antibodies on a Western blot. Additionally, actin was stained as a loading control. The analysis of the HeLa GFP-PP1γ cell line revealed that GFP-PP1γ is expressed near to endogenous levels and in comparable amounts to PP1γ in untreated HeLa cells (Figure 3.4 A). In HeLa SDS22-GFP cells, exogenous SDS22 is expressed from a bacterial artificial chromosome (BAC). On a BAC, the whole gene is encoded thus the expression is under control of the endogenous promoter. Western blot analysis revealed that the expression level of endogenous SDS22 together with the SDS22-GFP expression level in the stable cell line corresponds to the endogenous protein level in untransfected HeLa cells (Figure 3.4 B). Also GFP-I3 levels were examined by Western blot analysis. Staining the blot with I3 specific antibodies revealed that the GFP-I3 expression level is only moderately increased in comparison to the endogenous protein level (Figure 3.4 C).

3.2.2 Localization in HeLa cell lines stably expressing GFP-PP1γ, GFP-I3, or SDS22-GFP

As all three cell lines showed expression levels close to endogenous protein levels, they can be used for localization studies. In the next step, the localization of PP1γ, SDS22, and I3 was monitored at a confocal microscope to confirm the localization of PP1γ and SDS22 to kinetochores and to clarify, whether also I3 localizes to kinetochores. After fixation of HeLa GFP-PP1γ cells with paraformaldehyde, or imaging them live, PP1γ could be observed at kinetochores, but a large fraction also localized diffusely around the metaphase chromatin. In contrast, simultaneous fixing and permeabilizing with 0.1 % Triton-X-100, generated cells with chromatin free of PP1γ, so that the kinetochore localization was clearly visible (Figure 3.5 A). Also, HeLa SDS22-GFP cells were imaged live and after diverse fixation methods, but under none of these conditions SDS22 could be observed at kinetochores (Figure 3.5 B), which is in line with the observation of Liu and colleagues (Liu et al., 2010).

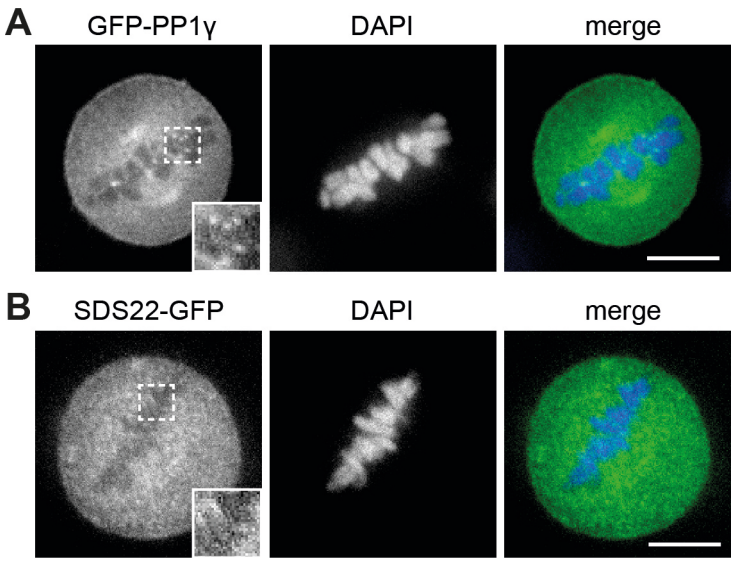

Figure 3.5 Localization of the GFP-fusions of PP1γ or SDS22 in stably expressing HeLa cells. A HeLa cells, stably expressing GFP-PP1γ, were fixed with PFA containing 0.1 % Triton X-100, then stained with DAPI and imaged at a confocal microscope. Scale bar, 10µm. **B** HeLa cells stably expressing SDS22-GFP, were fixed with PFA and stained with DAPI, before imaging at a confocal microscope. Scale bar, 10 µm.

I3 was published to localize in the nucleus and in the nucleoli during interphase (Lesage et al., 2007) and to centrosomes in mitosis (Huang et al., 2005). To confirm these observations and to clarify, whether I3 might also be observable at kinetochores, GFP-I3 cells were imaged live or paraformaldehyde-fixed. Under both conditions the interphase localization to the nucleus and the nucleoli could be verified, but a localization of I3 to centrosomes or other mitotic compartments could not be observed at any stage of mitosis (Figure 3.6), indicating that I3 does not regulate chromosome congression directly at kinetochores.

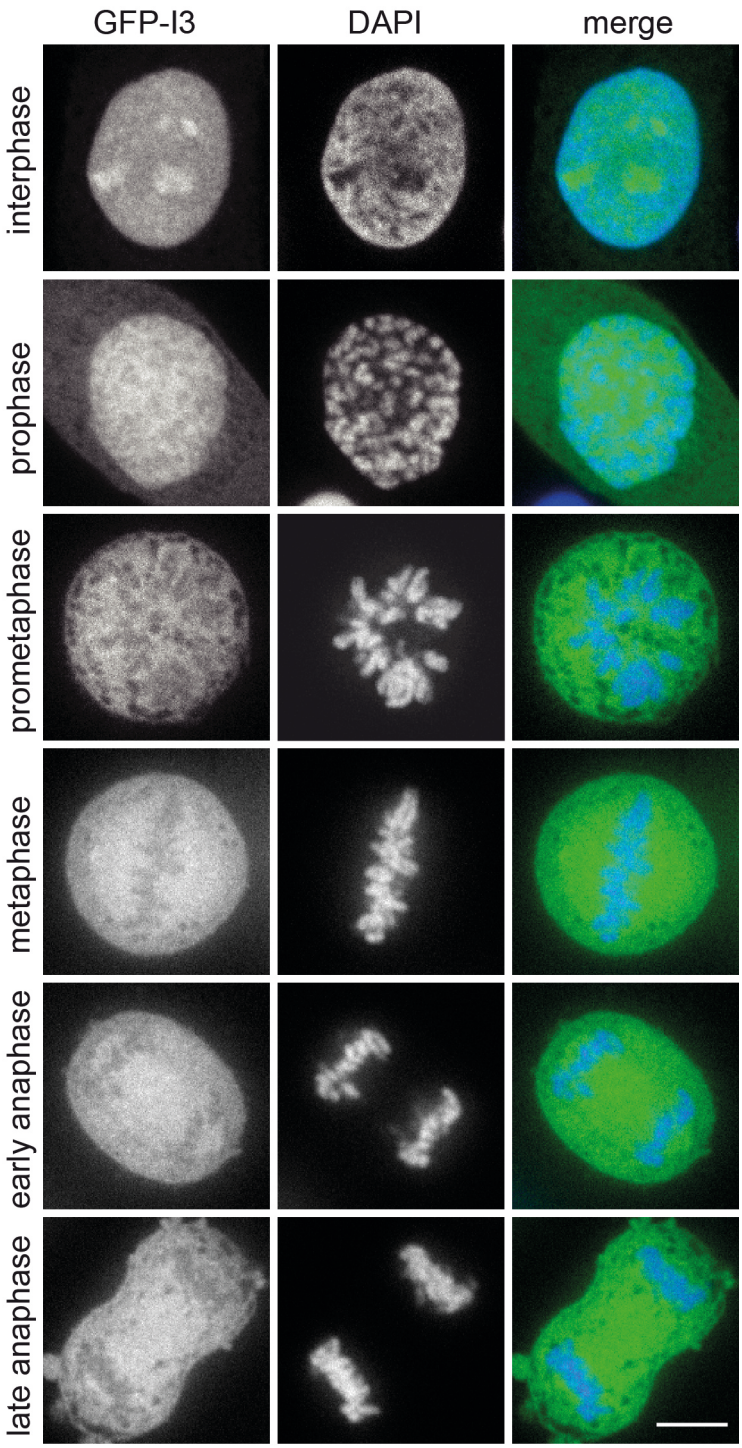

Figure 3.6 Localization of GFP-I3 in stably expressing HeLa cells. Representative images of HeLa cells, stably expressing GFP-I3, in interphase and in mitosis after fixation with PFA and staining with DAPI. Scale bar, 10 µm.

3.3 Localization of PP1γ and SDS22 upon depletion or overexpression of I3 or SDS22

I3 does not localize to kinetochores, where it could directly affect chromosome congression, hence it might regulate chromosomal attachment indirectly. Since I3 is known to form a complex with PP1-SDS22, it could possibly influence the binding of PP1 and SDS22 to kinetochores. Such regulatory function already has been found for SDS22, as Swedlow and colleagues detected decreased amounts of PP1 at kinetochores in the background of SDS22 depletion (Posch et al., 2010). To address the question we tested whether I3 depletion influences PP1γ or SDS22 localization. Additional, we revisited the effect of SDS22 silencing on PP1γ localization.

3.3.1 PP1γ localization is unaltered in the absence of I3 or SDS22

To test, whether I3 (and SDS22) regulates PP1 localization, HeLa GFP-PP1γ cells were treated with I3, SDS22, NIPP1, or Luc siRNA for 48 h. Afterwards the cells were fixed while permeabilizing them with Triton-X-100, stained with DAPI and analyzed at a confocal microscope. In Luc and NIPP1 depleted cells PP1γ localized, as expected, to kinetochores. But, surprisingly, the kinetochore localization of PP1γ was also unchanged in SDS22 or I3 depleted metaphase cells (Figure 3.7). However, a slightly higher expression level of PP1γ and a diffuse coating of metaphase chromatin could be found in SDS22 knockdown cells. Therefore, an SDS22-dependent localization of PP1γ to kinetochores could not be confirmed, suggesting that SDS22 does not regulate PP1γ in its localization. Furthermore, this result indicates that PP1γ localization is also independent of I3.

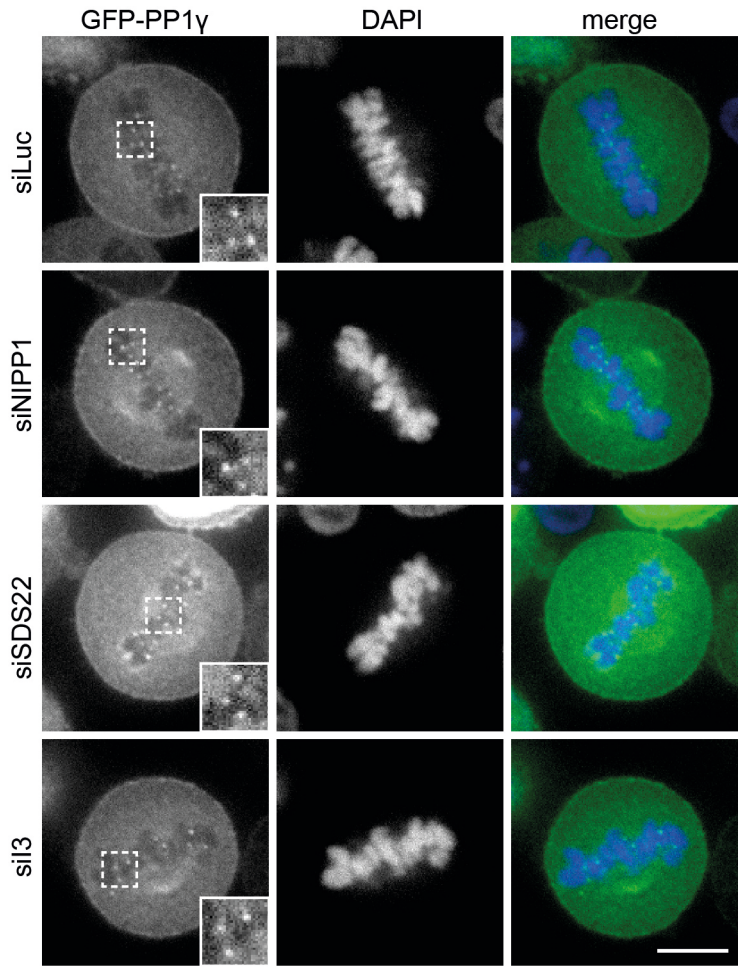

Figure 3.7 PP1γ localization is unchanged upon siRNA-mediated depletion of SDS22 or I3. HeLa cells stably expressing GFP-PP1γ were treated with siRNA specific for the indicated proteins for 48 h. Cells were fixed while permeabilizing and imaged at a confocal microscope. Representative images are shown. Scale bar, 10 µm.

3.3.2 SDS22 localizes to metaphase kinetochores in the absence of I3

To test, whether I3 depletion might regulate SDS22 localization, HeLa cells stably expressing SDS22-GFP were treated with siRNA against Luc, NIPP1 and with two different siRNAs against I3 (I3 S1 and I3 S2) for 48 h. The knockdown efficiency in HeLa SDS22-GFP cells was determined by performing a Western blot analysis on cell extracts. Both I3 siRNAs, as well as NIPP1 siRNA produced a specific knockdown (Figure 3.8 A).

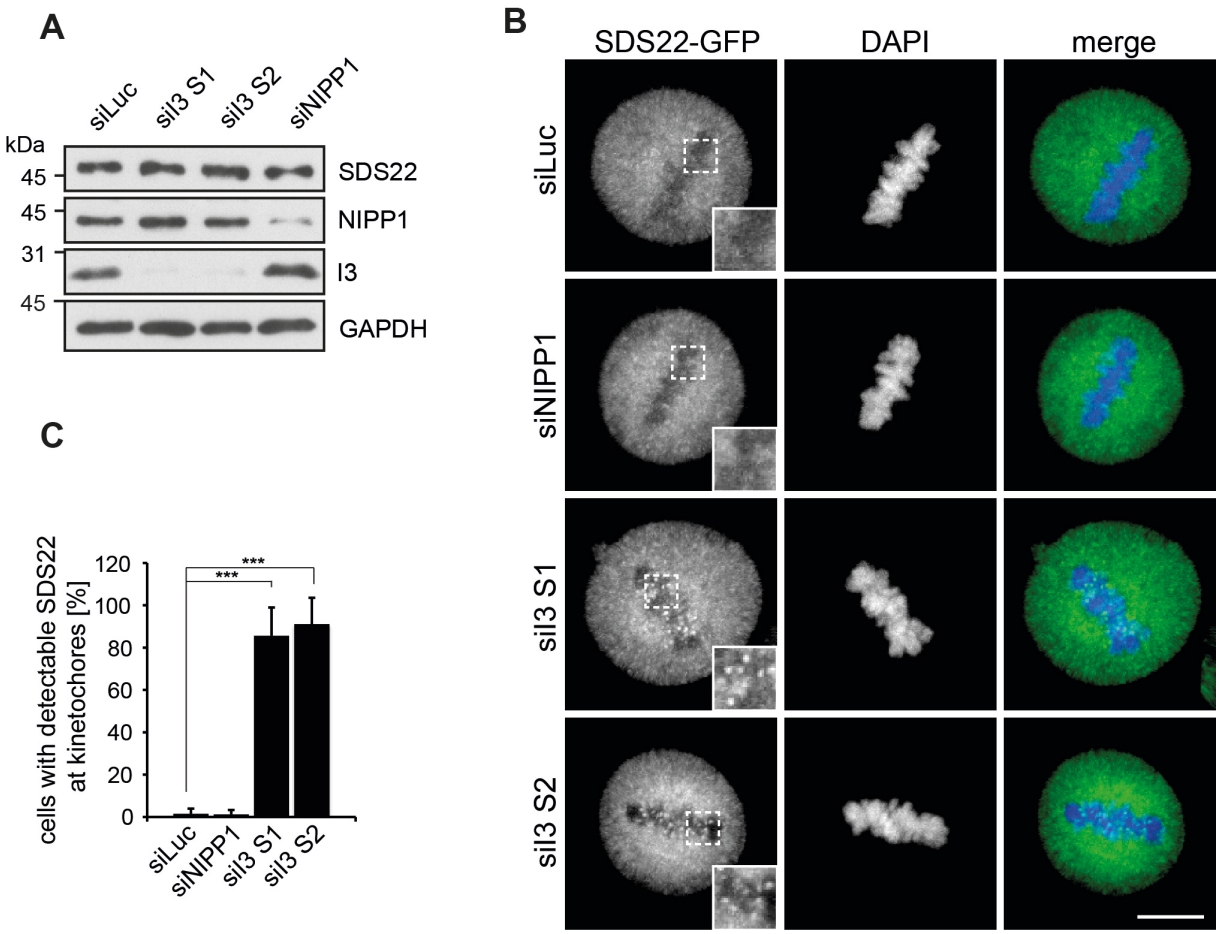

Figure 3.8 SDS22 localizes to metaphase kinetochores in the absence of I3. A HeLa cells stably expressing SDS22-GFP were treated with the indicated siRNAs for 48 h, then lysed and analyzed by Western blotting with respective antibodies. GAPDH served as a loading control. **B** Cells, treated as in **A**, were fixed and stained with DAPI. Maximum intensity projections of representative confocal fluorescence microscopy images are shown. Scale bar, 10 µm. **C** At least 30 metaphase cells per condition were analyzed for kinetochore localization of SDS22 in 3 independent experiments. Error bars show the standard deviation. P-values were calculated using a Mann-Whitney-*U* test (***, $p \leq 0.001$).

Next, depleted HeLa SDS22-GFP cells were fixed and stained with DAPI for subsequent analysis at a confocal microscope. In metaphase cells, which were silenced for Luc or NIPP1, SDS22 showed no specific localization to mitotic compartments as also found in untreated cells. However, a localization of SDS22 to kinetochores could be observed in cells treated with I3 S1 or S2 siRNA (Figure 3.8

B). The relative number of metaphase cells with a visible kinetochore localization of SDS22 was counted in three independent experiments. More than 85 % of all metaphase cells treated with either I3 S1 or S2 siRNA showed a redistribution of SDS22 to kinetochores (Figure 3.8 C).

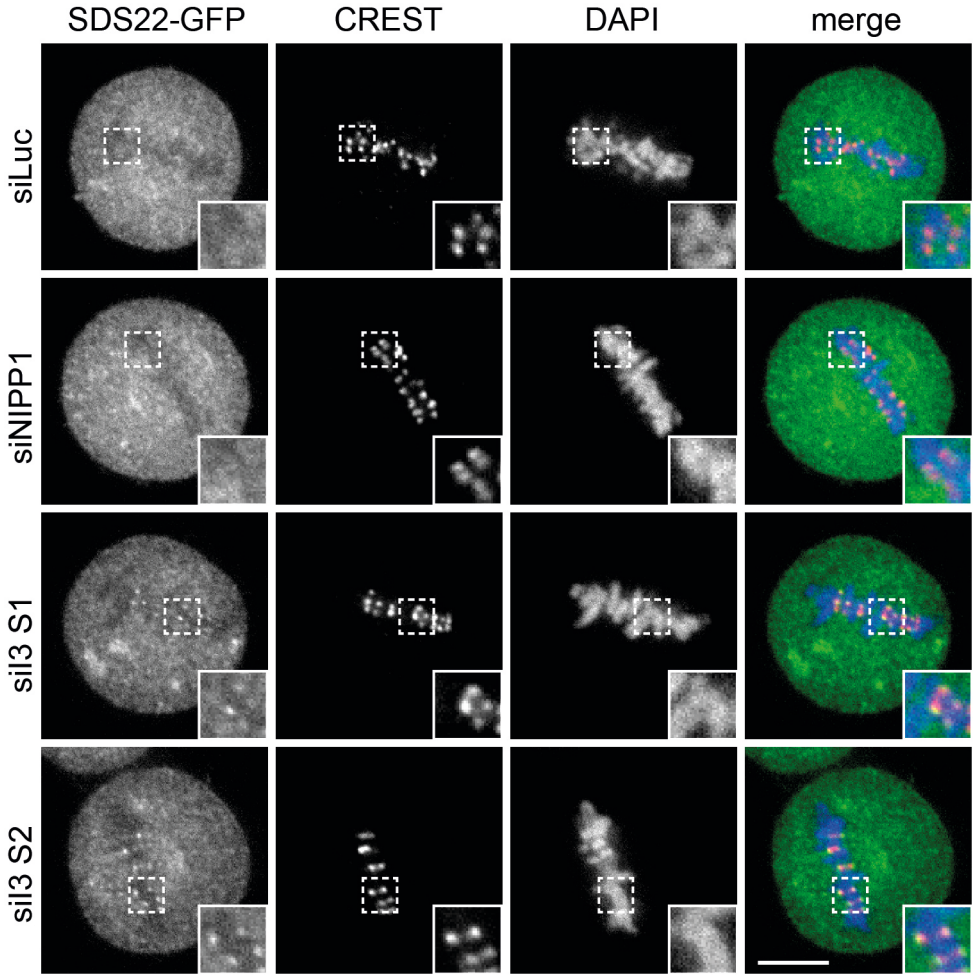

Figure 3.9 SDS22 colocalizes with CREST-marked inner kinetochores in the absence of I3. HeLa cells stably expressing SDS22-GFP were treated with the indicated siRNAs for 48h, then fixed and stained with a CREST serum and with DAPI. Representative confocal images are shown. Scale bar, 10 µm.

To verify that the localization of SDS22, found in the background of I3 depletion, indeed refers to a binding to kinetochores, I3 silenced SDS22-GFP cells were fixed and stained with antibodies detecting inner kinetochore proteins (CREST). As expected no overlap of CREST signal with SDS22-GFP signal could be detected in

Luc or NIPP1 depleted cells (Figure 3.9). However, when depleting I3, the SDS22-GFP signal overlapped with the outer edge of the CREST signal, confirming the anticipated outer kinetochore localization of SDS22.

To assure that this effect was specific for I3 knockdown and was not caused by any off-target effect, mCherry-tagged I3, which is resistant to I3 S2 siRNA, (mCherry-I3^{res}), was expressed in SDS22-GFP cells, which were previously depleted for I3. After 24 h of treatment with I3 S2 siRNA, SDS22-GFP cells were transfected for additional 48 h with either mCherry or mCherry-I3^{res}. Afterwards, the cells were either lysed for Western blot analysis or fixed and stained with DAPI for analysis at a confocal microscope. Immunoblotting revealed that mCherry and mCherry-I3^{res} migrated as expected according to their molecular weights. Concomitantly, the silencing of endogenous I3 is maintained (Figure 3.10 A). A weaker band in the lane of mCherry-I3^{res} transfection with the same apparent molecular weight as I3 may originate from a degradation product of the overexpressed mCherry-I3^{res}. This is likely since we found GFP-I3 to be partially degraded when overexpressed (see Figure 3.2 B). Next, the SDS22 localization was analyzed. SDS22 localization to kinetochores was detectable in cells silenced for I3 and positive for mCherry, but SDS22 disappeared from kinetochores in cells expressing mCherry-I3^{res} instead of mCherry (Figure 3.10 B). Quantification of three independent experiments revealed that I3 depleted and mCherry expressing SDS22-GFP cells show kinetochore localization of SDS22 in 98 % of all metaphase cells, whereas the effect was diminished to 3 % in cells expressing mCherry-I3^{res} instead (Figure 3.10 C).

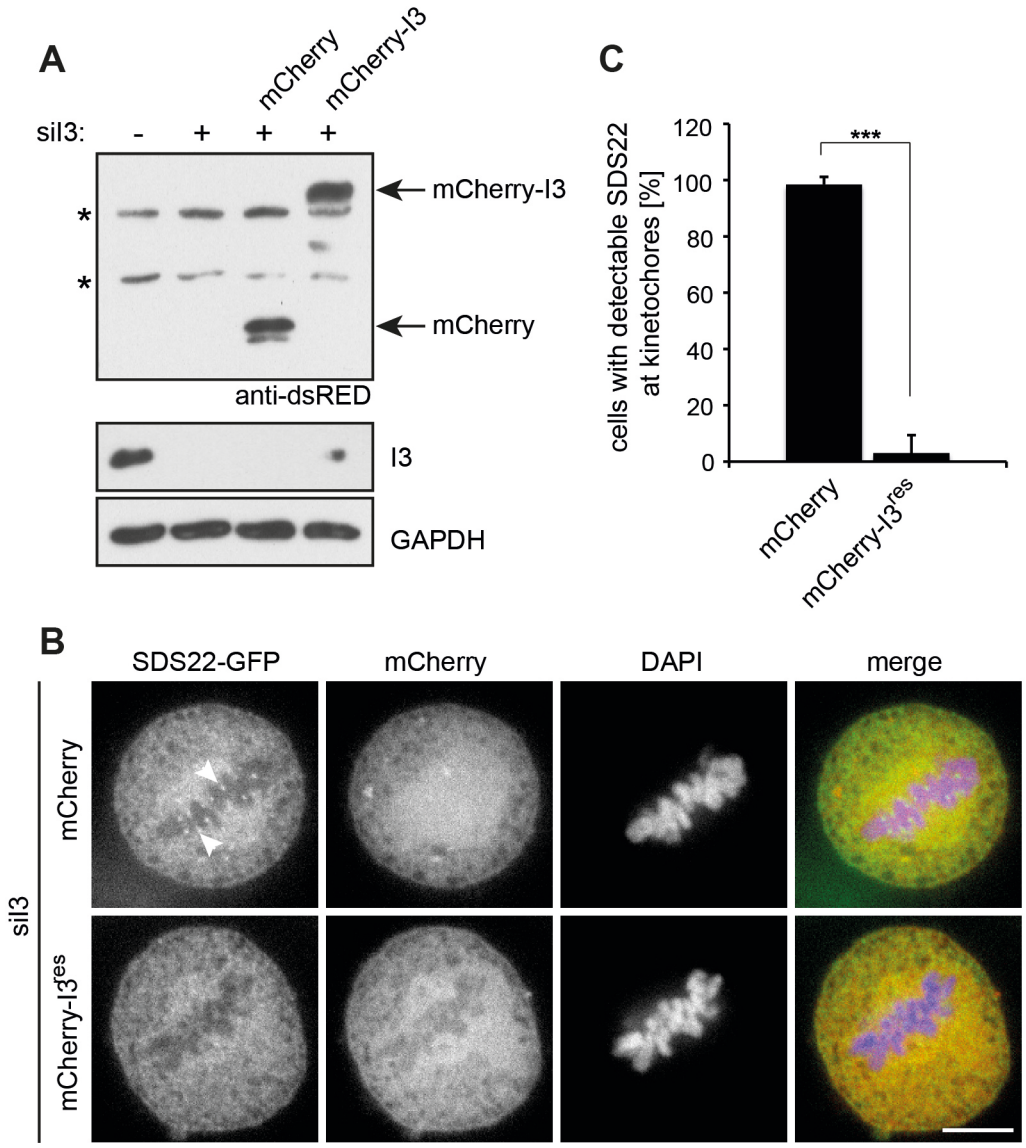

Figure 3.10 Overexpression of siRNA resistant I3 restores SDS22 localization. **A** HeLa cells stably expressing SDS22-GFP were treated with I3 S2 siRNA. After 24 h the cells were transfected for additional 48 h with constructs coding for mCherry or mCherry-I3^{res} cDNA, which is resistant to I3 S2 siRNA. Lysates were analyzed by Western blotting. mCherry and mCherry-I3^{res} were detected with anti-dsRED antibodies and endogenous I3 protein was detected with antibodies specific for I3. GAPDH served as a loading control. Asterisks mark unspecific bands. **B** Cells, treated like in **A**, were fixed and stained with DAPI. Representative confocal images are shown. Scale bar, 10 µm. **C** Quantification of **B**. The number of mitotic cells showing kinetochore localization of SDS22 was determined in 3 independent experiments with n ≥ 20 cells per condition. Error bars show the standard deviation. P-values were calculated using a Mann-Whitney-*U* test (***, p ≤ 0.001).

3.3.3 SDS22-PP1γ localization to outer kinetochores depends on KNL1

Together, the results so far suggest that I3 plays a role in chromosome segregation by balancing SDS22 localization to kinetochores without influencing PP1γ levels at that site. Since PP1γ localization to kinetochores also did not depend on SDS22, we asked whether PP1γ-SDS22 would bind to a known PP1 subunit at the kinetochore. Most PP1 localizes to kinetochores via binding to KNL1 (Liu et al., 2010), which, like I3, binds PP1 via an RVxF-motif. Therefore, we tested in a KNL1 knockdown experiment, whether the SDS22-bound fraction of PP1 localizes via binding to KNL1 to kinetochores.

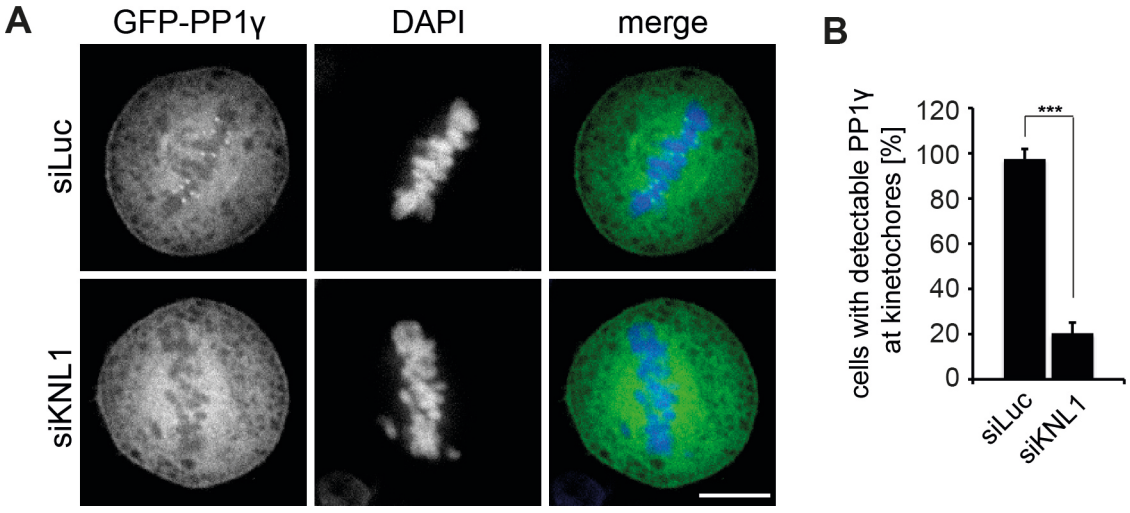

Figure 3.11 Knockdown of KNL1 depletes GFP-PP1γ from kinetochores. A HeLa cells stably expressing GFP-PP1γ were treated with Luc or KNL1 siRNA for 24 h, and then fixed while permeabilizing and stained with DAPI. Representative confocal images are shown. Scale bar, 10 µm. **B** Quantification of **A**. The number of mitotic cells showing kinetochore localization of PP1γ was determined in 3 independent experiments with n ≥ 25 cells per condition. Error bars show the standard deviation. P-values were calculated using a Mann-Whitney-*U* test (***, p ≤ 0.001).

The knockdown of KNL1 was previously shown to strongly diminish PP1 levels at kinetochores (Liu et al., 2010). Therefore, we first depleted KNL1 from HeLa GFP-PP1γ cells and analyzed metaphase cells for PP1γ localization to kinetochores to

test, whether the KNL1 knockdown was efficient. HeLa GFP-PP1γ cells were treated with Luc or KNL1 siRNA for 24 h and then fixed while permeabilizing with Triton-X-100 and stained with DAPI. Analysis at a confocal microscope revealed that, indeed, PP1γ was depleted from kinetochores in 80 % of all KNL1-silenced metaphase cells, whereas PP1γ was detectable in Luc-depleted cells (97 %), showing that the knockdown of KNL1 was efficient (Figure 3.11 A and B).

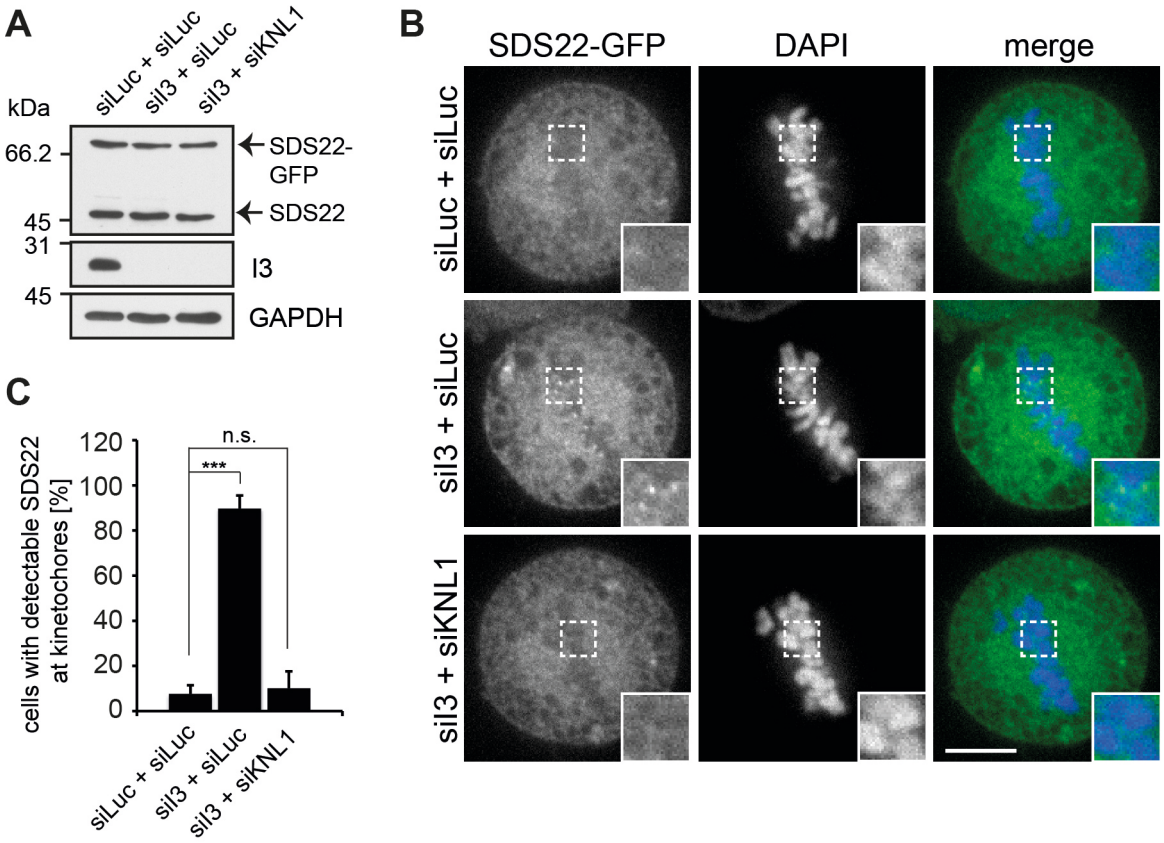

Figure 3.12 Knockdown of KNL1 abolishes SDS22 localization to kinetochores in I3 depleted HeLa SDS22-GFP cells. A HeLa cells stably expressing SDS22-GFP were treated with I3 S2 siRNA. After 24 h cells were additionally depleted of Luc or KNL1 for additional 24 h. Lysates were prepared and analyzed for I3 protein levels with I3 specific antibodies by Western blotting. GAPDH served as a loading control. **B** Cells, treated like in **A**, were fixed and stained with DAPI. Representative confocal images are shown. Scale bar, 10 µm. **C** Quantification of **B**. The number of mitotic cells showing kinetochore localization of SDS22 was determined in 3 independent experiments with n ≥ 25 cells per condition. Error bars show the standard deviation. P-values were calculated using a Mann-Whitney-*U* test (***, p ≤ 0.001).

Next, we treated HeLa SDS22-GFP cells, which were already silenced for I3 for 24 h, with KNL1 siRNA as before. Subsequently we prepared lysates and analyzed them by Western blotting to determine the I3 knockdown efficiency in the background of KNL1 depletion. Staining with I3 specific antibodies revealed that I3 depletion was efficient in the background of KNL1 knockdown. Also SDS22 expression levels were unchanged, as indicated by staining with SDS22 specific antibodies (Figure 3.12 A). Next we analyzed the localization of SDS22 in KNL1 and I3 depleted cells, which were fixed and stained with DAPI at a confocal microscope. KNL1 knockdown indeed abolished SDS22 binding to kinetochores in the background of I3 depletion in 90 % of all cells, whereas SDS22 still localized to kinetochores in 90 % of all I3 depleted cells, which were additionally treated with Luc siRNA (Figure 3.12 B and C). This experiment suggests a regulation of the KNL1-bound fraction of PP1γ by SDS22 binding.

3.3.4 SDS22 is detectable at kinetochores when overexpressed

To further elucidate the mechanism of SDS22 localization to kinetochores, we asked whether we could stimulate SDS22 localization to kinetochores by overexpression of SDS22. HeLa cells stably expressing GFP-PP1γ were transfected with mCherry, mCherry-SDS22, or its PP1-binding deficient mutants, mCherry-SDS22^{E192A} or mCherry-SDS22^{W302A}. The expression levels were determined by Western blot analysis. Like in HeLa cells (see Figure 2.2 A), also in GFP-PP1γ cells, SDS22 and its mutants were expressed to similar levels, whereas mCherry was slightly less expressed (Figure 3.13 A). Next, transfected cells were fixed while permeabilizing and afterwards stained with DAPI. The SDS22 localization was monitored at a confocal microscope. When overexpressing SDS22 in GFP-PP1γ cells, SDS22 could be observed at kinetochores, where it colocalizes with PP1γ, while PP1γ localization was unchanged in comparison to mCherry expressing cells (Figure 3.13 B). Precluding SDS22 binding to PP1 by mutating residue E192 or W302 to alanine abolished SDS22 localization to kinetochores. These data indicate that binding of SDS22 to kinetochores can be induced by strong overexpression and that SDS22 localization is PP1 dependent.

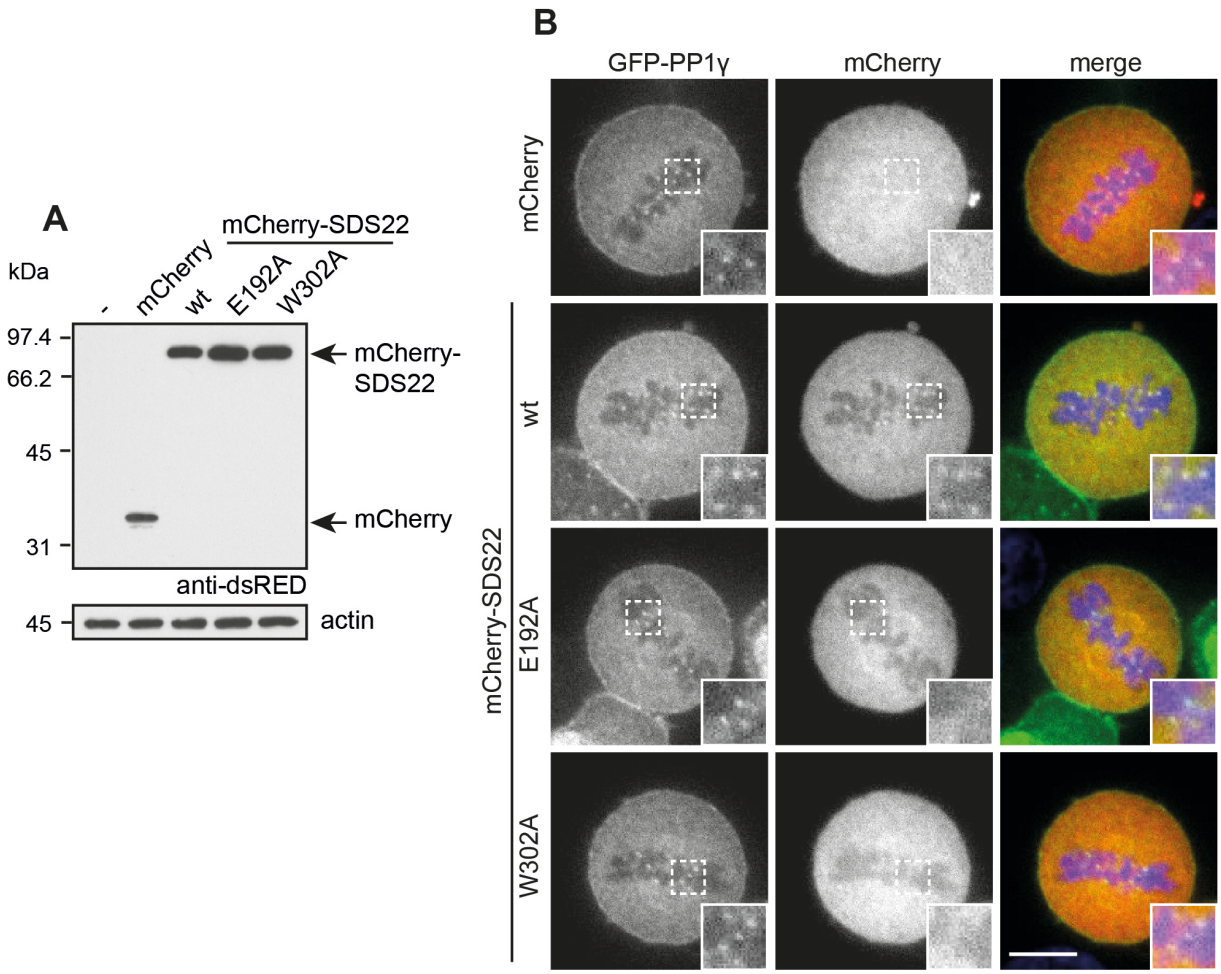

Figure 3.13 Localization of transiently overexpressed SDS22 to kinetochores depends on its PP1γ-binding ability. A HeLa cells stably expressing GFP-PP1γ were transfected with mCherry, mCherry-tagged wild type SDS22, SDS22^{E192A}, or SDS22^{W302A} for 48 h and then analyzed by Western blotting with anti-dsRED antibodies. Actin served as a loading control. **B** Cells treated as in **A** were fixed and stained with DAPI before localization analysis. Representative confocal images are shown. Scale bar, 10 µm.

3.3.5 Overexpression of RVxF motif-containing PP1 subunits extracts PP1γ from kinetochores

We used a similar experimental setup to address the question, which effect overexpression of I3 or NIPP1 might have on PP1γ localization. This is important, as we found congression defects upon overexpression of one or the other. HeLa GFP-

PP1γ cells were transfected with fluorescently tagged I3, NIPP1, SDS22, or the tag alone. The expression levels were again determined by Western blot analysis. All proteins were expressed on similar levels in HeLa GFP-PP1γ cells (Figure 3.14 A). Next, cells were transfected for 48 h and subsequently fixed and stained with DAPI for localization analysis. Again, colocalization of SDS22 with PP1γ could be observed. Interestingly, I3 or NIPP1 overexpression extracted PP1γ from kinetochores in metaphase cells (Figure 3.14 B). Absence of PP1γ from kinetochores could explain the congression defects upon I3 or NIPP1 overexpression, as mislocalized PP1γ fails to counteract Aurora B at kinetochores. The fact that also NIPP1 overexpression depleted PP1 from kinetochores indicates that this is a rather unspecific effect, caused by overexpression of an RVxF motif-containing protein, which competes with RVxF motif-containing PIPs at the kinetochore.

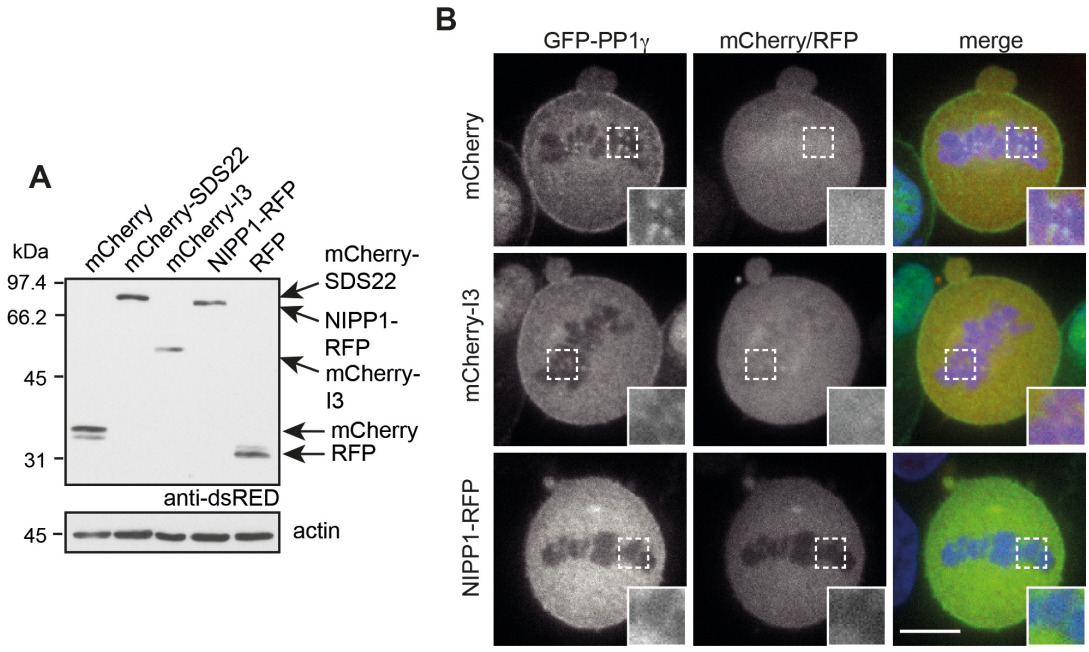

Figure 3.14 Overexpression of I3 or NIPP1 extracts PP1γ from kinetochores. A HeLa cells stably expressing GFP-PP1γ were transfected with I3, SDS22, NIPP1, tagged with red fluorophores or with a red fluorophore alone for 48 h and then lysed for Western blot analysis. Overexpression of the PP1 subunits was detected with anti-dsRED antibodies. Actin served as a loading control. **B** Cells treated as in **A** were fixed and stained with DAPI before localization analysis. Representative confocal images are shown. Scale bar, 10 µm.

3.4 PP1 activity at kinetochores is diminished by silencing as well as overexpression of I3 or SDS22

Our data so far indicate that the congression defects caused by I3 or SDS22 silencing are not an effect of altered PP1γ localization. Therefore we wanted to proceed with testing the possibility that the activity of kinetochore-localized PP1γ might be changed directly by I3 or SDS22 knockdown. Since PP1 counteracts Aurora B at kinetochores (Liu et al., 2010), an altered PP1 activity could in turn lead to an altered Aurora B activity. Two research groups already explored the effect of SDS22 depletion on Aurora B activity. However, their data are contradictory. Whereas Swedlow and colleagues found an increase in Aurora B activity upon SDS22 silencing, Gerlich and colleagues could not detect a change in Aurora B activity. Thus, the effect of both, SDS22 and I3 silencing, on Aurora B activity needs to be clarified.

3.4.1 I3, as well as SDS22 silencing increases the activity of Aurora B on metaphase chromatin

Aurora B activity can be measured by determining the level of autophosphorylation at T232 (Yasui et al., 2004). Antibodies detecting Aurora B phosphorylated at T232 are commercially available. To first test the specificity of the antibodies towards only the phosphorylated form of Aurora B, HeLa cells were either treated for 30 min with the Aurora B inhibitor Hesperadin or with DMSO, as a control. Subsequently, the cells were fixed and stained with Aurora B pT232 specific antibodies as well as with DAPI to visualize the chromatin. Hesperadin treatment strongly diminished the intensity of Aurora B pT232 staining on chromatin, but did not influence the signal intensity at centrosomes (Figure 3.15). Thus, the binding of the antibodies to centrosomes is an unspecific effect, whereas the chromatin-associated staining corresponds to the autophosphorylated form of Aurora B.

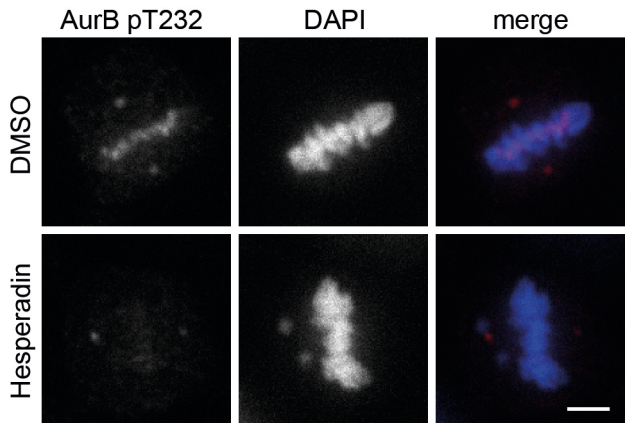

Figure 3.15 Aurora B pT232 antibodies are specific. HeLa cells were treated with 200 nM Hesperadin or with 0.02 % DMSO for 30 min and then stained with antibodies specific for Aurora B phosphorylated at T232 and with DAPI to visualize the chromatin. Representative confocal images are shown. Scale bar, 5 µm.

As the antibodies are suitable for Aurora B pT232 detection, the relative intensity in the different depletion backgrounds can be used to measure the Aurora B activity in that samples. HeLa cells were depleted for I3, SDS22, NIPP1, or Luc for 48 h before fixing and staining the samples with the Aurora B pT232 specific antibodies, with antibodies detecting whole Aurora B protein, and with DAPI. Analysis of the samples at a confocal microscope revealed an increase in Aurora B phosphorylation, as well as a small increase in Aurora B protein in metaphase cells silenced for SDS22 or I3 (Figure 3.16 A). The phosphorylation and protein levels in NIPP1 depleted cells were comparable to the levels in Luc depleted cells. Both, the Aurora B and the Aurora B pT232 signals were quantified with the program CellProfiler by building a mask on the DAPI signal to exclude centrosomal and cytoplasmic staining from the analysis. The mean intensity of both signals was measured within the mask in 50 metaphase cells per condition in 3 independent experiments. The quantification of Aurora B pT232 signal intensity, as well as the ratio between phosphorylated Aurora B and whole Aurora B protein signal intensity on chromatin is shown as a box plot in Figure 3.16 B.

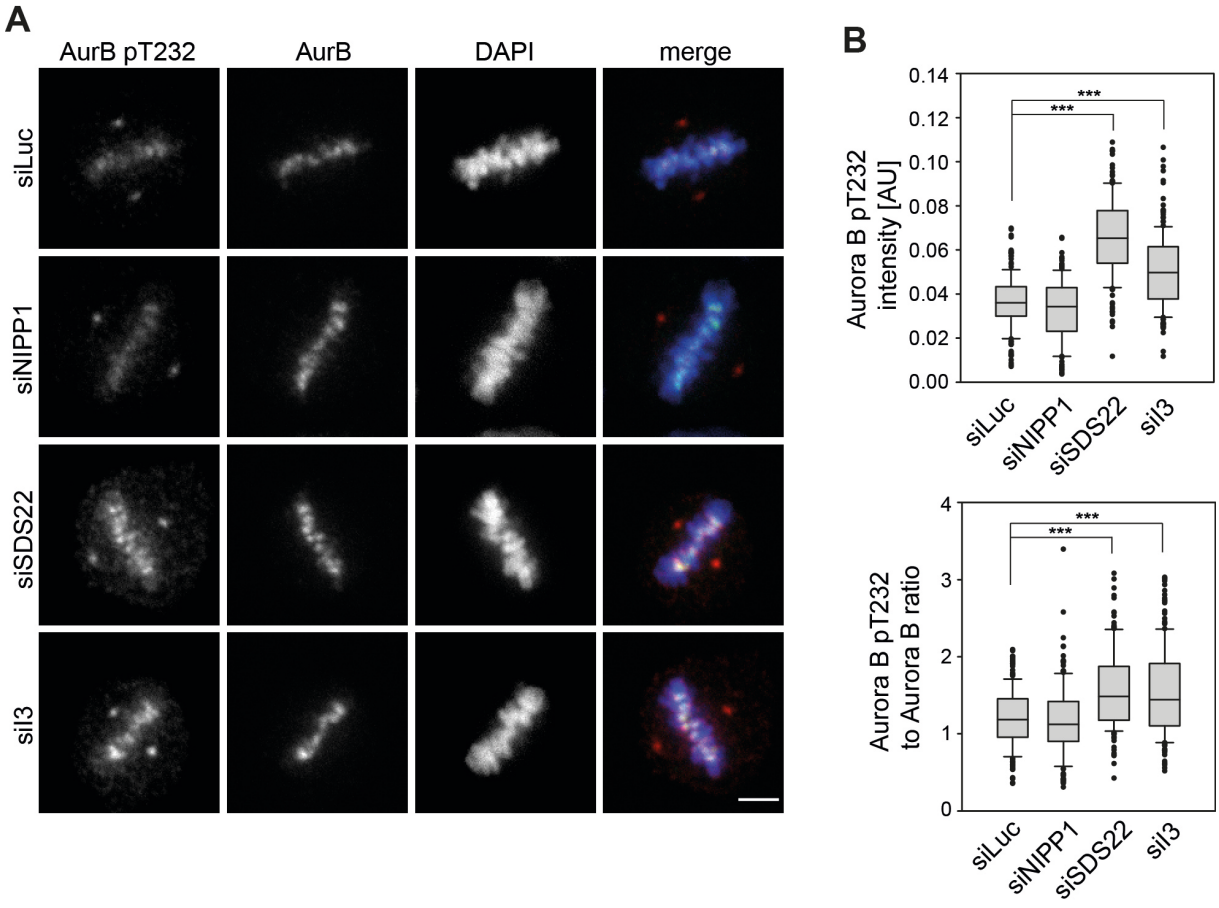

Figure 3.16 siRNA mediated depletion of SDS22 or I3 increases Aurora B activity on metaphase chromatin. A HeLa cells were treated with siRNA specific for the indicated proteins for 48 h before fixation. An immunofluorescence staining was performed with antibodies detecting Aurora B total protein and Aurora B phosphorylated at T232. Representative confocal images are shown. Scale bar, 5 µm. **B** Quantification of the signal intensities on chromatin using the software CellProfiler. The intensity of Aurora B total protein and Aurora B phosphorylation on chromatin was quantified in 3 independent experiments with n ≥ 50 cells per condition. The relative intensity of Aurora B pT232, as well as the ratio of Aurora B pT232 to Aurora B protein on chromatin was plotted as box plots with median, lower and upper quartiles (line and box), 10th and 90th percentiles (whiskers), and outliers (●). P-values were calculated using a Mann-Whitney-*U* test (***, p ≤ 0.001).

The box plots indicate that the significant increase in Aurora B activity is not solely explainable by the accumulation of Aurora B protein, as the phosphorylation level increased stronger than the protein level. However, the effect of SDS22 silencing on Aurora B activity was slightly stronger than the effect of I3 silencing. This result confirms Swedlow's data on SDS22, showing that SDS22 is required for PP1 activity at kinetochores. Furthermore, the result reveals that also I3 is required for PP1 activity. This indicates that SDS22 is needed for PP1 activity, but also that increased levels of SDS22 at kinetochores, caused by I3 silencing, inhibit PP1.

3.4.2 Overexpression of SDS22 increases Aurora B activity on metaphase chromatin

SDS22 overexpression phenocopies the effect of I3 silencing, as both treatments cause chromosomal congression defects and increase SDS22 localization to kinetochores. Therefore, we asked next, whether SDS22 overexpression also increases the activity of Aurora B, like I3 silencing does. To address this question, HeLa cells were transfected with fluorescently tagged SDS22 wild type or PP1-binding deficient mutants for 48 h. After fixing and staining with Aurora B pT232 specific antibodies and DAPI, the samples were applied to confocal microscopy analysis. In comparison to mCherry-transfected cells, the Aurora B phosphorylation level was strongly increased in mCherry-SDS22 transfected cells (Figure 3.17 A and B). This effect was not found when overexpressing either of the SDS22 mutants, suggesting that binding of SDS22 to PP1 inhibits PP1 in counteracting Aurora B. Furthermore, this result reveals that SDS22 overexpression phenocopies I3 silencing also in terms of Aurora B activity.

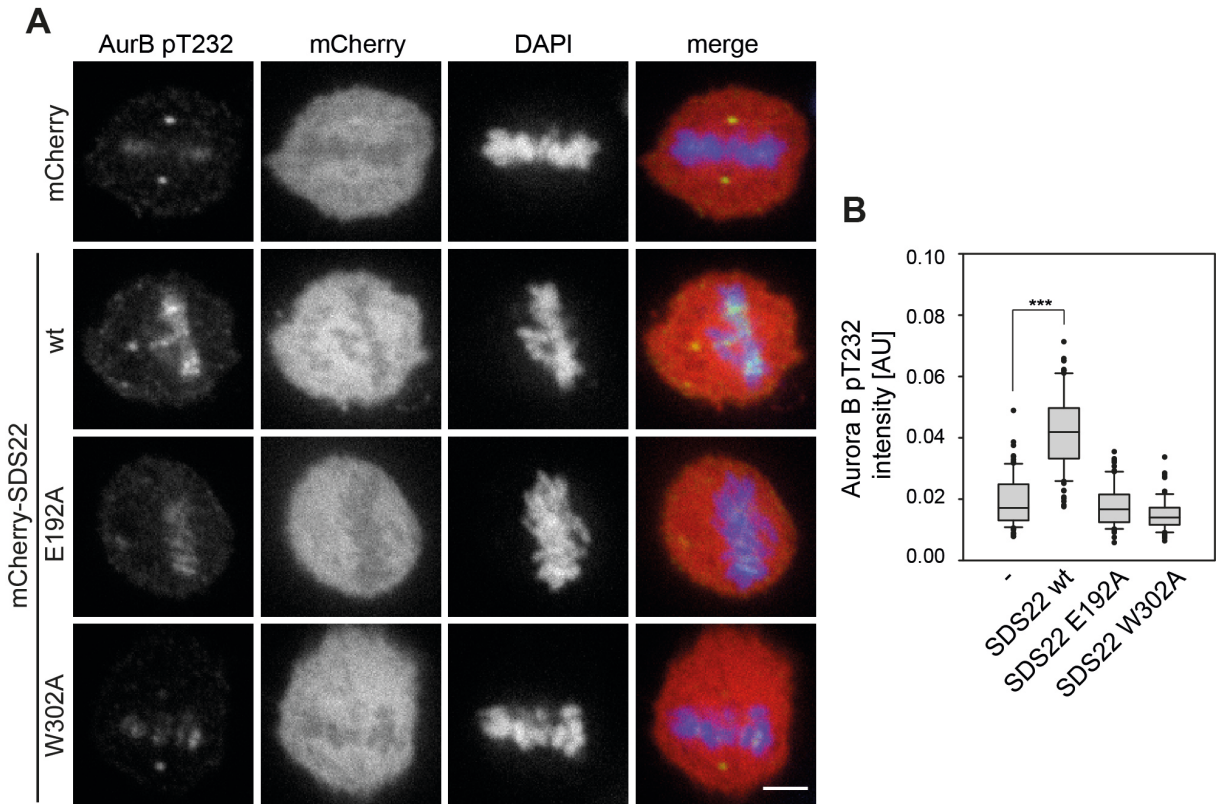

Figure 3.17 Increased Aurora B activity in SDS22 overexpressing cells depends on the PP1-binding ability of SDS22. A HeLa cells were transfected with wild type SDS22, SDS22^{E192A}, or SDS22^{W302A} tagged with a red fluorophore or with a red fluorophore alone for 48 h before fixation, and staining with anti-Aurora B pT232 antibodies and with DAPI. Representative confocal images are shown. **B** Quantification of **A**. The intensity of Aurora B pT232 staining on chromatin in transfected cells was quantified in 3 independent experiments with n ≥ 20 cells per condition and plotted as a box plot with median, lower and upper quartiles (line and box), 10th and 90th percentiles (whiskers), and outliers (●).P-values were calculated using a Mann-Whitney-*U* test (***, p ≤ 0.001).

In an identical experimental setup, also the influence of I3 or NIPP1 overexpression on the Aurora B phosphorylation level was tested. Before, we found that PP1γ is depleted from kinetochores, when I3 or NIPP1 was overexpressed. As PP1 localization to KNL1 is important for its function in opposing Aurora B activity (Liu et al., 2010), we expected to find increased Aurora B autophosphorylation upon I3 or NIPP1 overexpression. As a control, I3$^{V41A/W43A}$, which is deficient in binding to PP1, was expressed. HeLa cells were transfected with the respective constructs for 48 h

and Aurora B pT232 was monitored as before. As expected, GFP-I3 as well as NIPP1-GFP overexpression, but not GFP or GFP-I3$^{V41A/W43A}$ overexpression increased the level of active Aurora B on chromatin (Figure 3.18 A and B).

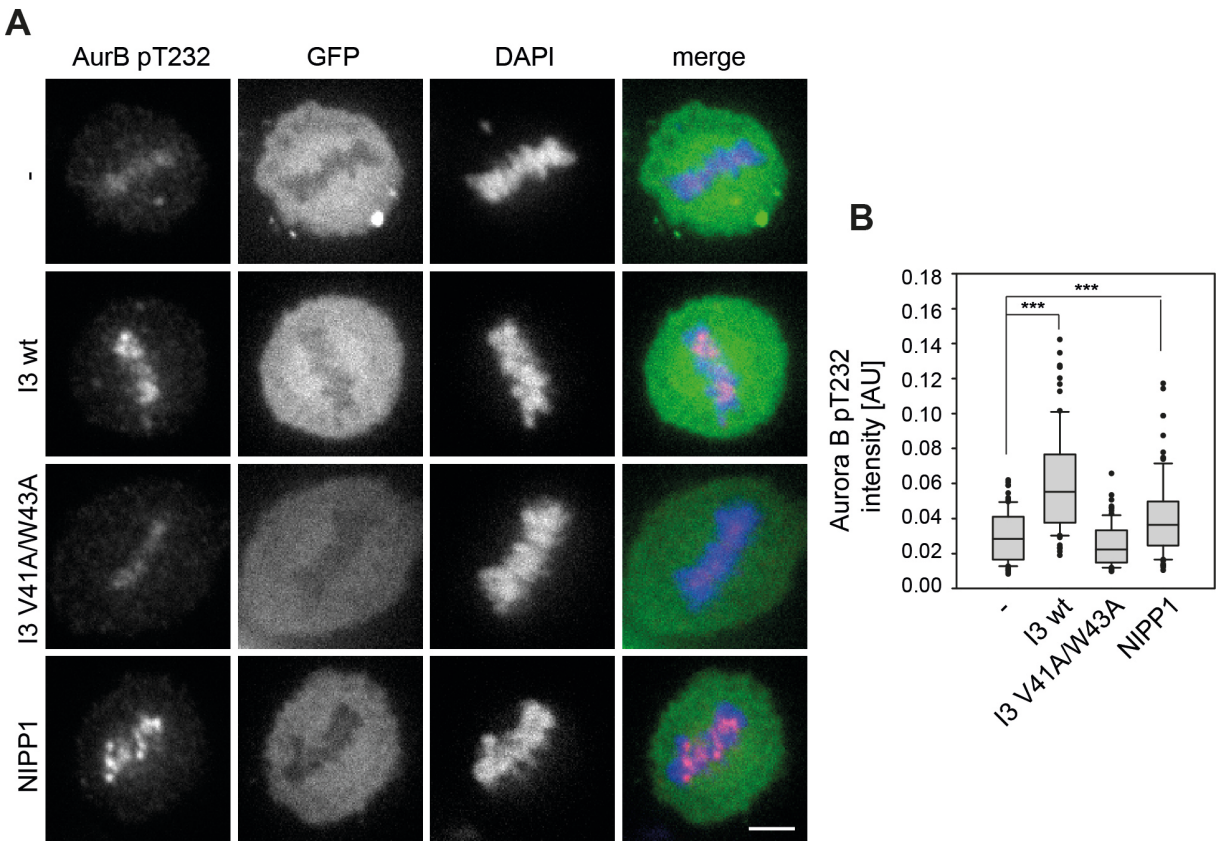

Figure 3.18 I3 or NIPP1 overexpression increases Aurora B activity. A HeLa cells were transfected with wild type I3, I3$^{V41A/W43A}$, or NIPP1 tagged with a green fluorophore or with a green fluorophore alone for 48 h before fixation and staining with anti-Aurora B pT232 antibodies and with DAPI. Representative confocal images are shown. **B** Quantification of **A**. The intensity of Aurora B pT232 staining on chromatin in transfected cells was quantified in 3 independent experiments with n ≥ 20 cells per condition and plotted as a box plot with median, lower and upper quartiles (line and box), 10th and 90th percentiles (whiskers), and outliers (●).P-values were calculated using a Mann-Whitney-*U* test (***, p ≤ 0.001).

3.5 I3 and SDS22 in anaphase

SDS22 silencing was published to cause not only metaphase defects, but also lead to anaphase defects, such as lagging chromosomes, anaphase bridges, and segregation pauses (Wurzenberger et al., 2012). Gerlich and colleagues connect these effects of SDS22 silencing with a function downstream of Aurora B, because they did not detect any effects on Aurora B activity in anaphase but on an Aurora B substrate (Wurzenberger et al., 2012). We wanted to confirm the anaphase defects caused by SDS22 silencing and asked whether SDS22 knockdown would affect Aurora B activity in anaphase. Knowing the relevance of I3 for metaphase progression, we also asked, whether I3 knockdown causes anaphase defects and changes SDS22 localization and Aurora B activity as well in anaphase.

3.5.1 I3 and SDS22 are required for faithful chromosome segregation in anaphase

To test, whether I3 or SDS22 depleted cells show anaphase defects, such as anaphase bridges and lagging chromosomes, HeLa cells were treated with I3, SDS22, NIPP1, or Luc siRNA for 48 h, then fixed and stained with DAPI. Analysis of the samples at a confocal microscope revealed that SDS22, as well as I3 silenced anaphase cells showed increased anaphase defects, compared to cells treated with Luc or NIPP1 siRNA (Figure 3.19 A). Quantification of 3 independent experiments revealed that the number of cells with anaphase defects doubled upon I3 or SDS22 silencing from 6.4 % and 8.6 % for Luc and NIPP1 depletion, to 16.2 % and 16.3 % for SDS22 and I3 depletion, respectively (Figure 3.19 B).

Besides anaphase defects, we also tested for defects in timely progression through anaphase. In contrast to the rather long and variable time span from nuclear envelope breakdown until anaphase onset, the time span for progression through anaphase has low variance, because the spindle assembly checkpoint assures that anaphase starts only from aligned metaphase plates. Hence, slight differences in anaphase timing already disclose a significant anaphase defect.

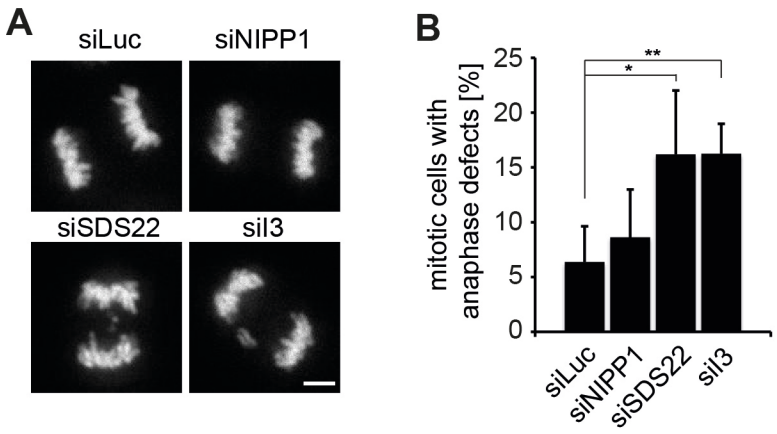

Figure 3.19 siRNA mediated depletion of SDS22 or I3 increases the number of cells with anaphase defects. A HeLa cells were treated with the indicated siRNAs for 48 h, then fixed and stained with DAPI. Representative confocal micrographs are shown. Scale bar, 5 µm. **B** Quantification of **A**. Percentage of mitotic cells with lagging chromosomes or chromosomal bridges. Data from 3 independent experiments with n ≥ 60 cells per condition. Error bars show the standard deviation. P-values were calculated using a Mann-Whitney-*U* test (**, p ≤ 0.01; *, p ≤ 0.05).

To measure the duration of anaphase, we again used the cell line stably expressing H2B-RFP and IBB-GFP. This tool enables us to detect anaphase onset (AO) as well as nuclear envelope formation (NEF) and thus to measure the duration from AO to NEF in movies obtained by live cell imaging. Cells were treated with siRNA against I3, SDS22, NIPP1, or Luc for 48 h then imaged at 37 °C, while supplied with 5 % CO_2 at a confocal microscope. Images were taken every 45 sec for 12.5 h. In Figure 3.20 image sequences of representative anaphase cells in different depletion backgrounds are shown. It is clearly visible that the influx of IBB-GFP starts later in cells depleted for SDS22 or I3 in comparison to cells depleted for Luc or NIPP1. The duration of anaphase was determined in 3 independent experiments and plotted as a histogram showing the relative number of mitotic cells against the time each cell needed until NEF (Figure 3.20 B). While Luc and NIPP1 depleted cells needed on average 5.8 min from AO to NEF, anaphase was prolonged to 7.0 min and 6.8 min in the background of SDS22 and I3 depletion, respectively. Taken into account that progression through anaphase is a very fast and highly regulated process, a delay of one min is already a considerable effect. These data confirm the relevance of SDS22

for proper anaphase progression, and furthermore indicate that also I3 is required for accurate anaphase progression.

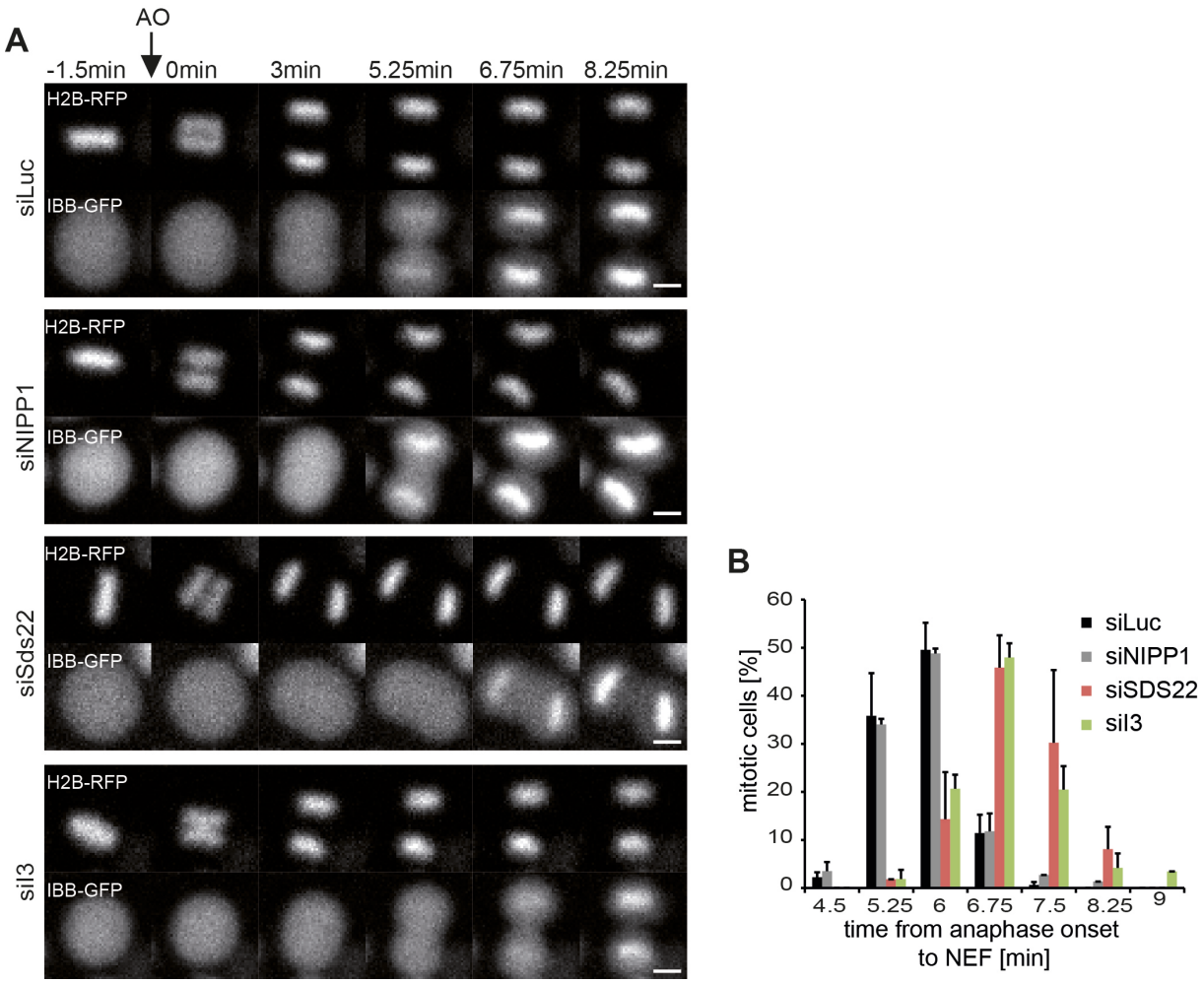

Figure 3.20 siRNA mediated depletion of SDS22 or I3 causes a delay in progression through anaphase. HeLa cells, stably expressing H2B-RFP and IBB-GFP, were depleted with the indicated siRNAs for 48 h, and then imaged in 45 sec intervals for 12.5 h. **A** Representative confocal image sequences from AO until NEF. Scale bar, 10 µm. **B** Mitotic timing from AO until NEF was measured in 3 independent experiments with n = 20-80 cells per condition. In a histogram, the relative number of mitotic cells was plotted against the time, which was needed for progression through anaphase. Error bars show the standard deviation. P-values were calculated using a Mann-Whitney-*U* test.

3.5.2 SDS22 localizes to anaphase kinetochores in the absence of I3

Since we found anaphase defects in cells depleted for I3, we asked next, whether these findings correlate with a persisting accumulation of SDS22 at kinetochores. We again treated SDS22-GFP cells with the respective siRNAs for 48 h and then fixed and stained the cells with DAPI. Analysis at a confocal microscope revealed that SDS22 localizes visibly to anaphase kinetochores in I3 depleted cells, whereas no localization of SDS22 could be observed in Luc and NIPP1 depleted cells (Figure 3.21 A).

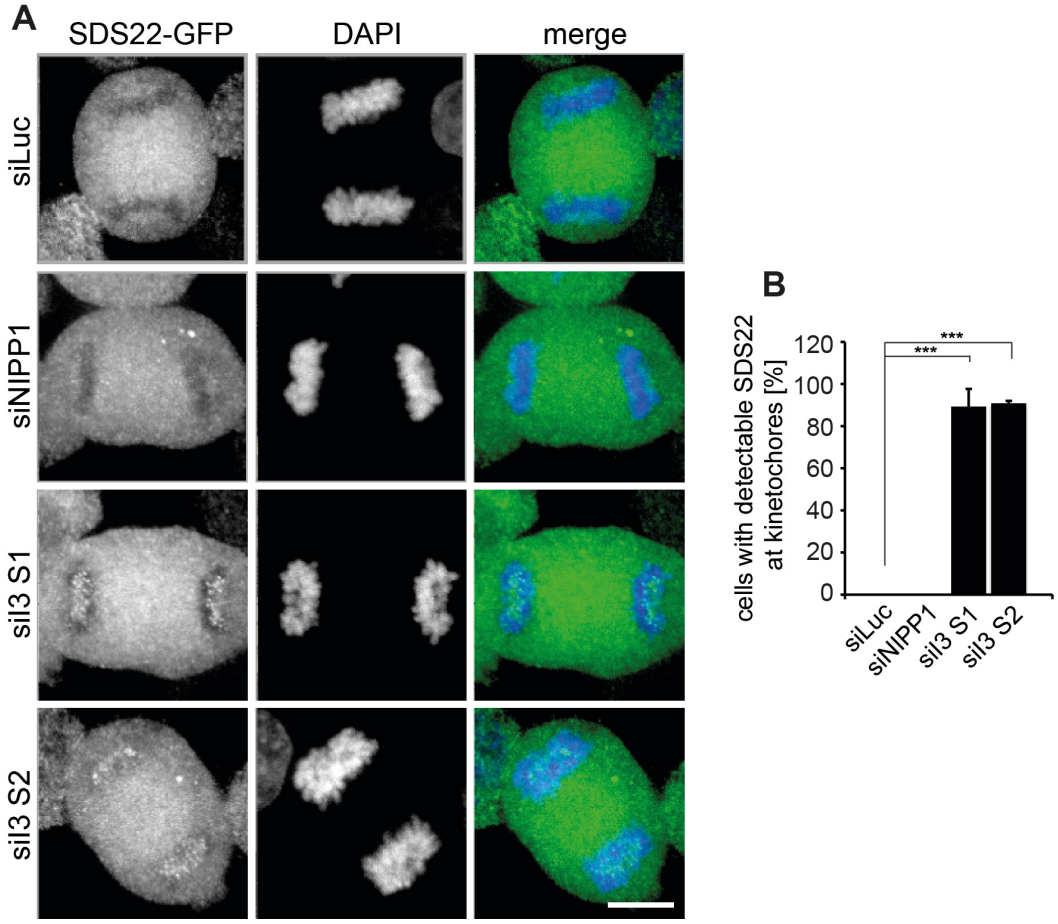

Figure 3.21 SDS22 localizes to anaphase kinetochores in the absence of I3. A HeLa cells stably expressing SDS22-GFP were treated with the indicated siRNAs for 48h and then fixed and stained with DAPI. Maximum intensity projections of representative confocal fluorescence microscopy images are shown. Scale bar, 10 µm. **B** At least 20 confocal images of cells in anaphase were analyzed for kinetochore localization of SDS22 in 3 independent experiments. Error bars show the standard deviation. P-values were calculated using a Mann-Whitney-*U* test (***, $p \leq 0.001$).

In 3 independent experiments, cells with visible amounts of SDS22 at anaphase kinetochores were counted. The quantification revealed that a kinetochore-localization was observable in more than 85 % of all I3-silenced anaphase cells (Figure 3.21 B). Therefore, the anaphase defects in I3 depleted cells correlate with a persisting accumulation of SDS22 at anaphase kinetochores.

3.5.3 Active Aurora B persists on anaphase chromatin in I3 or SDS22 silenced cells

Under normal conditions, Aurora B changes its localization from centromeres to the spindle midzone at anaphase onset. As SDS22 persisted on kinetochores in I3 depleted anaphase cells, we asked, whether also Aurora B persists on anaphase chromatin. Furthermore, also SDS22 depletion could potentially cause persistence of Aurora B on anaphase chromatin. To test this, HeLa cells were depleted for I3, SDS22, NIPP1, or Luc for 48 h, and Aurora B protein level and T232 phosphorylation level were monitored as before.

As expected, neither Aurora B nor phospho-Aurora B could be detected on chromatin in Luc or NIPP1 silenced anaphase cells. Intriguingly, in case of SDS22 or I3 depletion, Aurora B protein and phospho-Aurora B staining persisted on anaphase chromatin (Figure 3.22 A). Again the effect of SDS22 silencing on Aurora B was stronger than the effect of I3 silencing, as indicated from box plots showing the quantification of signal intensities from 3 independent experiments. However, both effects were significant (Figure 3.22 B). Hence, I3 and SDS22 are not only required for balancing Aurora B activity in metaphase, but also in anaphase.

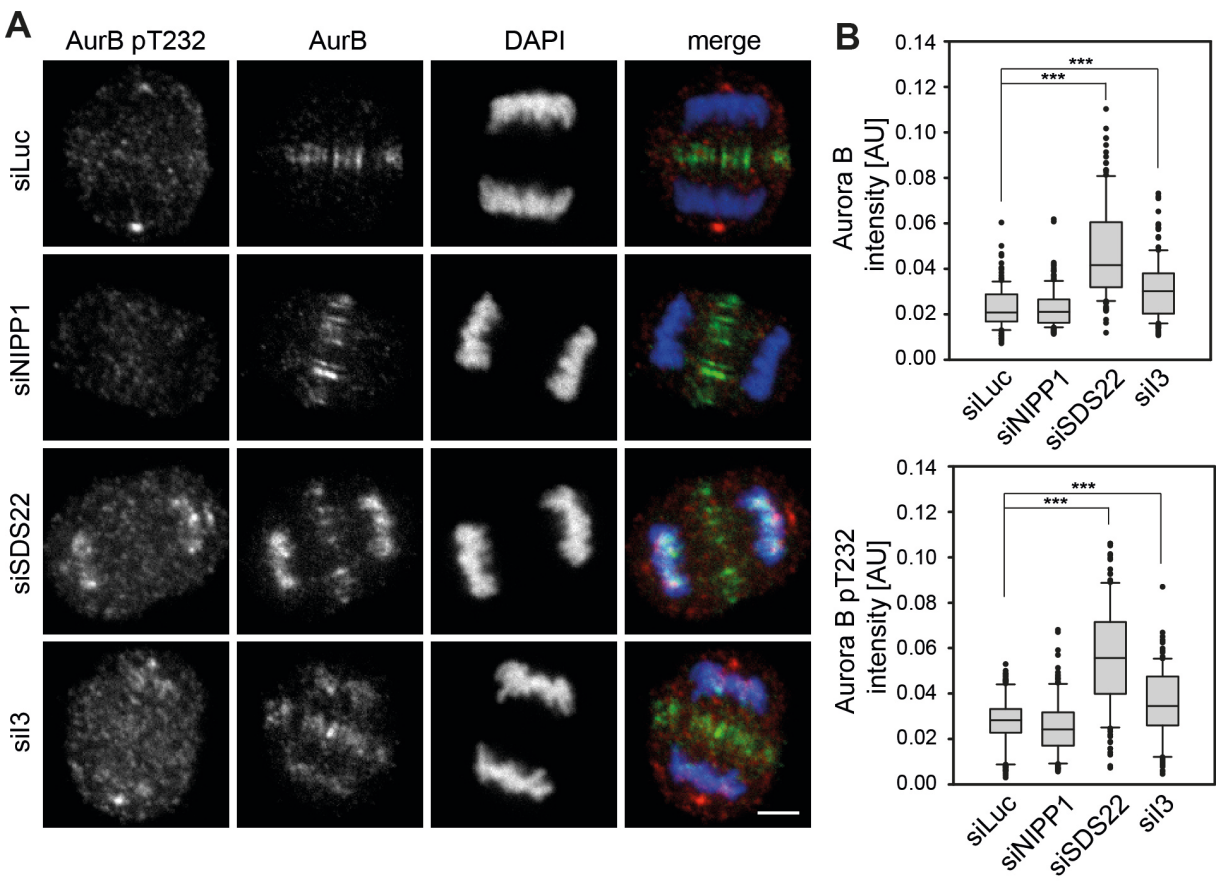

Figure 3.22 siRNA mediated depletion of SDS22 or I3 causes persistence of active Aurora B on anaphase chromatin. A HeLa cells were treated with siRNA for the indicated proteins for 48 h before fixation. Immunofluorescence staining was performed as in Figure 2.16. Representative confocal images are shown. Scale bar, 5 µm. **B** Quantification of **A**. The intensity of Aurora B total protein and Aurora B phosphorylation on chromatin was quantified in 3 independent experiments with n ≥ 50 cells per condition and plotted as box plots with median, lower and upper quartiles (line and box), 10th and 90th percentiles (whiskers), and outliers (●).P-values were calculated using a Mann-Whitney-*U* test (***, p ≤ 0.001).

3.6 Regulation of I3 in balancing PP1-SDS22 association with kinetochores

So far, we found that I3 balances SDS22 binding to kinetochores and thereby influences PP1 activity, because exaggerated SDS22 binding to kinetochore-localized PP1 has an inhibitory effect on PP1. To better understand this mechanism, we asked, if I3 is regulated so that it is able to balance SDS22 binding specifically. At least three ways of I3 regulation are thinkable. First, binding of I3 to PP1-SDS22 could be directly regulated via changes in its expression level during mitosis. Second, the binding affinity of I3 to PP1-SDS222 could be altered by posttranslational modifications. And third, an indirect regulation of I3 binding to PP1-SDS22 is possible, including further binding partners, which would interact with I3 or with the trimeric complex to change its properties. As part of this thesis we explored, whether I3 is regulated via its expression level or posttranslational modifications.

3.6.1 The trimeric complex exists in mitosis

First, we asked whether there are changes in the formation of the trimeric complex in mitotic cells in comparison to S-Phase cells and exponentially growing cells. To specifically test this, SDS22-GFP was immunoprecipitated from HeLa SDS22-GFP cell extracts using beads coupled to GFP-nanobodies. The immunoprecipitates were analyzed for co-immunoprecipitation of PP1 and I3 by Western blotting. To obtain mitotic cell extracts, the cells were treated for 16 h with nocodazole, which activates the SAC and arrests the cells in prometaphase. S-Phase cell extracts were obtained by treating the cells for 16 h with hydroxyurea, which leads to an S-Phase arrest due to activation of the intra-S checkpoint. Additionally, a sample was treated with DMSO and served as a control. To assure that only specific binding to the precipitated SDS22 is detected, a cell extract from HeLa cells stably expressing GFP treated for 16 h with DMSO was analyzed in parallel.

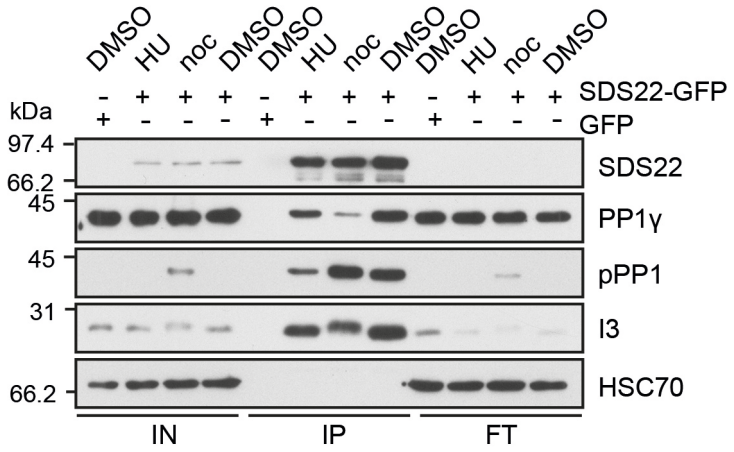

Figure 3.23 The ternary complex exists in mitosis. Extracts were prepared from HeLa cells stably expressing SDS22-GFP after treating for 16 h with hydroxyurea to arrest the cells in S-Phase, with nocodazole to arrest the cells in mitosis or with DMSO representing exponentially growing cells. As a control, HeLa cells stably expressing GFP were lysed after 16 h treatment with DMSO. GFP-SDS22 was isolated from cell extracts using beads coupled to recombinant GFP-nanobodies. The input samples (IN, 2 %), precipitates (IP, 100 %) and flow through samples (FT, 2 %) were analyzed by Western blotting with antibodies specific for the indicated proteins. HSC70 served as a loading control.

The Western blot analysis of input and immunoprecipitate samples revealed that similar amounts of SDS22-GFP were expressed and also precipitated in the different cell populations (Figure 3.23). PP1γ was co-isolated with SDS22 in all populations, but not with GFP alone. However, surprisingly, less PP1γ was found to bind SDS22 in the mitotic fraction. A possible reason for a decreased binding of PP1γ to SDS22 in mitosis could be the phosphorylation state of the phosphatase, as PP1 is phosphorylated by the mitotic kinase CDK1 at T320 in mitosis (Wu et al., 2009). When staining PP1 phosphorylated at T320 with specific antibodies, a signal is detected in the input lane of nocodazole treated cells, as expected. Interestingly, phosphorylated PP1 coprecipitates with SDS22 in all samples, while, as expected, less phosphorylated PP1 is found in S-Phase arrested cells. Thus, SDS22 binds PP1γ independently of its T320 phosphorylation.

Also I3 coprecipitated with all SDS22-GFP samples, but not with the GFP sample. However, also in the case of I3, we found less protein coprecipitating with SDS22-GFP in the mitotic fraction. This is expected, since I3 cannot bind SDS22 directly, but only via PP1. When analyzing I3 levels, it became apparent that mitotic I3 protein in the input lane as well as in the lane of the immunoprecipitation migrated slightly slower than interphase I3. This slight increase in the apparent molecular weight of I3 could hint to a posttranslational modification, which occurs specifically during mitosis.

3.6.2 SDS22 protein level, but not I3 protein level is slightly upregulated during mitosis

To test, whether the decreased binding of I3 and PP1γ to SDS22 during mitosis is caused by changes in the protein level during mitosis, cell extracts were prepared from synchronized HeLa cells at different cell cycle stages and the protein levels of I3, PP1γ and SDS22 were determined by Western blot analysis. To synchronize the cells, a double thymidine treatment was applied to HeLa cells to arrest them in S-Phase arrest. Cell extracts were prepared a different time points after release from S-Phase by thymidine wash out. Additionally, also cell extracts prepared from HeLa cells treated with hydroxyurea for S-Phase arrest, with nocodazole for mitotic arrest, or with DMSO as a control, were analyzed by Western blot analysis. To control the cell cycle state of the different samples, the blot was stained with antibodies specific for the S-Phase marker cyclin E and the mitosis marker Histone 3 phosphorylated at S10. As expected, hydroxyurea, as well as thymidine treated cell extracts displayed cyclin E staining (Figure 3.24). Nocodazole treated cell extracts, as well as extracts from cells released for 8-10 h from double thymidine block were in mitosis, as indicated by a Histone 3 pS10 staining in the corresponding lanes. Equal loading was verified by staining with HSC70 specific antibodies. Inspection of the I3 and PP1γ protein levels at different cell cycle stages revealed no differences in the expression level between S-Phase, mitosis, and G1 Phase. However, the SDS22 level was slightly increased during mitosis (10 h after release from double thymidine block). However, a regulation of I3 or PP1γ via their protein level can be excluded and also the slight increase in SDS22 protein level cannot fully explain the decrease in complex formation in mitosis.

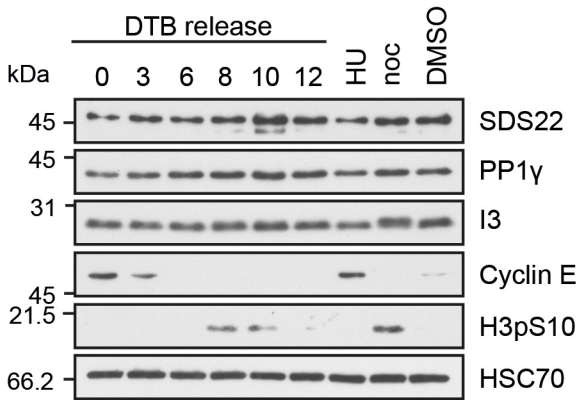

Figure 3.24 Expression levels of PP1γ and I3 are not altered during cell cycle but SDS22 protein level is slightly increased in mitosis. HeLa cells were arrested in S-Phase by double thymidine treatment. Extracts were prepared at the indicated time points (in hours) after release from S-Phase arrest. HeLa cells treated for 16 h with hydroxyurea (HU), nocodazole (noc), or DMSO were used as controls. Lysates were analyzed by Western blotting with antibodies specific for SDS22, PP1γ, and I3 as well as H3pS10 as a marker for mitosis, Cyclin E as a marker for S-Phase, and HSC70 as a loading control.

3.6.3 The non-phosphorylatable mutant of I3, $I3^{AAAEA}$, is less efficient in SDS22 binding

We found the Western blot band corresponding to I3 in mitosis to migrate slightly slower than the one corresponding to interphase I3. This is a possible hint for a mitotic posttranslational modification. Therefore we asked next, whether the binding of I3 to PP1 and SDS22 might be regulated by posttranslational modifications of I3. A mass spectrometry screen searching for mitotic phospho-sites revealed five phosphorylation sites in I3 (S73, S74, T75, S77, and T109) (Dephoure et al., 2008). Yet, the biological relevance of such phospho-sites is unclear. Therefore, we wondered, if these mitotic phospho-sites might specifically regulate I3 binding to PP1γ-SDS22. To address this question, we generated mutants mimicking the phosphorylated and the unphosphorylated state by exchanging the serine and threonine residues by glutamic acid or alanine. As four of the five phosphorylation sites are neighboring, the following four GFP tagged I3 mutants were generated: I3

S73A/S74A/T75A/S77A, I3 S73E/S74E/T75E/S77E, I3 T109A, and I3 T109E, (referred to as $I3^{AAAEA}$, $I3^{EEEEE}$, $I3^{TA}$, and $I3^{TE}$).

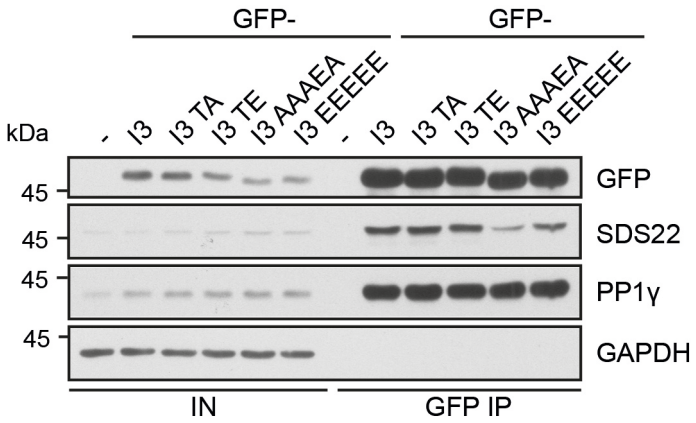

Figure 3.25 PP1 associated with the non-phosphorylatable mutant I3AAAEA binds SDS22 less efficiently. HeLa cells were transfected with GFP-tagged I3, $I3^{TA}$, $I3^{TE}$, $I3^{AAAEA}$, or $I3^{EEEEE}$, or with GFP alone for 48 h. GFP-I3 variants were pulled out from cell extracts by using beads coupled to GFP-nanobodies. The input samples (IN, 2 %) and precipitates (IP, 100 %) were analyzed by Western blotting with antibodies specific for SDS22, PP1γ and GFP to detect overexpressed I3. GAPDH served as a loading control.

To test the binding ability of the different I3 mutants to PP1-SDS22, the GFP-tagged I3 variants were overexpressed in HeLa cells for 48 h, then immunoprecipitated using beads coupled to GFP-nanobodies, and the amounts of co-immunoprecipitated PP1γ and SDS22 were detected by Western blot analysis with specific antibodies. Although the expression levels of the four mutants slightly varied (see input lanes, Figure 3.25), comparable levels were immunoprecipitated. Equal amounts of PP1γ were co-immunoprecipitated with all I3 variants, indicating equal binding affinities of all I3 mutants to PP1γ. However, binding of SDS22 to GFP-$I3^{AAAEA}$-bound PP1γ was clearly reduced, in comparison to binding of SDS22 to wild type I3-bound PP1γ. Also SDS22-binding to GFP-$I3^{EEEEE}$-bound PP1γ was slightly reduced. Both effects indicate that I3 phosphorylation might be relevant for the complex formation with PP1γ and SDS22, although it should be noted that the affinity for PP1γ seems to be unaffected.

3.7 I3-PP1-SDS22 and p97-p37/p47 complexes are both relevant for chromosomal alignment but have different effects on Aurora B

After reconciling the conflicting data on SDS22 and uncovering the relevance of I3 in chromosomal bi-orientation, we wanted to explore the functional link of the trimeric complex to the p97 system, in particular to p37 and p47. Since we identified I3 to balance Aurora B activity via SDS22 localization at the kinetochore and thereby playing a role in chromosome congression, we next wanted to test, whether p37 and p47 are also required for chromosome congression. In a second step, we asked, whether p37 or p47 might regulate Aurora B. These experiments provide only first hints on a potential role of p37 and p47 on Aurora B. However, due to time limitations, further experiments could not be performed.

3.7.1 p37 is required for chromosome congression

To address the question whether p37 or p47 is involved in chromosome congression, we tested the effect of p37 or p47 silencing on chromosomal alignment in metaphase cells. As p37 and p47 have highly homologous sequences they potentially have overlapping functions. Therefore we silenced not only one or the other protein, but also both in a double knockdown. HeLa cells were treated with siRNAs targeting Luc alone, p37 and Luc, p47 and Luc, or p37 and p47. After 48 h, extracts were prepared and the knockdown efficiency was determined by Western blot analysis. p37 and p47 siRNA, both deplete the respective proteins efficiently, although the siRNA targeting p47 also partially depletes p37 (Figure 3.26 A). In contrast, the protein level of p97 stayed unaffected by either of the knockdowns and served as a loading control. In a next step, cells depleted for the respective proteins were fixed and stained with DAPI for microscopic analysis of chromosomal congression. Consistent with Figure 3.1 C, under control conditions, 7 % of all metaphase cells displayed misaligned chromosomes (Figure 3.26 B). When depleting p37 and Luc, or p37 and p47 the number of cells with congression defects doubled, while only a minor increase was measured in the p47 and Luc depleted sample. However, only the increase in misalignment upon p37 and Luc knockdown was significant, because the number of cells with congression defects upon p37 and p47 depletion varied strongly between

single experiments (p = 0.0789). The slight increase in the number of cells with misaligned chromosomes in case of p47 depletion can be explained with the partial codepletion of p37. This result provides a first indication, that p37, but not p47 is required for proper chromosomal alignment.

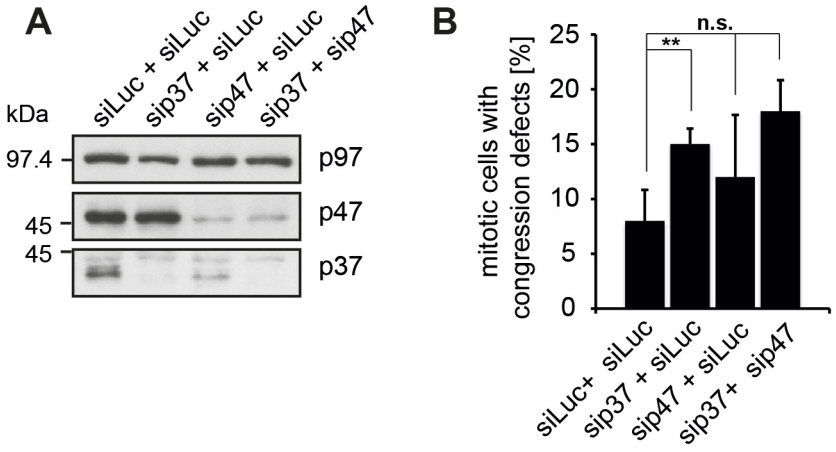

Figure 3.26 siRNA mediated depletion of p37 causes congression defects. A HeLa cells were treated with the indicated siRNAs for 48 h and lysates were analyzed by Western blotting with respective antibodies. **B** Cells treated as in **A** were fixed and stained with DAPI. The chromosomal alignment of cells in metaphase was quantified in 3 independent experiments with n ≥ 50 cells per condition. Error bars show the standard deviation. P-values were calculated using a Mann-Whitney-*U* test (**, p ≤ 0.01; n.s., not significant).

3.7.2 p37 and p47 silencing decreases Aurora B activity in metaphase

In a next step, we tested, whether the defects in chromosome congression found upon p37 silencing could originate from an altered Aurora B activity or localization. Such finding would also provide a potential functional link to the I3-PP1-SDS22 complex. So, HeLa cells were again treated with Luc, p37 and Luc, p47 and Luc, or p37 and p47 siRNA for 48 h. Then, the cells were fixed and stained for Aurora B and Aurora B pT232 with specific antibodies and with DAPI.

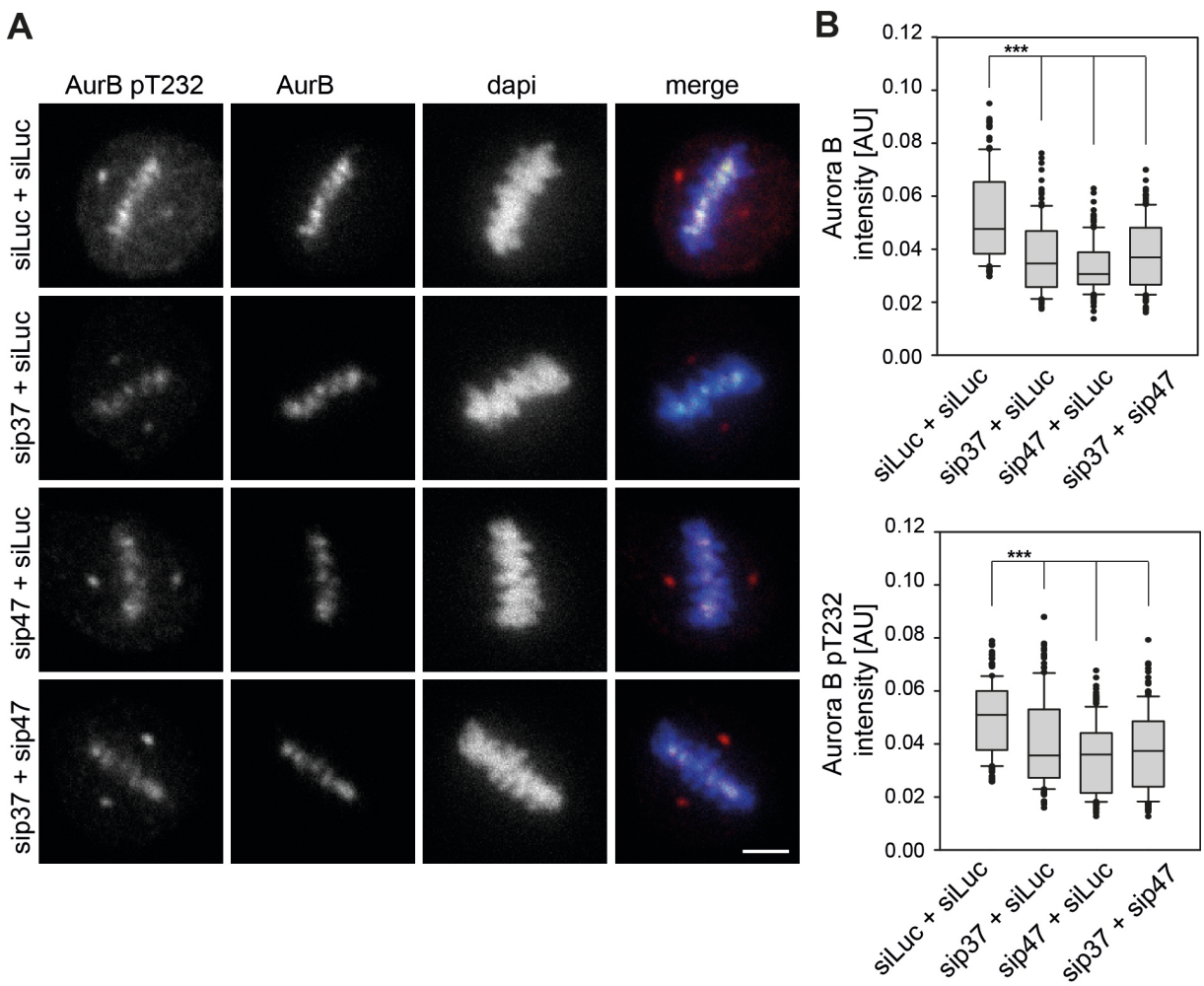

Figure 3.27 siRNA mediated depletion of p37 or p47 decreases Aurora B protein level and activity in metaphase. A HeLa cells were treated with siRNA for the indicated proteins for 48 h before fixation. An immunofluorescence staining was performed with antibodies specific for Aurora B and Aurora B phosphorylated at T232. Representative confocal images are shown. Scale bar, 5 µm. **B** Quantification of **A**. The intensities of Aurora B and Aurora B pT232 staining on chromatin were quantified in 3 independent experiments with n ≥ 50 cells per condition and plotted as box plots with median, lower and upper quartiles (line and box), 10th and 90th percentiles (whiskers), and outliers (●). P-values were calculated using a Mann-Whitney-*U* test (***, p ≤ 0.001).

Inspection at a confocal microscope revealed a decrease in Aurora B protein and activity on metaphase chromatin in p37, p47, as well as p37 and p47 depleted cells in comparison to Luc depleted cells (Figure 3.27 A). The signal intensities on chromatin were quantified in 3 independent experiments with at least 50 metaphase

cells per condition. The decrease in both Aurora B protein level, as well as Aurora B autophosphorylation was significant (Figure 3.27 B). As p47 siRNA codepletes p37, the effect of p47 depletion is possibly p37-related. This result suggests that Aurora B is possibly regulated by p37. Whether this regulation might be via I3-PP1-SDS22 could not be addressed in this thesis due to lack of time.

4 Discussion

PP1 and Aurora B activities have to be dynamically balanced to achieve chromosomal bi-orientation and to satisfy the spindle assembly checkpoint, allowing the cell to proceed through anaphase. PP1 activity at the kinetochore is so far thought to be controlled by the amount of PP1, which is localized to the kinetochore. Previous data suggest that the localization is mediated by KNL1 and SDS22 (as well as CENP-E and KIF18A), acting as targeting PIPs (Liu 2019, Posch 2010, Kim 2010, Meadows 2011). In this thesis, we find that SDS22 is not required for PP1 localization to kinetochores, but influences the activity of KNL1-bound PP1. Our data indicate furthermore that SDS22 is not a simple positive regulator of PP1 activity towards Aurora B, but could possibly act as a PP1 chaperone. Moreover, we find I3 to be required for PP1 activity at kinetochores by preventing SDS22 association with kinetochore-localized PP1. In addition, we collected initial indications that mitotic phosphorylation of I3 could possibly regulate the SDS22-binding affinity for I3-PP1. We also find potential hints that p97-p37/p47 could participate in the regulating of Aurora B activity by PP1.

In summary, the data collected in this thesis provide new insights into the function of SDS22 on PP1, which question a specific role of SDS22 at the kinetochore. Moreover, we identified I3 as a factor, which balances SDS22 localization at the kinetochore. Additionally, the data obtained from this work provide first insights into a possible role of p97-p47/p37 on I3-PP1-SDS22, which will facilitate further studies revealing the functional relationship between I3-PP1-SDS22 and p97-p47/p37.

4.1 The role of SDS22 in regulating PP1 activity at the kinetochore

The role of SDS22 at mitotic kinetochores has been investigated previously by two independent research groups. However, their data are contradictory in two crucial points. In 2010, Swedlow and colleagues found SDS22 to localize to kinetochores

from prometaphase until anaphase (Posch et al., 2010). They furthermore identified SDS22 as a PP1 subunit, that mediates targeting PP1 to kinetochores in mammalian cells, as they found depletion of SDS22 to decrease PP1 levels at kinetochores (Posch et al., 2010). Additionally, they showed that PP1-targeting by SDS22 is required for PP1 activity in counteracting Aurora B, as SDS22 depletion increased Aurora B autophosphorylation, and that silencing of SDS22 causes chromosome segregation defects. In 2012, Gerlich and coworkers provided additional data confirming the congression defects upon SDS22 depletion, and SDS22-dependent counteraction of Aurora B by PP1 (Wurzenberger et al., 2012). However, they could not detect effects on Aurora B autophosphorylation at the kinetochore, but found increased Aurora B substrate phosphorylation when depleting SDS22. Therefore, they suggested PP1 to act downstream of Aurora B. Furthermore, they could not detect SDS22 at kinetochores (Wurzenberger, personal communication), which is in line with results published by Lampson and colleagues (Liu et al., 2010) and with results obtained by Bollen and colleagues (Lesage, personal communication), who as well failed to detect SDS22 at kinetochores.

Our data confirmed SDS22 to be required for chromosomal congression. However, we did not observe decreased levels of PP1 at kinetochores in SDS22-depleted cells, which questions PP1 localization to kinetochores being SDS22-dependent. Furthermore, we did not detect SDS22 at kinetochores, when expressed at endogenous levels. Only by transiently overexpressing SDS22, a colocalization with PP1 at kinetochores could be observed, suggesting that SDS22 does not localize quantitatively to kinetochores under control conditions. We conclude from these results that SDS22 does not function as a targeting subunit of PP1. Still our data provide evidence that the discrepancy between Swedlow's group, who detected SDS22 at kinetochores and Lampson's, Gerlich's, and Bollen's groups, who failed to detect SDS22 at that site, could be explained by differences in the expression level.

We also revisited the effect of SDS22 depletion on Aurora B activity. Consistent with Swedlow's data, we found an increase in Aurora B autophosphorylation at T232upon SDS22 silencing. In addition, we also detected a slight increase in Aurora B protein level at kinetochores, which was not observed by Swedlow and colleagues (Posch et al., 2010). However, this increase is explainable by the positive feedback loop between Aurora B and PP1-Repo-Man, which allows active Aurora B to promote its

own targeting to chromosomes, as inhibitory phosphorylation of Repo-Man by Aurora B prevents PP1-dependent dephosphorylation of the Aurora B targeting site H3pT3 (Qian et al., 2013). From the increase in Aurora B activity upon SDS22 depletion, we conclude that SDS22 is required for PP1 activity, without being required for PP1 targeting to kinetochores.

As PP1 binding to kinetochores is SDS22 independent and SDS22 is not detectable at kinetochores under control conditions, one could question whether the effects caused by SDS22 depletion are mediated by PP1. However, our experiments indicate that wild type SDS22, but not its PP1-binding deficient mutants, have an effect on Aurora B activity and are able to localize to kinetochores when overexpressed, showing that SDS22 acts in a PP1-dependent manner. Furthermore, these experiments revealed a second effect: SDS22 overexpression inhibited PP1 activity, monitored as an increase in Aurora B activity. This seems to contradict our suggestion that SDS22 is a positive regulator of PP1, as suggested from SDS22 depletion experiments. However these seemingly contradictory findings are in line with genetic interaction experiments in yeast, as here the temperature-sensitive lethality of *ipl1* mutant strains could be rescued by expression of high copy numbers of Sds22, as well as by expression of *sds22* mutants (Peggie et al., 2002; Pinsky et al., 2006; Robinson et al., 2012). The fact that SDS22 is required for PP1 activity, but SDS22 localization to kinetochores upon SDS22 overexpression inhibits PP1 activity, suggests that SDS22 levels at kinetochores have to be tightly regulated. Additionally, it supports our notion that SDS22 is not a simple targeting subunit of PP1.

Based on these findings, we propose that SDS22 acts as a chaperone for PP1, rather than acting as a PP1-targeting PIP. Recently, α4, a PP2A-binding protein, was shown to be a chaperone of PP2A (Jiang et al., 2013). PP2A is a phosphatase, which is closely related to PP1 (Guo et al., 2014). Like PP1, it requires subunit-binding to gain specificity and it’s catalytic site coordinates as well two metal ions to gain enzymatic activity (Bollen et al., 2009). Because of the high structural similarity between PP1 and PP2A, one could possibly draw conclusions from the regulation of one phosphatase to the other. α4 binds preferentially inactive PP2A and stabilizes it in its inactive state. Binding to PP2A is accompanied with a partially unfolding of the phosphatase near the active site, which may help recharging PP2A with metal ions (Jiang et al., 2013). Our data support the hypothesis of a similar function of SDS22

for PP1. We show that SDS22 is required for PP1 activity. Furthermore, SDS22 does not bind PP1 via the RVxF-motif, which is frequently found in PP1 targeting proteins. Instead, SDS22 binds PP1 via leucine-rich repeats, whose binding to the PP1 surface is thought to induce a conformational change in PP1, as Bollen and colleagues found PP1 to become trypsin-sensitive upon binding to SDS22 (Lesage et al., 2007). Moreover, SDS22-binding to PP1 keeps it in an inactive state, as indicated by our overexpression experiments and as shown *in vitro* by Bollen and colleagues (Lesage et al., 2007). Thus, SDS22 could stabilize PP1 in its inactive form, thereby possibly allowing re-activation of PP1 by a different protein.

To further strengthen the hypothesis that SDS22 is a PP1 chaperone, one would have to clarify whether also other PP1-mediated signaling pathways show phenotypes, which could be caused by decreased PP1 activity in the background of SDS22 depletion or overexpression. For example, one would expect Aurora A activity at centrosomes to be increased when SDS22 levels are changed, as PP1 inhibits Aurora A by dephosphorylating it (Satinover et al., 2004). One the other hand, one could argue that Aurora A is closely related to Aurora B, so that an effect on Aurora A does not allow the conclusion of SDS22 being a general factor for PP1. However it is difficult to find PP1 targets, which are definitely not affected by a change in Aurora B activity.

Additionally, one could ask whether there are more similarities between the PP1-SDS22 interaction and the PP2A-α4 interaction. For example, it would be interesting to know whether SDS22 binds preferentially PP1, which is inactive due to loss of its two catalytic metal ions. Finally, a challenging task would be to address the question whether there is a PP1 subunit, which is capable of activating PP1, when bound to SDS22. This would prove that SDS22 does not only stabilize inactive PP1, but is part of a mechanism for PP1 re-activation.

4.2 The role of I3 in regulating SDS22-bound PP1

In this work, the role of I3 in mammalian mitosis was analyzed for the first time. Our data indicate that I3 is essential for proper chromosome bi-orientation, as I3 depletion causes chromosomal misalignment and delays progression through mitosis. As I3 is a PIP, the mitotic defects upon I3 silencing could possibly be explained with a

function of I3 in PP1 regulation at the kinetochore. Indeed, we found an increase in Aurora B activity on metaphase chromosomes upon I3 depletion, suggesting that I3 might be a positive regulator of PP1 in counteracting Aurora B. Such positive regulation of PP1 by I3 was also found in yeast, where Bharucha and colleagues, as well as Robinson and colleagues independently identified mutants of the yeast homologue of I3, Ypi1, to suppress the temperature-sensitive lethality of the *ipl1-2* mutant strain (Bharucha et al., 2008; Robinson et al., 2012). However, also overexpression of Ypi1 was shown to suppress *ipl1* mutant strain lethality, pointing to an inhibitory function of I3 on PP1 (Pedelini et al., 2007). Our data are consistent with an inhibitory effect of I3 overexpression on PP1 activity, as we found increased Aurora B activity on chromatin in metaphase upon overexpression of I3. However, our data also indicate that this is an unspecific effect, as we found that also overexpression of the RVxF motif-containing PIP, NIPP1, increased Aurora B activity on chromatin. Furthermore, overexpression of I3, as well as overexpression of NIPP1 extracted PP1 from the kinetochore, which explains the effect on Aurora B activity. Only overexpression of the I3 mutant, which is deficient PP1-binding, failed to extract PP1 from kinetochores, suggesting that the effect is caused by a competition of RVxF motif-containing PIPs in the cytoplasm (I3 and NIPP1) and kinetochore-localized RVxF motif-containing PIPs (for instance KNL1).

While overexpression of I3 causes unspecific effects in mitosis, the effects caused by I3 silencing were specific, as depletion of NIPP1 did not cause mitotic defects. To further elucidate the phenotype of congression defects and increased Aurora B activity in the background of I3 depletion, we asked whether I3 might localize to kinetochores to balance PP1 activity. However, we could not detect I3 at chromosomes during mitosis. Nevertheless, I3 could also balance PP1 activity at the kinetochore as a cytosolic factor. Thus, we next explored the effect of I3 depletion on the composition of the kinetochore. While, we did not observe any changes in PP1 localization upon I3 silencing, we found increased levels of SDS22 at outer kinetochores in metaphase cells silenced for I3. This phenotype was confirmed to be specific, as silencing with two different siRNA oligomers targeting I3 had the same effect and NIPP1 depletion did not cause SDS22 accumulation at kinetochores. Also reintroducing mCherry-tagged I3, which is resistant to the siRNA, restored the phenotype. However, the informative value of the restoration experiment is limited,

since strong overexpression of RVxF motif-containing PIPs extracted PP1 from kinetochores. Since SDS22 localizes to the kinetochore via PP1-binding, PP1 extraction is likely to remove also SDS22 from kinetochores. Nevertheless, the fact that treatment with two different I3 siRNAs, but not with NIPP1 siRNA led to SDS22 accumulation at kinetochores indicates that this is not an off-target effect. These data suggest I3 does not regulate PP1 localization, but balances PP1 activity indirectly by restricting SDS22 localization to kinetochores. We therefore propose that I3 is essential for the localization of active and SDS22-free PP1 to kinetochores. This could be either achieved by sequestration of SDS22-bound PP1 and thereby preventing its binding to kinetochores, or by releasing SDS22 from SDS22-bound PP1, thereby activating PP1. However, the mechanism of sequestering PP1-SDS22 seems to be more likely, than a release of SDS22 from PP1-SDS22, since Lesage and colleagues showed the I3 builds a stable trimeric complex with PP1-SDS22 (Lesage et al., 2007).

We found that SDS22 itself is not responsible for PP1 targeting to kinetochores. Yet, the fact that we detect SDS22 at kinetochores in I3-depleted cells enables us to investigate by which kinetochore-targeting PIP SDS22-bound PP1 is anchored instead. Localization analysis of SDS22 in I3-silenced metaphase cells, which were additionally depleted of KNL1, revealed that KNL1 is the targeting PIP required for localization of SDS22-bound PP1. Additionally, J. Seiler, a member of our group, further confirmed binding of SDS22 to KNL1-associated PP1 in immunoprecipitations of a soluble KNL1 fragment, which contains the RVxF motif. Also increased binding of SDS22 to KNL1-localized PP1 in the background of I3 depletion in comparison to control conditions could be confirmed by immunoprecipitation experiments (J. Seiler unpublished data). Since KNL1 binds PP1 via an RVxF motif, the formation of a trimeric complex with SDS22, comparable with the ternary complex of SDS22, PP1 and I3, is likely. Furthermore, KNL1 and I3 might compete for binding to PP1-SDS22. However, since the sequence of the RVxF motif is degenerative and differs from PIP to PIP (Heroes et al., 2013), their RVxF motifs may not have the same affinity for PP1. Presumably, unphosphorylated KNL1 might have a higher binding affinity for PP1 than I3, because the RVxF motif of I3 contains a glutamic acid, which is supposed to hinder PP1 binding (Meiselbach et al., 2006). However, the affinity of SDS22-bound PP1 for the respective RVxF motif-containing proteins could be

different from the affinity of PP1 alone, especially, as SDS22 binding leads to a conformational change in PP1 (Lesage et al., 2007).

In conclusion, we propose a model, in which SDS22 binds PP1 to stabilize it in its inactive form (Figure 4.1). This could possibly be part of a regulatory mechanism, which involves charging the catalytic site of inactive or newly synthesized PP1 with metal ions to activate it. I3 binds specifically the PP1-SDS22 complex and thereby prevents its association with other RVxF motif-containing PIPs, like KNL1 at the kinetochore. This mechanism allows binding of active SDS22-free PP1 to KNL1, which is able to fulfill its function in counteracting Aurora B activity.

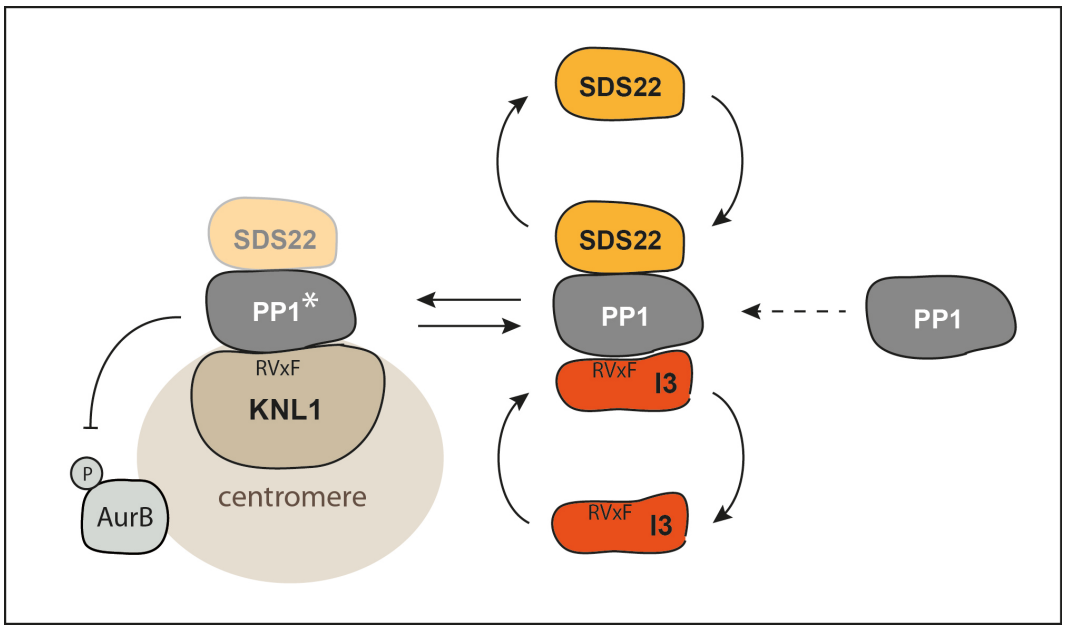

Figure 4.1 Model showing the role of SDS22 and I3 in the regulation of kinetochore-bound PP1. Inactive PP1, which is possibly newly synthesized, is bound by SDS22. I3 binds SDS22-bound PP1 via its RVxF motif, thereby preventing association of inactive SDS22-bound PP1 with other RVxF motif-containing proteins, like KNL1 at the kinetochore. This mechanism allows binding of active PP1 from an SDS22-free pool to the kinetochore, which is able to counteract Aurora B activity. The asterisk marks active PP1.

4.3 The I3-PP1-SDS22 complex in anaphase

With anaphase onset, Aurora B translocates from chromatin to the spindle midzone. The kinesin 6 protein, Mklp2, transports Aurora B to the midzone in a CDK1-dependent manner and PP1-Repo-Man dephosphorylates the Aurora B binding site on chromatin to prevent re-localization of Aurora B to chromatin (Gruneberg et al., 2004; Hummer and Mayer, 2009; Qian et al., 2013). Moreover, chromatin-localized Aurora B is ubiquitinated by Cullin 3 and extracted from chromatin by the p97-Ufd1-Npl4 complex (Dobrynin et al., 2011; Maerki et al., 2009; Sumara et al., 2007).

Wurzenberger and colleagues previously showed that SDS22 silencing causes anaphase defects, like lagging chromosomes, chromosomal bridges and segregation pauses (Wurzenberger et al., 2012). In this work, we confirmed that SDS22 depletion causes anaphase defects and found that also I3 is required for proper progression through anaphase. In contrast to Wurzenberger and colleagues, we furthermore found that Aurora B persisted on chromatin at anaphase onset upon SDS22 or I3 silencing (Wurzenberger et al., 2012). Since our data also indicate that this fraction of Aurora B is active, we conclude that I3-PP1-SDS22-mediated balancing of Aurora B activity in metaphase is a prerequisite for the transfer of Aurora B to the spindle midzone. Furthermore, we suggest that the persistence of active Aurora B on anaphase chromatin is the cause for the detected anaphase defects.

In I3 silenced cells, we additionally detected SDS22 at anaphase kinetochores. This finding suggests that also PP1 is still localized to kinetochores in I3-depleted anaphase cells. Whether PP1 also stays bound to anaphase-kinetochores under control conditions is difficult to detect, as Repo-Man targets PP1 to chromatin in anaphase (Qian et al., 2013; Trinkle-Mulcahy and Lamond, 2006), thereby covering a potentially kinetochore-localized fraction of PP1. However, this result provides first hints that PP1 might be required at anaphase kinetochores under control conditions. Potentially, PP1 could be involved in maintaining stable kinetochore-microtubule attachments in anaphase, as Wurzenberger and colleagues found pauses in chromatin segregation during anaphase in SDS22-depleted cells (Wurzenberger et al., 2012).

4.4 A possible mechanism for I3 function

Our data so far suggest that SDS22 acts as a chaperone, which stabilizes inactive PP1. Additionally, we showed that increased localization of SDS22 to kinetochores by overexpression, as well as by I3 depletion inhibits PP1 activity in counteracting Aurora B. These data indicate that I3 is required for restricting SDS22 localization to kinetochores, so that instead SDS22-free PP1 can localize to kinetochores, which is active and capable in counteracting Aurora B. But what is the actual function of I3 when bound to PP1-SDS22? There are at least two possible explanations for its properties.

First, I3 could function as a chaperone assisting SDS22 in stabilizing and reactivating PP1. This would imply that the effects of I3 silencing on Aurora B activity and SDS22 localization to kinetochores are side effects, which would also be observable in other PP1-related pathways. Under the assumption that SDS22 acts on PP1, like the chaperone α4 on PP2A, the function of I3 could be similar to the function of PTPA on PP2A, which may act in concert with α4 (Guo et al., 2014). By binding of PTPA to PP2A, it orients the ATP phosphoryl groups, so that they bind directly the active site of PP2A, thereby modulating its metal-ion binding preferences (Guo et al., 2014). Via this mechanism PP2A is activated by PTPA binding. However, there is no strong evidence for such function of I3. The only indication is provided by Zhang and colleagues, as they found a second PP1-binding motif in I3, which, as they propose, could possibly bind the active site of PP1 (Zhang et al., 2008). However, Lesage and colleagues found the inactivation of PP1 by SDS22 *in vitro* not to be affected by the addition of I3 (Lesage et al., 2007), which argues against a function of I3 in activating SDS22-bound PP1.

Second, I3 could function by controlling the amount of SDS22-bound PP1, which is accessible for other RVxF motif-containing proteins, by specifically sequestering PP1-SDS22. Thereby it would increase the relative fraction of active PP1, which is free to bind RVxF motif-containing proteins, for instance at the kinetochore. If sequestration of PP1-SDS22 would be the main function of I3, it is likely that I3 binding to PP1-SDS22 is regulated to guarantee that a proper level PP1-SDS22 is kept in an I3-bound state. Such regulation would allow dynamic I3 binding to PP1-SDS22, that would be adaptable to different cellular needs.

When examining possible ways of I3 regulation, we found that the I3 protein level is unchanged throughout the cell cycle. However, we found decreased binding of SDS22 to I3-PP1, when mutating S73, S74, T75, and S77 of I3 to alanine or glutamic acid. This sequence of serine and threonine residues is part of a second PP1-binding site found by Zhang and colleagues (Zhang et al., 2008) and was identified as being phosphorylated in mitosis in a mass spectrometry screen by Dephoure and colleagues (Dephoure et al., 2008). The biological relevance of these phospho-sites is unknown so far, but, as they are part of a PP1-binding site, phosphorylation could possibly influence the PP1-binding affinity of I3. Although we find no evidence for an altered binding affinity of I3 for PP1, our data suggest that this second PP1-binding motif may be of importance for the interaction between I3-PP1 and SDS22. However, whether the altered SDS22-binding affinity is a result of phosphorylation or dephosphorylation events, still needs to be tested. As we found decreased SDS22 binding for both, the phospho-mimicking and the unphosphorylatable mutant, also general structural changes in the second PP1-binding motif caused by mutating four neighboring residues could explain the altered SDS22 binding affinity.

However, another piece of data strengthens the hypothesis that SDS22 binding to I3-PP1 might be regulated via phosphorylation. The Western blot band corresponding to I3 from mitotic extracts migrated slightly slower, which is an indication for a mitotic post-translational modification. This could potentially originate from mitotic phosphorylation of S73, S74, T75, and S77. Interestingly, this potential mitotic phosphorylation correlated with a decreased binding of PP1-I3 to SDS22, as found in immunoprecipitations from mitotic extracts. This result is in line with our data, showing that less SDS22 coprecipitated with I3 mutated at S73, S74, T75, and S77. Together, these data provide first evidence that binding of SDS22 to I3-PP1 might be regulated via phosphorylation. However, it is an open question whether the slower migrating variant of I3 is phosphorylated at S73, S74, T75, and S77. Furthermore, it also still needs to be clarified whether this phosphorylation is the cause for the decreased binding of I3-PP1 to SDS22, as there are also other explanations for a decrease in SDS22 binding to PP1 in mitosis. For instance, SDS22 could, in its function as a chaperone, bind preferentially newly synthesized PP1 to activate it. However, protein synthesis is paused during mitosis.

To further elucidate this potential I3 regulation, one could first test, if dephosphorylation of I3, which was immunoprecipitated from mitotic cell extracts, would reverse the shift of the Western blot band corresponding to mitotic I3 to higher molecular weights. Furthermore, one could test in an *in vitro* experiment whether phosphorylation of I3 has an impact on the affinity of SDS22 to PP1-I3. Additionally, it would be also interesting to apply a structural analysis to address the question whether the second PP1-binding motif of I3 binds PP1 at its active site under any condition. Finally, it would be interesting to identify the kinase, which is responsible for I3 phosphorylation. Candidates would be mitotic kinases, like CDK1, SAC kinases as well as Aurora B. Uncovering the responsible kinase would associate I3 phosphorylation with a cellular context and thereby help to understand the relevance of I3 phosphorylation.

4.5 The role of p37 and p47 in regulating Aurora B activity

In yeast, the p47 homologue, Shp1, binds the PP1 homologue, Glc7, and positively regulates it, as shown by physical and genetic interactions (Bohm and Buchberger, 2013). Lethality caused by Glc7 overexpression, as well as lethality due to the temperature sensitive *Ipl1-321* (Aurora) mutation could be restored by expression of a Shp1 mutant (Bohm and Buchberger, 2013; Robinson et al., 2012; Zhang et al., 1995). These data indicate that Shp1 is required for Glc7 activity in counteracting Ipl1 in yeast. The fact that D. Ritz from our group found a physical interaction between p97 with the cofactor p47 and PP1, SDS22, as well as I3 in mammalian cells, suggests that also p97 and PP1 act in concert in mammals.

p47 and p37 were shown to extract Aurora A from centrosomes already in prophase of mammalian cells (Kress et al., 2013). Yet, PP1 and SDS22 have only been linked to the regulation of Aurora B (Posch et al., 2010; Wurzenberger et al., 2012). The data presented in this thesis underline the relevance of SDS22 and I3 for balancing PP1 and Aurora B activity. Therefore we tested, whether p47 and p37 may also be required for proper Aurora B activity. Our data show that p37, as well as p47 depletion decreases Aurora B localization on chromatin, which is accompanied with a decrease in Aurora B activity. Additionally, p37 depletion also caused chromosomal congression defects. However, these data do not indicate that Aurora B regulation is

the functional link between I3-PP1-SDS22 and p37/p47, since both, depletion, as well as overexpression of I3 or SDS22 increased Aurora B activity. Still, p97-p47/p37 could be required for PP1 extraction from kinetochores. An increased level of PP1 at kinetochores in the case of p47/p37 silencing would lead to more efficient dephosphorylation of Aurora B. As Aurora B regulates its own targeting (Qian et al., 2013), decreased Aurora B activity would also lead to decreased Aurora B protein level on chromatin. However this scenario would not explain why also SDS22 and I3 were found to bind p97-p47/p37.

Besides PP1 extraction, there is also another possible explanation for the decrease in Aurora B level on chromatin in the case of p47 and p37 depletion. It is known that p97 with its cofactors Ufd1 and Npl4 extracts Aurora B from chromatin to restrict its localization to the centromeric region (Dobrynin et al., 2011). Thus, p47 and p37 depletion could shift p97 complex formation towards complexes containing Ufd1-Npl4, and thereby enforce Aurora B extraction from chromatin by p97 with the help of Ufd1-Npl4.

So, the functional link between p97-p47/p37 and I3-PP1-SDS22 still remains unclear. However, since our data suggest that SDS22 is a chaperone of PP1, which binds and stabilizes inactive PP1, it is unlikely that I3-PP1-SDS22 acts on p97-p47/p37 by dephosphorylating it. Therefore, we assume that rather the p97-p47/p37 complex acts on I3-PP1-SDS22. Possibly, p97-p47/p37 could extract SDS22 or I3 from PP1, or it could specifically bind the I3-PP1-SDS22 complex, for example, to target it for degradation. When further investigating the functional link between p97-p47/p37 and I3-PP1-SDS22, it will be important to test, whether at least one of the complex members is ubiquitinated, when bound by p97-p47/p37. However, the fact that PP1 was found to be ubiquitinated in two independent screens performed in yeast (Peng et al., 2003; Starita et al., 2012), supports the notion that p97-p47/p37 could bind ubiquitinated PP1.

5 References

Acquaviva, C., and Pines, J. (2006). The anaphase-promoting complex/cyclosome: APC/C. Journal of cell science *119*, 2401-2404.

Adams, R.R., Wheatley, S.P., Gouldsworthy, A.M., Kandels-Lewis, S.E., Carmena, M., Smythe, C., Gerloff, D.L., and Earnshaw, W.C. (2000). INCENP binds the Aurora-related kinase AIRK2 and is required to target it to chromosomes, the central spindle and cleavage furrow. Current biology : CB *10*, 1075-1078.

Ainsztein, A.M., Kandels-Lewis, S.E., Mackay, A.M., and Earnshaw, W.C. (1998). INCENP centromere and spindle targeting: identification of essential conserved motifs and involvement of heterochromatin protein HP1. The Journal of cell biology *143*, 1763-1774.

Alessi, D.R., Street, A.J., Cohen, P., and Cohen, P.T. (1993). Inhibitor-2 functions like a chaperone to fold three expressed isoforms of mammalian protein phosphatase-1 into a conformation with the specificity and regulatory properties of the native enzyme. European journal of biochemistry / FEBS *213*, 1055-1066.

Alexandru, G., Graumann, J., Smith, G.T., Kolawa, N.J., Fang, R., and Deshaies, R.J. (2008). UBXD7 binds multiple ubiquitin ligases and implicates p97 in HIF1alpha turnover. Cell *134*, 804-816.

Ballar, P., Shen, Y., Yang, H., and Fang, S. (2006). The role of a novel p97/valosin-containing protein-interacting motif of gp78 in endoplasmic reticulum-associated degradation. The Journal of biological chemistry *281*, 35359-35368.

Barford, D., Das, A.K., and Egloff, M.P. (1998). The structure and mechanism of protein phosphatases: insights into catalysis and regulation. Annual review of biophysics and biomolecular structure *27*, 133-164.

Bayliss, R., Sardon, T., Vernos, I., and Conti, E. (2003). Structural basis of Aurora-A activation by TPX2 at the mitotic spindle. Molecular cell *12*, 851-862.

Beardmore, V.A., Ahonen, L.J., Gorbsky, G.J., and Kallio, M.J. (2004). Survivin dynamics increases at centromeres during G2/M phase transition and is regulated by microtubule-attachment and Aurora B kinase activity. Journal of cell science *117*, 4033-4042.

Berdougo, E., Nachury, M.V., Jackson, P.K., and Jallepalli, P.V. (2008). The nucleolar phosphatase Cdc14B is dispensable for chromosome segregation and mitotic exit in human cells. Cell cycle *7*, 1184-1190.

Bergink, S., Ammon, T., Kern, M., Schermelleh, L., Leonhardt, H., and Jentsch, S. (2013). Role of Cdc48/p97 as a SUMO-targeted segregase curbing Rad51-Rad52 interaction. Nature cell biology *15*, 526-532.

Beskow, A., Grimberg, K.B., Bott, L.C., Salomons, F.A., Dantuma, N.P., and Young, P. (2009). A conserved unfoldase activity for the p97 AAA-ATPase in proteasomal degradation. Journal of molecular biology *394*, 732-746.

Beuron, F., Dreveny, I., Yuan, X., Pye, V.E., McKeown, C., Briggs, L.C., Cliff, M.J., Kaneko, Y., Wallis, R., Isaacson, R.L.*, et al.* (2006). Conformational changes in the AAA ATPase p97-p47 adaptor complex. The EMBO journal *25*, 1967-1976.

Bharucha, J.P., Larson, J.R., Gao, L., Daves, L.K., and Tatchell, K. (2008). Ypi1, a positive regulator of nuclear protein phosphatase type 1 activity in Saccharomyces cerevisiae. Molecular biology of the cell *19*, 1032-1045.

Bishop, J.D., and Schumacher, J.M. (2002). Phosphorylation of the carboxyl terminus of inner centromere protein (INCENP) by the Aurora B Kinase stimulates Aurora B kinase activity. The Journal of biological chemistry *277*, 27577-27580.

Black, B.E., and Bassett, E.A. (2008). The histone variant CENP-A and centromere specification. Current opinion in cell biology *20*, 91-100.

Bohm, S., and Buchberger, A. (2013). The budding yeast Cdc48(Shp1) complex promotes cell cycle progression by positive regulation of protein phosphatase 1 (Glc7). PloS one *8*, e56486.

Bollen, M., Gerlich, D.W., and Lesage, B. (2009). Mitotic phosphatases: from entry guards to exit guides. Trends in cell biology *19*, 531-541.

Bollen, M., Peti, W., Ragusa, M.J., and Beullens, M. (2010). The extended PP1 toolkit: designed to create specificity. Trends in biochemical sciences *35*, 450-458.

Bruderer, R.M., Brasseur, C., and Meyer, H.H. (2004). The AAA ATPase p97/VCP interacts with its alternative co-factors, Ufd1-Npl4 and p47, through a common bipartite binding mechanism. The Journal of biological chemistry *279*, 49609-49616.

Buchberger, A. (2013). Roles of cdc48 in regulated protein degradation in yeast. Sub-cellular biochemistry *66*, 195-222.

Carmena, M., Ruchaud, S., and Earnshaw, W.C. (2009). Making the Auroras glow: regulation of Aurora A and B kinase function by interacting proteins. Current opinion in cell biology *21*, 796-805.

Carmena, M., Wheelock, M., Funabiki, H., and Earnshaw, W.C. (2012). The chromosomal passenger complex (CPC): from easy rider to the godfather of mitosis. Nature reviews Molecular cell biology *13*, 789-803.

Ceulemans, H., and Bollen, M. (2004). Functional diversity of protein phosphatase-1, a cellular economizer and reset button. Physiological reviews *84*, 1-39.

Ceulemans, H., Stalmans, W., and Bollen, M. (2002). Regulator-driven functional diversification of protein phosphatase-1 in eukaryotic evolution. BioEssays : news and reviews in molecular, cellular and developmental biology *24*, 371-381.

Chan, C.S., and Botstein, D. (1993). Isolation and characterization of chromosome-gain and increase-in-ploidy mutants in yeast. Genetics *135*, 677-691.

Chan, Y.W., Jeyaprakash, A.A., Nigg, E.A., and Santamaria, A. (2012). Aurora B controls kinetochore-microtubule attachments by inhibiting Ska complex-KMN network interaction. The Journal of cell biology *196*, 563-571.

Cheeseman, I.M., Chappie, J.S., Wilson-Kubalek, E.M., and Desai, A. (2006). The conserved KMN network constitutes the core microtubule-binding site of the kinetochore. Cell *127*, 983-997.

Cheng, Y.L., and Chen, R.H. (2010). The AAA-ATPase Cdc48 and cofactor Shp1 promote chromosome bi-orientation by balancing Aurora B activity. Journal of cell science *123*, 2025-2034.

Chou, T.F., Brown, S.J., Minond, D., Nordin, B.E., Li, K., Jones, A.C., Chase, P., Porubsky, P.R., Stoltz, B.M., Schoenen, F.J.*, et al.* (2011). Reversible inhibitor of p97, DBeQ, impairs both ubiquitin-dependent and autophagic protein clearance pathways. Proceedings of the National Academy of Sciences of the United States of America *108*, 4834-4839.

Crosio, C., Fimia, G.M., Loury, R., Kimura, M., Okano, Y., Zhou, H., Sen, S., Allis, C.D., and Sassone-Corsi, P. (2002). Mitotic phosphorylation of histone H3: spatio-temporal regulation by mammalian Aurora kinases. Molecular and cellular biology *22*, 874-885.

Dai, R.M., and Li, C.C. (2001). Valosin-containing protein is a multi-ubiquitin chain-targeting factor required in ubiquitin-proteasome degradation. Nature cell biology *3*, 740-744.

Dantuma, N.P., and Hoppe, T. (2012). Growing sphere of influence: Cdc48/p97 orchestrates ubiquitin-dependent extraction from chromatin. Trends in cell biology *22*, 483-491.

Dargemont, C., and Ossareh-Nazari, B. (2012). Cdc48/p97, a key actor in the interplay between autophagy and ubiquitin/proteasome catabolic pathways. Biochimica et biophysica acta *1823*, 138-144.

Decottignies, A., Evain, A., and Ghislain, M. (2004). Binding of Cdc48p to a ubiquitin-related UBX domain from novel yeast proteins involved in intracellular proteolysis and sporulation. Yeast *21*, 127-139.

DeLaBarre, B., and Brunger, A.T. (2005). Nucleotide dependent motion and mechanism of action of p97/VCP. Journal of molecular biology *347*, 437-452.

DeLuca, J.G., Gall, W.E., Ciferri, C., Cimini, D., Musacchio, A., and Salmon, E.D. (2006). Kinetochore microtubule dynamics and attachment stability are regulated by Hec1. Cell *127*, 969-982.

Dephoure, N., Zhou, C., Villen, J., Beausoleil, S.A., Bakalarski, C.E., Elledge, S.J., and Gygi, S.P. (2008). A quantitative atlas of mitotic phosphorylation. Proceedings of the National Academy of Sciences of the United States of America *105*, 10762-10767.

Ditchfield, C., Johnson, V.L., Tighe, A., Ellston, R., Haworth, C., Johnson, T., Mortlock, A., Keen, N., and Taylor, S.S. (2003). Aurora B couples chromosome alignment with anaphase by targeting BubR1, Mad2, and Cenp-E to kinetochores. The Journal of cell biology *161*, 267-280.

Dobrynin, G., Popp, O., Romer, T., Bremer, S., Schmitz, M.H., Gerlich, D.W., and Meyer, H. (2011). Cdc48/p97-Ufd1-Npl4 antagonizes Aurora B during chromosome segregation in HeLa cells. Journal of cell science *124*, 1571-1580.

Emanuele, M.J., Lan, W., Jwa, M., Miller, S.A., Chan, C.S., and Stukenberg, P.T. (2008). Aurora B kinase and protein phosphatase 1 have opposing roles in modulating kinetochore assembly. The Journal of cell biology *181*, 241-254.

Ernst, R., Mueller, B., Ploegh, H.L., and Schlieker, C. (2009). The otubain YOD1 is a deubiquitinating enzyme that associates with p97 to facilitate protein dislocation from the ER. Molecular cell *36*, 28-38.

Erzberger, J.P., and Berger, J.M. (2006). Evolutionary relationships and structural mechanisms of AAA+ proteins. Annual review of biophysics and biomolecular structure *35*, 93-114.

Espeut, J., Cheerambathur, D.K., Krenning, L., Oegema, K., and Desai, A. (2012). Microtubule binding by KNL-1 contributes to spindle checkpoint silencing at the kinetochore. The Journal of cell biology *196*, 469-482.

Fededa, J.P., and Gerlich, D.W. (2012). Molecular control of animal cell cytokinesis. Nature cell biology *14*, 440-447.

Fischle, W., Tseng, B.S., Dormann, H.L., Ueberheide, B.M., Garcia, B.A., Shabanowitz, J., Hunt, D.F., Funabiki, H., and Allis, C.D. (2005). Regulation of HP1-chromatin binding by histone H3 methylation and phosphorylation. Nature *438*, 1116-1122.

Foley, E.A., and Kapoor, T.M. (2013). Microtubule attachment and spindle assembly checkpoint signalling at the kinetochore. Nature reviews Molecular cell biology *14*, 25-37.

Foley, E.A., Maldonado, M., and Kapoor, T.M. (2011). Formation of stable attachments between kinetochores and microtubules depends on the B56-PP2A phosphatase. Nature cell biology *13*, 1265-1271.

Francisco, L., Wang, W., and Chan, C.S. (1994). Type 1 protein phosphatase acts in opposition to IpL1 protein kinase in regulating yeast chromosome segregation. Molecular and cellular biology *14*, 4731-4740.

Franz, A., Orth, M., Pirson, P.A., Sonneville, R., Blow, J.J., Gartner, A., Stemmann, O., and Hoppe, T. (2011). CDC-48/p97 coordinates CDT-1 degradation with GINS chromatin dissociation to ensure faithful DNA replication. Molecular cell *44*, 85-96.

Fuller, B.G., Lampson, M.A., Foley, E.A., Rosasco-Nitcher, S., Le, K.V., Tobelmann, P., Brautigan, D.L., Stukenberg, P.T., and Kapoor, T.M. (2008). Midzone activation of aurora B in anaphase produces an intracellular phosphorylation gradient. Nature *453*, 1132-1136.

Funabiki, H., and Wynne, D.J. (2013). Making an effective switch at the kinetochore by phosphorylation and dephosphorylation. Chromosoma *122*, 135-158.

Garcia-Gimeno, M.A., Munoz, I., Arino, J., and Sanz, P. (2003). Molecular characterization of Ypi1, a novel Saccharomyces cerevisiae type 1 protein phosphatase inhibitor. The Journal of biological chemistry *278*, 47744-47752.

Ghosh, A., and Cannon, J.F. (2013). Analysis of protein phosphatase-1 and aurora protein kinase suppressors reveals new aspects of regulatory protein function in Saccharomyces cerevisiae. PloS one *8*, e69133.

Gibbons, J.A., Kozubowski, L., Tatchell, K., and Shenolikar, S. (2007). Expression of human protein phosphatase-1 in Saccharomyces cerevisiae highlights the role of

phosphatase isoforms in regulating eukaryotic functions. The Journal of biological chemistry *282*, 21838-21847.

Gruneberg, U., Neef, R., Honda, R., Nigg, E.A., and Barr, F.A. (2004). Relocation of Aurora B from centromeres to the central spindle at the metaphase to anaphase transition requires MKlp2. The Journal of cell biology *166*, 167-172.

Guo, F., Stanevich, V., Wlodarchak, N., Sengupta, R., Jiang, L., Satyshur, K.A., and Xing, Y. (2014). Structural basis of PP2A activation by PTPA, an ATP-dependent activation chaperone. Cell research *24*, 190-203.

Guttinger, S., Laurell, E., and Kutay, U. (2009). Orchestrating nuclear envelope disassembly and reassembly during mitosis. Nature reviews Molecular cell biology *10*, 178-191.

Hanzelmann, P., Buchberger, A., and Schindelin, H. (2011). Hierarchical binding of cofactors to the AAA ATPase p97. Structure *19*, 833-843.

Hauf, S., Cole, R.W., LaTerra, S., Zimmer, C., Schnapp, G., Walter, R., Heckel, A., van Meel, J., Rieder, C.L., and Peters, J.M. (2003). The small molecule Hesperadin reveals a role for Aurora B in correcting kinetochore-microtubule attachment and in maintaining the spindle assembly checkpoint. The Journal of cell biology *161*, 281-294.

Hendrickx, A., Beullens, M., Ceulemans, H., Den Abt, T., Van Eynde, A., Nicolaescu, E., Lesage, B., and Bollen, M. (2009). Docking motif-guided mapping of the interactome of protein phosphatase-1. Chemistry & biology *16*, 365-371.

Heo, J.M., Livnat-Levanon, N., Taylor, E.B., Jones, K.T., Dephoure, N., Ring, J., Xie, J., Brodsky, J.L., Madeo, F., Gygi, S.P.*, et al.* (2010). A stress-responsive system for mitochondrial protein degradation. Molecular cell *40*, 465-480.

Heroes, E., Lesage, B., Gornemann, J., Beullens, M., Van Meervelt, L., and Bollen, M. (2013). The PP1 binding code: a molecular-lego strategy that governs specificity. The FEBS journal *280*, 584-595.

Howell, B.J., McEwen, B.F., Canman, J.C., Hoffman, D.B., Farrar, E.M., Rieder, C.L., and Salmon, E.D. (2001). Cytoplasmic dynein/dynactin drives kinetochore protein transport to the spindle poles and has a role in mitotic spindle checkpoint inactivation. The Journal of cell biology *155*, 1159-1172.

Huang, H.S., and Lee, E.Y. (2008). Protein phosphatase-1 inhibitor-3 is an in vivo target of caspase-3 and participates in the apoptotic response. The Journal of biological chemistry *283*, 18135-18146.

Huang, H.S., Pozarowski, P., Gao, Y., Darzynkiewicz, Z., and Lee, E.Y. (2005). Protein phosphatase-1 inhibitor-3 is co-localized to the nucleoli and centrosomes with PP1gamma1 and PP1alpha, respectively. Archives of biochemistry and biophysics *443*, 33-44.

Hummer, S., and Mayer, T.U. (2009). Cdk1 negatively regulates midzone localization of the mitotic kinesin Mklp2 and the chromosomal passenger complex. Current biology : CB *19*, 607-612.

Hurley, T.D., Yang, J., Zhang, L., Goodwin, K.D., Zou, Q., Cortese, M., Dunker, A.K., and DePaoli-Roach, A.A. (2007). Structural basis for regulation of protein phosphatase 1 by inhibitor-2. The Journal of biological chemistry *282*, 28874-28883.

Ito, H., Koyama, Y., Takano, M., Ishii, K., Maeno, M., Furukawa, K., and Horigome, T. (2007). Nuclear envelope precursor vesicle targeting to chromatin is stimulated by protein phosphatase 1 in Xenopus egg extracts. Experimental cell research *313*, 1897-1910.

Jagiello, I., Van Eynde, A., Vulsteke, V., Beullens, M., Boudrez, A., Keppens, S., Stalmans, W., and Bollen, M. (2000). Nuclear and subnuclear targeting sequences of the protein phosphatase-1 regulator NIPP1. Journal of cell science *113 Pt 21*, 3761-3768.

Jelluma, N., Brenkman, A.B., van den Broek, N.J., Cruijsen, C.W., van Osch, M.H., Lens, S.M., Medema, R.H., and Kops, G.J. (2008). Mps1 phosphorylates Borealin to control Aurora B activity and chromosome alignment. Cell *132*, 233-246.

Jentsch, S., and Rumpf, S. (2007). Cdc48 (p97): a "molecular gearbox" in the ubiquitin pathway? Trends in biochemical sciences *32*, 6-11.

Jia, L., Kim, S., and Yu, H. (2013). Tracking spindle checkpoint signals from kinetochores to APC/C. Trends in biochemical sciences *38*, 302-311.

Jiang, L., Stanevich, V., Satyshur, K.A., Kong, M., Watkins, G.R., Wadzinski, B.E., Sengupta, R., and Xing, Y. (2013). Structural basis of protein phosphatase 2A stable latency. Nature communications *4*, 1699.

Ju, J.S., and Weihl, C.C. (2010). p97/VCP at the intersection of the autophagy and the ubiquitin proteasome system. Autophagy *6*, 283-285.

Kallio, M.J., McCleland, M.L., Stukenberg, P.T., and Gorbsky, G.J. (2002). Inhibition of aurora B kinase blocks chromosome segregation, overrides the spindle checkpoint, and perturbs microtubule dynamics in mitosis. Current biology : CB *12*, 900-905.

Kawashima, S.A., Tsukahara, T., Langegger, M., Hauf, S., Kitajima, T.S., and Watanabe, Y. (2007). Shugoshin enables tension-generating attachment of kinetochores by loading Aurora to centromeres. Genes & development *21*, 420-435.

Kawashima, S.A., Yamagishi, Y., Honda, T., Ishiguro, K., and Watanabe, Y. (2010). Phosphorylation of H2A by Bub1 prevents chromosomal instability through localizing shugoshin. Science *327*, 172-177.

Kelly, A.E., and Funabiki, H. (2009). Correcting aberrant kinetochore microtubule attachments: an Aurora B-centric view. Current opinion in cell biology *21*, 51-58.

Kelly, A.E., Ghenoiu, C., Xue, J.Z., Zierhut, C., Kimura, H., and Funabiki, H. (2010). Survivin reads phosphorylated histone H3 threonine 3 to activate the mitotic kinase Aurora B. Science *330*, 235-239.

Kemmler, S., Stach, M., Knapp, M., Ortiz, J., Pfannstiel, J., Ruppert, T., and Lechner, J. (2009). Mimicking Ndc80 phosphorylation triggers spindle assembly checkpoint signalling. The EMBO journal *28*, 1099-1110.

Kim, Y., Holland, A.J., Lan, W., and Cleveland, D.W. (2010). Aurora kinases and protein phosphatase 1 mediate chromosome congression through regulation of CENP-E. Cell *142*, 444-455.

Kirchner, P., Bug, M., and Meyer, H. (2013). Ubiquitination of the N-terminal region of caveolin-1 regulates endosomal sorting by the VCP/p97 AAA-ATPase. The Journal of biological chemistry *288*, 7363-7372.

Kiyomitsu, T., Obuse, C., and Yanagida, M. (2007). Human Blinkin/AF15q14 is required for chromosome alignment and the mitotic checkpoint through direct interaction with Bub1 and BubR1. Developmental cell *13*, 663-676.

Kobayashi, T., Manno, A., and Kakizuka, A. (2007). Involvement of valosin-containing protein (VCP)/p97 in the formation and clearance of abnormal protein aggregates. Genes to cells : devoted to molecular & cellular mechanisms *12*, 889-901.

Kops, G.J., Weaver, B.A., and Cleveland, D.W. (2005). On the road to cancer: aneuploidy and the mitotic checkpoint. Nature reviews Cancer *5*, 773-785.

Krenn, V., Wehenkel, A., Li, X., Santaguida, S., and Musacchio, A. (2012). Structural analysis reveals features of the spindle checkpoint kinase Bub1-kinetochore subunit Knl1 interaction. The Journal of cell biology *196*, 451-467.

Kress, E., Schwager, F., Holtackers, R., Seiler, J., Prodon, F., Zanin, E., Eiteneuer, A., Toya, M., Sugimoto, A., Meyer, H*., et al.* (2013). The UBXN-2/p37/p47 adaptors of CDC-48/p97 regulate mitosis by limiting the centrosomal recruitment of Aurora A. The Journal of cell biology *201*, 559-575.

Kruse, T., Zhang, G., Larsen, M.S., Lischetti, T., Streicher, W., Kragh Nielsen, T., Bjorn, S.P., and Nilsson, J. (2013). Direct binding between BubR1 and B56-PP2A phosphatase complexes regulate mitotic progression. Journal of cell science *126*, 1086-1092.

Kuhlbrodt, K., Janiesch, P.C., Kevei, E., Segref, A., Barikbin, R., and Hoppe, T. (2011). The Machado-Joseph disease deubiquitylase ATX-3 couples longevity and proteostasis. Nature cell biology *13*, 273-281.

Lampson, M.A., and Cheeseman, I.M. (2011). Sensing centromere tension: Aurora B and the regulation of kinetochore function. Trends in cell biology *21*, 133-140.

Lampson, M.A., Renduchitala, K., Khodjakov, A., and Kapoor, T.M. (2004). Correcting improper chromosome-spindle attachments during cell division. Nature cell biology *6*, 232-237.

Lan, W., Zhang, X., Kline-Smith, S.L., Rosasco, S.E., Barrett-Wilt, G.A., Shabanowitz, J., Hunt, D.F., Walczak, C.E., and Stukenberg, P.T. (2004). Aurora B phosphorylates centromeric MCAK and regulates its localization and microtubule depolymerization activity. Current biology : CB *14*, 273-286.

Landsverk, H.B., Kirkhus, M., Bollen, M., Kuntziger, T., and Collas, P. (2005). PNUTS enhances in vitro chromosome decondensation in a PP1-dependent manner. The Biochemical journal *390*, 709-717.

Lesage, B., Beullens, M., Pedelini, L., Garcia-Gimeno, M.A., Waelkens, E., Sanz, P., and Bollen, M. (2007). A complex of catalytically inactive protein phosphatase-1 sandwiched between Sds22 and inhibitor-3. Biochemistry *46*, 8909-8919.

Lesage, B., Qian, J., and Bollen, M. (2011). Spindle checkpoint silencing: PP1 tips the balance. Current biology : CB *21*, R898-903.

Li, M., Satinover, D.L., and Brautigan, D.L. (2007). Phosphorylation and functions of inhibitor-2 family of proteins. Biochemistry *46*, 2380-2389.

Lipp, J.J., Hirota, T., Poser, I., and Peters, J.M. (2007). Aurora B controls the association of condensin I but not condensin II with mitotic chromosomes. Journal of cell science *120*, 1245-1255.

Liu, D., Vader, G., Vromans, M.J., Lampson, M.A., and Lens, S.M. (2009). Sensing chromosome bi-orientation by spatial separation of aurora B kinase from kinetochore substrates. Science *323*, 1350-1353.

Liu, D., Vleugel, M., Backer, C.B., Hori, T., Fukagawa, T., Cheeseman, I.M., and Lampson, M.A. (2010). Regulated targeting of protein phosphatase 1 to the outer kinetochore by KNL1 opposes Aurora B kinase. The Journal of cell biology *188*, 809-820.

Lobrich, M., and Jeggo, P.A. (2007). The impact of a negligent G2/M checkpoint on genomic instability and cancer induction. Nature reviews Cancer *7*, 861-869.

London, N., Ceto, S., Ranish, J.A., and Biggins, S. (2012). Phosphoregulation of Spc105 by Mps1 and PP1 regulates Bub1 localization to kinetochores. Current biology : CB *22*, 900-906.

Ma, H.T., and Poon, R.Y. (2011). How protein kinases co-ordinate mitosis in animal cells. The Biochemical journal *435*, 17-31.

MacKelvie, S.H., Andrews, P.D., and Stark, M.J. (1995). The Saccharomyces cerevisiae gene SDS22 encodes a potential regulator of the mitotic function of yeast type 1 protein phosphatase. Molecular and cellular biology *15*, 3777-3785.

Madsen, L., Seeger, M., Semple, C.A., and Hartmann-Petersen, R. (2009). New ATPase regulators--p97 goes to the PUB. The international journal of biochemistry & cell biology *41*, 2380-2388.

Maerki, S., Olma, M.H., Staubli, T., Steigemann, P., Gerlich, D.W., Quadroni, M., Sumara, I., and Peter, M. (2009). The Cul3-KLHL21 E3 ubiquitin ligase targets aurora B to midzone microtubules in anaphase and is required for cytokinesis. The Journal of cell biology *187*, 791-800.

Margolis, S.S., Perry, J.A., Forester, C.M., Nutt, L.K., Guo, Y., Jardim, M.J., Thomenius, M.J., Freel, C.D., Darbandi, R., Ahn, J.H.*, et al.* (2006a). Role for the PP2A/B56delta phosphatase in regulating 14-3-3 release from Cdc25 to control mitosis. Cell *127*, 759-773.

Margolis, S.S., Perry, J.A., Weitzel, D.H., Freel, C.D., Yoshida, M., Haystead, T.A., and Kornbluth, S. (2006b). A role for PP1 in the Cdc2/Cyclin B-mediated positive feedback activation of Cdc25. Molecular biology of the cell *17*, 1779-1789.

Margolis, S.S., Walsh, S., Weiser, D.C., Yoshida, M., Shenolikar, S., and Kornbluth, S. (2003). PP1 control of M phase entry exerted through 14-3-3-regulated Cdc25 dephosphorylation. The EMBO journal *22*, 5734-5745.

Martin-Lluesma, S., Stucke, V.M., and Nigg, E.A. (2002). Role of Hec1 in spindle checkpoint signaling and kinetochore recruitment of Mad1/Mad2. Science *297*, 2267-2270.

Meadows, J.C., Shepperd, L.A., Vanoosthuyse, V., Lancaster, T.C., Sochaj, A.M., Buttrick, G.J., Hardwick, K.G., and Millar, J.B. (2011). Spindle checkpoint silencing requires association of PP1 to both Spc7 and kinesin-8 motors. Developmental cell *20*, 739-750.

Meerang, M., Ritz, D., Paliwal, S., Garajova, Z., Bosshard, M., Mailand, N., Janscak, P., Hubscher, U., Meyer, H., and Ramadan, K. (2011). The ubiquitin-selective segregase VCP/p97 orchestrates the response to DNA double-strand breaks. Nature cell biology *13*, 1376-1382.

Meiselbach, H., Sticht, H., and Enz, R. (2006). Structural analysis of the protein phosphatase 1 docking motif: molecular description of binding specificities identifies interacting proteins. Chemistry & biology *13*, 49-59.

Meusser, B., Hirsch, C., Jarosch, E., and Sommer, T. (2005). ERAD: the long road to destruction. Nature cell biology *7*, 766-772.

Meyer, H., Bug, M., and Bremer, S. (2012). Emerging functions of the VCP/p97 AAA-ATPase in the ubiquitin system. Nature cell biology *14*, 117-123.

Meyer, H.H., Wang, Y., and Warren, G. (2002). Direct binding of ubiquitin conjugates by the mammalian p97 adaptor complexes, p47 and Ufd1-Npl4. The EMBO journal *21*, 5645-5652.

Minnebo, N., Gornemann, J., O'Connell, N., Van Dessel, N., Derua, R., Vermunt, M.W., Page, R., Beullens, M., Peti, W., Van Eynde, A.*, et al.* (2013). NIPP1 maintains EZH2 phosphorylation and promoter occupancy at proliferation-related target genes. Nucleic acids research *41*, 842-854.

Moir, D., Stewart, S.E., Osmond, B.C., and Botstein, D. (1982). Cold-sensitive cell-division-cycle mutants of yeast: isolation, properties, and pseudoreversion studies. Genetics *100*, 547-563.

Moore, A., and Wordeman, L. (2004). C-terminus of mitotic centromere-associated kinesin (MCAK) inhibits its lattice-stimulated ATPase activity. The Biochemical journal *383*, 227-235.

Mora-Bermudez, F., Gerlich, D., and Ellenberg, J. (2007). Maximal chromosome compaction occurs by axial shortening in anaphase and depends on Aurora kinase. Nature cell biology *9*, 822-831.

Mouysset, J., Deichsel, A., Moser, S., Hoege, C., Hyman, A.A., Gartner, A., and Hoppe, T. (2008). Cell cycle progression requires the CDC-48UFD-1/NPL-4 complex for efficient DNA replication. Proceedings of the National Academy of Sciences of the United States of America *105*, 12879-12884.

Murata-Hori, M., and Wang, Y.L. (2002). Both midzone and astral microtubules are involved in the delivery of cytokinesis signals: insights from the mobility of aurora B. The Journal of cell biology *159*, 45-53.

Musacchio, A. (2011). Spindle assembly checkpoint: the third decade. Philosophical transactions of the Royal Society of London Series B, Biological sciences *366*, 3595-3604.

Musacchio, A., and Salmon, E.D. (2007). The spindle-assembly checkpoint in space and time. Nature reviews Molecular cell biology *8*, 379-393.

Nicklas, R.B. (1997). How cells get the right chromosomes. Science *275*, 632-637.

Nicklas, R.B., and Koch, C.A. (1969). Chromosome micromanipulation. 3. Spindle fiber tension and the reorientation of mal-oriented chromosomes. The Journal of cell biology *43*, 40-50.

Nuytten, M., Beke, L., Van Eynde, A., Ceulemans, H., Beullens, M., Van Hummelen, P., Fuks, F., and Bollen, M. (2008). The transcriptional repressor NIPP1 is an essential player in EZH2-mediated gene silencing. Oncogene *27*, 1449-1460.

Ogura, T., and Wilkinson, A.J. (2001). AAA+ superfamily ATPases: common structure--diverse function. Genes to cells : devoted to molecular & cellular mechanisms *6*, 575-597.

Ohi, R., Sapra, T., Howard, J., and Mitchison, T.J. (2004). Differentiation of cytoplasmic and meiotic spindle assembly MCAK functions by Aurora B-dependent phosphorylation. Molecular biology of the cell *15*, 2895-2906.

Pedelini, L., Marquina, M., Arino, J., Casamayor, A., Sanz, L., Bollen, M., Sanz, P., and Garcia-Gimeno, M.A. (2007). YPI1 and SDS22 proteins regulate the nuclear localization and function of yeast type 1 phosphatase Glc7. The Journal of biological chemistry *282*, 3282-3292.

Peggie, M.W., MacKelvie, S.H., Bloecher, A., Knatko, E.V., Tatchell, K., and Stark, M.J. (2002). Essential functions of Sds22p in chromosome stability and nuclear localization of PP1. Journal of cell science *115*, 195-206.

Peng, J., Schwartz, D., Elias, J.E., Thoreen, C.C., Cheng, D., Marsischky, G., Roelofs, J., Finley, D., and Gygi, S.P. (2003). A proteomics approach to understanding protein ubiquitination. Nature biotechnology *21*, 921-926.

Pereira, G., and Schiebel, E. (2003). Separase regulates INCENP-Aurora B anaphase spindle function through Cdc14. Science *302*, 2120-2124.

Petersen, J., and Hagan, I.M. (2003). S. pombe aurora kinase/survivin is required for chromosome condensation and the spindle checkpoint attachment response. Current biology : CB *13*, 590-597.

Petronczki, M., Glotzer, M., Kraut, N., and Peters, J.M. (2007). Polo-like kinase 1 triggers the initiation of cytokinesis in human cells by promoting recruitment of the RhoGEF Ect2 to the central spindle. Developmental cell *12*, 713-725.

Petrovic, A., Pasqualato, S., Dube, P., Krenn, V., Santaguida, S., Cittaro, D., Monzani, S., Massimiliano, L., Keller, J., Tarricone, A*., et al.* (2010). The MIS12 complex is a protein interaction hub for outer kinetochore assembly. The Journal of cell biology *190*, 835-852.

Pinsky, B.A., Kotwaliwale, C.V., Tatsutani, S.Y., Breed, C.A., and Biggins, S. (2006). Glc7/protein phosphatase 1 regulatory subunits can oppose the Ipl1/aurora protein kinase by redistributing Glc7. Molecular and cellular biology *26*, 2648-2660.

Pinsky, B.A., Nelson, C.R., and Biggins, S. (2009). Protein phosphatase 1 regulates exit from the spindle checkpoint in budding yeast. Current biology : CB *19*, 1182-1187.

Posch, M., Khoudoli, G.A., Swift, S., King, E.M., Deluca, J.G., and Swedlow, J.R. (2010). Sds22 regulates aurora B activity and microtubule-kinetochore interactions at mitosis. The Journal of cell biology *191*, 61-74.

Poser, I., Sarov, M., Hutchins, J.R., Heriche, J.K., Toyoda, Y., Pozniakovsky, A., Weigl, D., Nitzsche, A., Hegemann, B., Bird, A.W*., et al.* (2008). BAC TransgeneOmics: a high-throughput method for exploration of protein function in mammals. Nature methods *5*, 409-415.

Pye, V.E., Dreveny, I., Briggs, L.C., Sands, C., Beuron, F., Zhang, X., and Freemont, P.S. (2006). Going through the motions: the ATPase cycle of p97. Journal of structural biology *156*, 12-28.

Qian, J., Beullens, M., Lesage, B., and Bollen, M. (2013). Aurora B defines its own chromosomal targeting by opposing the recruitment of the phosphatase scaffold Repo-Man. Current biology : CB *23*, 1136-1143.

Queralt, E., and Uhlmann, F. (2008). Cdk-counteracting phosphatases unlock mitotic exit. Current opinion in cell biology *20*, 661-668.

Ramadan, K., Bruderer, R., Spiga, F.M., Popp, O., Baur, T., Gotta, M., and Meyer, H.H. (2007). Cdc48/p97 promotes reformation of the nucleus by extracting the kinase Aurora B from chromatin. Nature *450*, 1258-1262.

Raman, M., Havens, C.G., Walter, J.C., and Harper, J.W. (2011). A genome-wide screen identifies p97 as an essential regulator of DNA damage-dependent CDT1 destruction. Molecular cell *44*, 72-84.

Rezvani, K., Teng, Y., Pan, Y., Dani, J.A., Lindstrom, J., Garcia Gras, E.A., McIntosh, J.M., and De Biasi, M. (2009). UBXD4, a UBX-containing protein, regulates the cell surface number and stability of alpha3-containing nicotinic acetylcholine receptors. The Journal of neuroscience : the official journal of the Society for Neuroscience *29*, 6883-6896.

Richly, H., Rape, M., Braun, S., Rumpf, S., Hoege, C., and Jentsch, S. (2005). A series of ubiquitin binding factors connects CDC48/p97 to substrate multiubiquitylation and proteasomal targeting. Cell *120*, 73-84.

Rieder, C.L., Khodjakov, A., Paliulis, L.V., Fortier, T.M., Cole, R.W., and Sluder, G. (1997). Mitosis in vertebrate somatic cells with two spindles: implications for the metaphase/anaphase transition checkpoint and cleavage. Proceedings of the National Academy of Sciences of the United States of America *94*, 5107-5112.

Riemer, A., Dobrynin, G., Dressler, A., Bremer, S., Soni, A., Iliakis, G., and Meyer, H. (2014). The p97-Ufd1-Npl4 ATPase complex ensures robustness of the G /M checkpoint by facilitating CDC25A degradation. Cell cycle *13*.

Robinson, L.C., Phillips, J., Brou, L., Boswell, E.P., and Tatchell, K. (2012). Suppressors of ipl1-2 in components of a Glc7 phosphatase complex, Cdc48 AAA ATPase, TORC1, and the kinetochore. G3 *2*, 1687-1701.

Rosenberg, J.S., Cross, F.R., and Funabiki, H. (2011). KNL1/Spc105 recruits PP1 to silence the spindle assembly checkpoint. Current biology : CB *21*, 942-947.

Ruchaud, S., Carmena, M., and Earnshaw, W.C. (2007). Chromosomal passengers: conducting cell division. Nature reviews Molecular cell biology *8*, 798-812.

Salimian, K.J., Ballister, E.R., Smoak, E.M., Wood, S., Panchenko, T., Lampson, M.A., and Black, B.E. (2011). Feedback control in sensing chromosome biorientation by the Aurora B kinase. Current biology : CB *21*, 1158-1165.

Santaguida, S., and Musacchio, A. (2009). The life and miracles of kinetochores. The EMBO journal *28*, 2511-2531.

Santaguida, S., Vernieri, C., Villa, F., Ciliberto, A., and Musacchio, A. (2011). Evidence that Aurora B is implicated in spindle checkpoint signalling independently of error correction. The EMBO journal *30*, 1508-1519.

Satinover, D.L., Leach, C.A., Stukenberg, P.T., and Brautigan, D.L. (2004). Activation of Aurora-A kinase by protein phosphatase inhibitor-2, a bifunctional signaling protein. Proceedings of the National Academy of Sciences of the United States of America *101*, 8625-8630.

Saurin, A.T., van der Waal, M.S., Medema, R.H., Lens, S.M., and Kops, G.J. (2011). Aurora B potentiates Mps1 activation to ensure rapid checkpoint establishment at the onset of mitosis. Nature communications *2*, 316.

Schlaitz, A.L., Srayko, M., Dammermann, A., Quintin, S., Wielsch, N., MacLeod, I., de Robillard, Q., Zinke, A., Yates, J.R., 3rd, Muller-Reichert, T.*, et al.* (2007). The C. elegans RSA complex localizes protein phosphatase 2A to centrosomes and regulates mitotic spindle assembly. Cell *128*, 115-127.

Schmitz, M.H., Held, M., Janssens, V., Hutchins, J.R., Hudecz, O., Ivanova, E., Goris, J., Trinkle-Mulcahy, L., Lamond, A.I., Poser, I.*, et al.* (2010). Live-cell imaging RNAi screen identifies PP2A-B55alpha and importin-beta1 as key mitotic exit regulators in human cells. Nature cell biology *12*, 886-893.

Schuberth, C., and Buchberger, A. (2008). UBX domain proteins: major regulators of the AAA ATPase Cdc48/p97. Cellular and molecular life sciences : CMLS *65*, 2360-2371.

Schuberth, C., Richly, H., Rumpf, S., and Buchberger, A. (2004). Shp1 and Ubx2 are adaptors of Cdc48 involved in ubiquitin-dependent protein degradation. EMBO reports *5*, 818-824.

Starita, L.M., Lo, R.S., Eng, J.K., von Haller, P.D., and Fields, S. (2012). Sites of ubiquitin attachment in Saccharomyces cerevisiae. Proteomics *12*, 236-240.

Steen, R.L., Martins, S.B., Tasken, K., and Collas, P. (2000). Recruitment of protein phosphatase 1 to the nuclear envelope by A-kinase anchoring protein AKAP149 is a prerequisite for nuclear lamina assembly. The Journal of cell biology *150*, 1251-1262.

Stegmeier, F., and Amon, A. (2004). Closing mitosis: the functions of the Cdc14 phosphatase and its regulation. Annual review of genetics *38*, 203-232.

Stolz, A., Hilt, W., Buchberger, A., and Wolf, D.H. (2011). Cdc48: a power machine in protein degradation. Trends in biochemical sciences *36*, 515-523.

Suijkerbuijk, S.J., Vleugel, M., Teixeira, A., and Kops, G.J. (2012). Integration of kinase and phosphatase activities by BUBR1 ensures formation of stable kinetochore-microtubule attachments. Developmental cell *23*, 745-755.

Sullivan, M., and Morgan, D.O. (2007). Finishing mitosis, one step at a time. Nature reviews Molecular cell biology *8*, 894-903.

Sumara, I., and Peter, M. (2007). A Cul3-based E3 ligase regulates mitosis and is required to maintain the spindle assembly checkpoint in human cells. Cell cycle *6*, 3004-3010.

Sumara, I., Quadroni, M., Frei, C., Olma, M.H., Sumara, G., Ricci, R., and Peter, M. (2007). A Cul3-based E3 ligase removes Aurora B from mitotic chromosomes, regulating mitotic progression and completion of cytokinesis in human cells. Developmental cell *12*, 887-900.

Sun, L., Gao, J., Dong, X., Liu, M., Li, D., Shi, X., Dong, J.T., Lu, X., Liu, C., and Zhou, J. (2008). EB1 promotes Aurora-B kinase activity through blocking its

inactivation by protein phosphatase 2A. Proceedings of the National Academy of Sciences of the United States of America *105*, 7153-7158.

Surana, U., Amon, A., Dowzer, C., McGrew, J., Byers, B., and Nasmyth, K. (1993). Destruction of the CDC28/CLB mitotic kinase is not required for the metaphase to anaphase transition in budding yeast. The EMBO journal *12*, 1969-1978.

Takemoto, A., Murayama, A., Katano, M., Urano, T., Furukawa, K., Yokoyama, S., Yanagisawa, J., Hanaoka, F., and Kimura, K. (2007). Analysis of the role of Aurora B on the chromosomal targeting of condensin I. Nucleic acids research *35*, 2403-2412.

Takeuchi, K., and Fukagawa, T. (2012). Molecular architecture of vertebrate kinetochores. Experimental cell research *318*, 1367-1374.

Tanaka, K. (2013). Regulatory mechanisms of kinetochore-microtubule interaction in mitosis. Cellular and molecular life sciences : CMLS *70*, 559-579.

Terrak, M., Kerff, F., Langsetmo, K., Tao, T., and Dominguez, R. (2004). Structural basis of protein phosphatase 1 regulation. Nature *429*, 780-784.

Tresse, E., Salomons, F.A., Vesa, J., Bott, L.C., Kimonis, V., Yao, T.P., Dantuma, N.P., and Taylor, J.P. (2010). VCP/p97 is essential for maturation of ubiquitin-containing autophagosomes and this function is impaired by mutations that cause IBMPFD. Autophagy *6*, 217-227.

Trinkle-Mulcahy, L., Andrews, P.D., Wickramasinghe, S., Sleeman, J., Prescott, A., Lam, Y.W., Lyon, C., Swedlow, J.R., and Lamond, A.I. (2003). Time-lapse imaging reveals dynamic relocalization of PP1gamma throughout the mammalian cell cycle. Molecular biology of the cell *14*, 107-117.

Trinkle-Mulcahy, L., and Lamond, A.I. (2006). Mitotic phosphatases: no longer silent partners. Current opinion in cell biology *18*, 623-631.

Tsukahara, T., Tanno, Y., and Watanabe, Y. (2010). Phosphorylation of the CPC by Cdk1 promotes chromosome bi-orientation. Nature *467*, 719-723.

Uchiyama, K., Jokitalo, E., Lindman, M., Jackman, M., Kano, F., Murata, M., Zhang, X., and Kondo, H. (2003). The localization and phosphorylation of p47 are important for Golgi disassembly-assembly during the cell cycle. The Journal of cell biology *161*, 1067-1079.

Uchiyama, K., Totsukawa, G., Puhka, M., Kaneko, Y., Jokitalo, E., Dreveny, I., Beuron, F., Zhang, X., Freemont, P., and Kondo, H. (2006). p37 is a p97 adaptor required for Golgi and ER biogenesis in interphase and at the end of mitosis. Developmental cell *11*, 803-816.

Vader, G., Cruijsen, C.W., van Harn, T., Vromans, M.J., Medema, R.H., and Lens, S.M. (2007). The chromosomal passenger complex controls spindle checkpoint function independent from its role in correcting microtubule kinetochore interactions. Molecular biology of the cell *18*, 4553-4564.

Vader, G., Kauw, J.J., Medema, R.H., and Lens, S.M. (2006). Survivin mediates targeting of the chromosomal passenger complex to the centromere and midbody. EMBO reports *7*, 85-92.

Vagnarelli, P., Hudson, D.F., Ribeiro, S.A., Trinkle-Mulcahy, L., Spence, J.M., Lai, F., Farr, C.J., Lamond, A.I., and Earnshaw, W.C. (2006). Condensin and Repo-Man-PP1

co-operate in the regulation of chromosome architecture during mitosis. Nature cell biology *8*, 1133-1142.

Vagnarelli, P., Ribeiro, S., Sennels, L., Sanchez-Pulido, L., de Lima Alves, F., Verheyen, T., Kelly, D.A., Ponting, C.P., Rappsilber, J., and Earnshaw, W.C. (2011). Repo-Man coordinates chromosomal reorganization with nuclear envelope reassembly during mitotic exit. Developmental cell *21*, 328-342.

van der Waal, M.S., Saurin, A.T., Vromans, M.J., Vleugel, M., Wurzenberger, C., Gerlich, D.W., Medema, R.H., Kops, G.J., and Lens, S.M. (2012). Mps1 promotes rapid centromere accumulation of Aurora B. EMBO reports *13*, 847-854.

Vanoosthuyse, V., and Hardwick, K.G. (2009). A novel protein phosphatase 1-dependent spindle checkpoint silencing mechanism. Current biology : CB *19*, 1176-1181.

Vazquez-Novelle, M.D., Mirchenko, L., Uhlmann, F., and Petronczki, M. (2010). The 'anaphase problem': how to disable the mitotic checkpoint when sisters split. Biochemical Society transactions *38*, 1660-1666.

Vembar, S.S., and Brodsky, J.L. (2008). One step at a time: endoplasmic reticulum-associated degradation. Nature reviews Molecular cell biology *9*, 944-957.

Verdecia, M.A., Huang, H., Dutil, E., Kaiser, D.A., Hunter, T., and Noel, J.P. (2000). Structure of the human anti-apoptotic protein survivin reveals a dimeric arrangement. Nature structural biology *7*, 602-608.

Vong, Q.P., Cao, K., Li, H.Y., Iglesias, P.A., and Zheng, Y. (2005). Chromosome alignment and segregation regulated by ubiquitination of survivin. Science *310*, 1499-1504.

Wakula, P., Beullens, M., Ceulemans, H., Stalmans, W., and Bollen, M. (2003). Degeneracy and function of the ubiquitous RVXF motif that mediates binding to protein phosphatase-1. The Journal of biological chemistry *278*, 18817-18823.

Wang, F., Dai, J., Daum, J.R., Niedzialkowska, E., Banerjee, B., Stukenberg, P.T., Gorbsky, G.J., and Higgins, J.M. (2010). Histone H3 Thr-3 phosphorylation by Haspin positions Aurora B at centromeres in mitosis. Science *330*, 231-235.

Wang, Q., Song, C., and Li, C.C. (2004). Molecular perspectives on p97-VCP: progress in understanding its structure and diverse biological functions. Journal of structural biology *146*, 44-57.

Welburn, J.P., Vleugel, M., Liu, D., Yates, J.R., 3rd, Lampson, M.A., Fukagawa, T., and Cheeseman, I.M. (2010). Aurora B phosphorylates spatially distinct targets to differentially regulate the kinetochore-microtubule interface. Molecular cell *38*, 383-392.

Wheatley, S.P., Henzing, A.J., Dodson, H., Khaled, W., and Earnshaw, W.C. (2004). Aurora-B phosphorylation in vitro identifies a residue of survivin that is essential for its localization and binding to inner centromere protein (INCENP) in vivo. The Journal of biological chemistry *279*, 5655-5660.

Whyte, J., Bader, J.R., Tauhata, S.B., Raycroft, M., Hornick, J., Pfister, K.K., Lane, W.S., Chan, G.K., Hinchcliffe, E.H., Vaughan, P.S.*, et al.* (2008). Phosphorylation regulates targeting of cytoplasmic dynein to kinetochores during mitosis. The Journal of cell biology *183*, 819-834.

Wilcox, A.J., and Laney, J.D. (2009). A ubiquitin-selective AAA-ATPase mediates transcriptional switching by remodelling a repressor-promoter DNA complex. Nature cell biology *11*, 1481-1486.

Wolf, D.H., and Stolz, A. (2012). The Cdc48 machine in endoplasmic reticulum associated protein degradation. Biochimica et biophysica acta *1823*, 117-124.

Wu, J.Q., Guo, J.Y., Tang, W., Yang, C.S., Freel, C.D., Chen, C., Nairn, A.C., and Kornbluth, S. (2009). PP1-mediated dephosphorylation of phosphoproteins at mitotic exit is controlled by inhibitor-1 and PP1 phosphorylation. Nature cell biology *11*, 644-651.

Wurzenberger, C., and Gerlich, D.W. (2011). Phosphatases: providing safe passage through mitotic exit. Nature reviews Molecular cell biology *12*, 469-482.

Wurzenberger, C., Held, M., Lampson, M.A., Poser, I., Hyman, A.A., and Gerlich, D.W. (2012). Sds22 and Repo-Man stabilize chromosome segregation by counteracting Aurora B on anaphase kinetochores. The Journal of cell biology *198*, 173-183.

Xu, P., Raetz, E.A., Kitagawa, M., Virshup, D.M., and Lee, S.H. (2013). BUBR1 recruits PP2A via the B56 family of targeting subunits to promote chromosome congression. Biology open *2*, 479-486.

Xu, S., Peng, G., Wang, Y., Fang, S., and Karbowski, M. (2011). The AAA-ATPase p97 is essential for outer mitochondrial membrane protein turnover. Molecular biology of the cell *22*, 291-300.

Yamagishi, Y., Honda, T., Tanno, Y., and Watanabe, Y. (2010). Two histone marks establish the inner centromere and chromosome bi-orientation. Science *330*, 239-243.

Yamashiro, S., Yamakita, Y., Totsukawa, G., Goto, H., Kaibuchi, K., Ito, M., Hartshorne, D.J., and Matsumura, F. (2008). Myosin phosphatase-targeting subunit 1 regulates mitosis by antagonizing polo-like kinase 1. Developmental cell *14*, 787-797.

Yasui, Y., Urano, T., Kawajiri, A., Nagata, K., Tatsuka, M., Saya, H., Furukawa, K., Takahashi, T., Izawa, I., and Inagaki, M. (2004). Autophosphorylation of a newly identified site of Aurora-B is indispensable for cytokinesis. The Journal of biological chemistry *279*, 12997-13003.

Ye, Y. (2006). Diverse functions with a common regulator: ubiquitin takes command of an AAA ATPase. Journal of structural biology *156*, 29-40.

Ye, Y., Meyer, H.H., and Rapoport, T.A. (2001). The AAA ATPase Cdc48/p97 and its partners transport proteins from the ER into the cytosol. Nature *414*, 652-656.

Ye, Y., Shibata, Y., Yun, C., Ron, D., and Rapoport, T.A. (2004). A membrane protein complex mediates retro-translocation from the ER lumen into the cytosol. Nature *429*, 841-847.

Yeong, F.M., Lim, H.H., Padmashree, C.G., and Surana, U. (2000). Exit from mitosis in budding yeast: biphasic inactivation of the Cdc28-Clb2 mitotic kinase and the role of Cdc20. Molecular cell *5*, 501-511.

Yeung, H.O., Kloppsteck, P., Niwa, H., Isaacson, R.L., Matthews, S., Zhang, X., and Freemont, P.S. (2008). Insights into adaptor binding to the AAA protein p97. Biochemical Society transactions *36*, 62-67.

Yuan, X., Simpson, P., McKeown, C., Kondo, H., Uchiyama, K., Wallis, R., Dreveny, I., Keetch, C., Zhang, X., Robinson, C.*, et al.* (2004). Structure, dynamics and interactions of p47, a major adaptor of the AAA ATPase, p97. The EMBO journal *23*, 1463-1473.

Yuce, O., Piekny, A., and Glotzer, M. (2005). An ECT2-centralspindlin complex regulates the localization and function of RhoA. The Journal of cell biology *170*, 571-582.

Zhang, L., Qi, Z., Gao, Y., and Lee, E.Y. (2008). Identification of the interaction sites of Inhibitor-3 for protein phosphatase-1. Biochemical and biophysical research communications *377*, 710-713.

Zhang, S., Guha, S., and Volkert, F.C. (1995). The Saccharomyces SHP1 gene, which encodes a regulator of phosphoprotein phosphatase 1 with differential effects on glycogen metabolism, meiotic differentiation, and mitotic cell cycle progression. Molecular and cellular biology *15*, 2037-2050.

Abbreviations

aa	amino acid
AAA	ATPase associated with various cellular activities
AP2	adaptor protein 2
APC/C	anaphase promoting complex/cyclosome
ATP	adenosine 5’-triphosphate
ATPase	adenosine 5’-triphosphatase
BAC	bacterial artificial chromosome
BIR	baculovirus IAP repeat
BS1	binding site 1
Bub	budding inhibited by benomyl
BubR	Bub-related
CCAN	constitutive centromere associated network
CDC	cell division control
CDK1	Cyclin-dependent kinase 1
CDT1	chromatin licensing and DNA replication factor 1
CENP	centromere protein
CPC	chromosomal passenger complex
DAPI	4',6-diamidino-2-phenylindole
DNA	deoxyribonucleic acid
DUB	deubiquitination enzyme
E3	ubiquitin ligase
ER	endoplasmic reticulum
ERAD	ER-associated degradation
FCS	fetal calf serum
FRET	fluorescence resonance energy transfer
GAPDH	glyceraldehyde 3’-phosphate dehydrogenase
GFP	green fluorescent protein
H	Histone
HA tag	hemagglutinin epitope tag (YPYDVPDYA)

HP1	heterochromatin protein-1
HRP	horseradish peroxidase
I	inhibitor
IAP	inhibitor of aptoptosis
IBB	importin β binding
INCENP	inner centromere protein
KMN	KNL1/Mis12 complex/Ndc80 complex
KNL1	Kinetochore-null protein 1
LRR	leucine-rich repeat
MAD	mitotic arrest deficient
MCAK	Mitotic centromere-associated kinesin
MCC	mitotic checkpoint complex
mCherry	monomeric cherry fluorescent protein
Mklp	mitotic kinesin-like protein
MPF	maturation-promoting factor
Mps1	monopolar spindle protein 1
MyPhoNE	myosin phosphatase N-terminal element
Mypt1	Myosin phosphatase 1
NEBD.	nuclear envelope break down
NIPP1	nuclear inhibitor of PP1
Npl	nuclear protein localization
PAGE	polyacrylamid gel electrophoresis
PBS	phosphate buffered saline
PCR	polymerase chain reaction
PFA	paraformaldehyde
PIP	PP1 interacting protein
PKA	protein kinase A
PLK1	Polo-like kinase 1
PNGase	peptide *N*-glycanase enzyme
PNUTS	PP1 uclear targeting subunit
PP	protein phosphatase
PTPA	PP2A phosphatase activator

PUB	PNGase/UBA or UBX domain
Repo-Man	Recruits PP1 onto mitotic chromatin at anaphase protein
RFP	red fluorescent protein
RNA	ribonucleic acid
RNAi	RNA interference
SAC	spindle assembly checkpoint
SEP	Shp1, eye-closed, p47
Shp1	Suppressor of high-copy PP1
SDS	sodium dodecyl sulfate
siRNA	small interfering RNA
Ska	spindle- and kinetochore-associated
Strep	streptavidin
SUMO	small ubiquitin-related modifier
UBA	ubiquitin-associated domain
UBL	ubiquitin-like domain
Ubx	UBX domain-containing protein
UBXD	ubiquitin regulatory X domain
Ufd	ubiquitin fusion degradation
VBM	VCP-binding motif
VCP	valosin-containing protein
VIM	VCP-interacting motif

Acknowledgements

I would like to thank Prof. Dr. Hemmo Meyer for the opportunity to work in the field of mitosis, which entails not only exciting research, but also beautiful microscopy images. I am grateful for his constant support and useful criticism.

I also would like to thank Prof. Dr. Mathieu Bollen and Prof. Dr. Andrea Musacchio for valuable discussions concerning the fields of phosphatases and bipolar spindle attachment. In that context, I furthermore would like to thank Monique Beullens and Bart Lesage, who supported us with ideas and material.

Special thanks go to Jonas, who launched together with me the PP1 subgroup and who had always time for a little chat on PP1, its fellows, and the troubles they caused.

Thank you to all the members of the Meyer lab for daily support in the lab. To mention here are Christina and Sabine, who keep the lab running and who constantly supply us with buffers, ordered material, and so on.
It was a great time with lots of fun inside the lab, during lunch, coffee, ice and all other breaks, as well as outside the lab during dinners, parties, movie nights, and cocktail nights. I will miss our great working atmosphere.

Finally, I wish to thank my family and friends, with whom I always have lots of fun, totally independent of issues in science.

Curriculum Vitae

For data privacy reasons, the CV is omitted from the online version.

For data privacy reasons, the CV is omitted from the online version.

Affidavits/Erklärungen

Erklärung:

Hiermit erkläre ich, gem. § 6 Abs. 2, Nr. 7 der Promotionsordnung der Math.-Nat.-Fachbreiche zur Erlangung des Dr. rer. nat., dass ich das Arbeitgebiet, dem das Thema „The functional relationship between Inhibitor-3, SDS22 and PP1 in the process of bipolar spindle attachment“ zuzuordnen ist, in Forschung und Lehre vertrete und den Antrag von Annika Eiteneuer befürworte.

Essen, den _____ _____

Unterschrift eines Mitglieds der Universität Duisburg-Essen

Erklärung:

Hiermit erkläre ich, gem. § 6 Abs. 2, Nr. 6 der Promotionsordnung der Math.-Nat.-Fachbereiche zur Erlangung des Dr. rer. nat., dass ich die vorliegende Dissertation selbständig verfasst und mich keiner anderen als der angegebenen Hilfsmittel bedient habe.

Essen, den _____ _____

Unterschrift des/r Doktoranden/in

Erklärung:

Hiermit erkläre ich, gem. § 6 Abs. 2, Nr. 8 der Promotionsordnung der Math.-Nat.-Fachbereiche zur Erlangung des Dr. rer. nat., dass ich keine anderen Promotionen bzw. Promotionsversuche in der Vergangenheit durchgeführt habe und dass diese Arbeit von keiner anderen Fakultät/Fachbereich abgelehnt worden ist.

Essen, den _____ _____

Unterschrift des/r Doktoranden/in